The CD40/CD40L axis as potential therapeutic target in abdominal aortic aneurysm

Inaugural-Dissertation

zur Erlangung des Doktorgrades
der Mathematisch-Naturwissenschaftlichen Fakultät
der Heinrich-Heine-Universität Düsseldorf

vorgelegt von
Miriam Ommer-Bläsius
aus Lindlar

Düsseldorf, Mai 2024

aus der Klinik für Kardiologie, Pneumologie und Angiologie
der Heinrich-Heine-Universität Düsseldorf
Klinikdirektor: Prof. Dr. med. Malte Kelm

Gedruckt mit der Genehmigung der
Mathematisch-Naturwissenschaftlichen Fakultät der
Heinrich-Heine-Universität Düsseldorf

Berichterstatter:
1. Prof. Dr. rer. nat. Norbert Gerdes
2. Prof. Dr. rer. nat. Gerhard Fritz

Tag der mündlichen Prüfung: 09.10.2024

Eidesstattliche Erklärung

Ich, Miriam Ommer-Bläsius, versichere an Eides Statt, dass die Dissertation von mir selbständig und ohne unzulässige fremde Hilfe unter Beachtung der „Grundsätze zur Sicherung guter wissenschaftlicher Praxis“ an der Heinrich-Heine-Universität Düsseldorf erstellt worden ist.

Die vorliegende Dissertation wurde in keiner anderen Fakultät vorgelegt und es gab bisher noch keine vorherigen erfolglosen oder erfolgreichen Promotionsversuche.

Düsseldorf, den _____

Unterschrift

Parts of this dissertation were already published in a scientific journal or presented on scientific conferences:

Original publication:

Ommer-Bläsius M, Vajen T, Elster C, et al. Inhibition of CD40-TRAF6 signaling protects against aneurysm development and progression. bioRxiv. 2023:2023.03.24.534110. http://dx.doi.org/10.1101/2023.03.24.534110

Posters:

May 21 - 24, 2023
91st European Atherosclerosis Society (EAS) congress in Mannheim, Germany
Miriam Ommer-Bläsius, Christin Elster, Tanja Vajen, Sarah Verheyen, Susanne Pfeiler, Malte Kelm, Esther Lutgens, Norbert Gerdes. Inhibition of CD40-TRAF6 signaling reduces AAA progression.

March 23 - 25, 2022
3rd International Symposium of the Collaborative Research Center/Transregio TRR 259 in Bonn, Germany
Miriam Ommer, Christin Elster, Tanja Vajen, Milena Feige, Julia Pauli, Susanne Pfeiler, Malte Kelm, Esther Lutgens, Norbert Gerdes. Inhibition of CD40-TRAF6 signaling diminishes AAA incidence and rupture.

Abstract

Background: Progressive degeneration of the aortic wall and extensive inflammatory processes are main pathological drivers of abdominal aortic aneurysm (AAA), a life-threatening and multifactorial disease. In particular, the activation of proteolytic enzymes and the release of pro-inflammatory cytokines both associated with the degradation of important structural proteins of the aortic wall are key processes in which inflammation is involved. These immune responses are among others regulated by the interaction of co-stimulatory molecules, such as CD40 and CD40L. This regulation should prevent detrimental dysregulated and prolonged activation of immune cells under physiologic conditions. CD40 and CD40L, cell surface proteins, are widely expressed on hematopoietic cells, such as monocytes, macrophages, B cells, T cells, and platelets but also on non-hematopoietic cells as fibroblasts, endothelial cells and smooth muscle cells. However, the mechanisms underlying inflammatory activation and processes contributing to AAA formation and progression remain incompletely understood.

Hypothesis & Aim: In this work, it was hypothesized that in the context of AAA, the activation of the CD40/CD40L signalling pathway contributes to extensive stimulation of immune cells, resulting in the release of proteolytic enzymes and pro-inflammatory cytokines that further promote AAA pathology. Therefore, this study evaluated the inhibition of the CD40/CD40L axis as potential therapeutic target in AAA in different experimental models.

Methods: To unravel the role of CD40/CD40L signalling in AAA pathology, AAAs were induced in mice with C57BL/6J background by transient porcine pancreatic elastase (PPE) perfusion of an infrarenal aortic segment or by continuous infusion with angiotensin (Ang) II into mice with apolipoprotein E–deficient (*Apoe*$^{-/-}$) background for 28 days. C57BL/6J and *Apoe*$^{-/-}$ mice on standard chow or western diet were treated with a small molecule inhibitor, which specifically blocks the interaction between CD40 and tumor necrosis factor (TNF) receptor-associated factor (TRAF)-6, referred to as TRAF-STOP or solvent control for 28 days. Aortic dilation and rupture, as well as degradation of structural proteins, expression and activation of proteolytic enzymes, immune cell infiltration, and the presence of inflammatory cytokines in aneurysmal tissue were investigated using ultrasound imaging, histological staining, flow cytometry, and gene profiling by transcriptomics.
In addition, global, tamoxifen-inducible genetic ablation of CD40 as well as cell type-specific persistent CD40 or CD40L deficiency on B-cells, myeloid cells or T cells was used to further examine the role of CD40/CD40L signalling in AAA formation and progression. AAAs were induced using the PPE or AngII model and aortic expansion and rupture was investigated by ultrasound imaging.

Results: Inhibition of CD40-TRAF6 signalling resulted in a significant reduced aortic dilation and collagen type IV degradation, probably due to decreased *Mmp2* mRNA expression in aneurysmal tissue after PPE-induced AAA formation. Furthermore, TRAF-STOP administration led to a significant decrease in the myeloid cell proportion as well as a significant decrease in *Tnfa* mRNA expression in aneurysmal tissue. Plasma concentration of pro-inflammatory cytokines, IL-12 and IL-17, were also reduced after PPE-induced AAA formation.
Moreover, CD40-TRAF6 signalling inhibition slightly protected against AAA rupture in *Apoe*$^{-/-}$ mice on standard chow and western diet reflected by increased survival rates after TRAF-STOP administration 28 days after AngII-induced AAA formation. TRAF-STOP-treated *Apoe*$^{-/-}$ mice on western diet also exhibited a reduced aortic diameter 28 days after AngII-induced AAA formation.

Furthermore, tamoxifen-inducible, global CD40 deficiency prevented AAA rupture, whereas aortic expansion was similar compared to their CD40-expressing littermates 28 days after AngII-induced AAA formation. However, B cell- and myeloid cell-specific CD40 deficiency did not affect AAA formation and progression 28 days after AngII-induced AAA formation. Persistent CD40L ablation on T cells showed similar mortality rates as well as similar abdominal aortic expansion compared to their CD40L-expressing littermates 28 days after PPE- and AngII-induced AAA formation.

Conclusion: The results of this study suggest that pharmacological inhibition of CD40-TRAF6 signalling limits AAA growth by partially attenuating structural protein degradation and partially reducing inflammation following PPE-induced AAA formation. In the AngII model, pharmacological CD40-TRAF6 blockage as well as tamoxifen-inducible, global CD40 deficiency seem to slightly prevent AAA rupture, whereas AAA dilation is not affected. Furthermore, this work provides evidence that CD40 on B cells and myeloid cells and that CD40L on T cells do not substantially contribute to AAA formation and progression in the AngII- as well as in the PPE-induced experimental AAA model, as demonstrated by cell type-specific CD40/CD40L genetic ablation.

Zusammenfassung

Hintergrund: Zwei der wichtigsten pathologischen Ursachen für die Entstehung eines Bauchaortenaneurysmas (AAA), eine lebensbedrohliche und komplexe Erkrankung, sind die andauernde Degeneration der Aortenwand und beträchtliche Entzündungsprozesse. Die Aktivierung von Membran-abbauenden Enzymen und die Freisetzung von entzündungsfördernden Zytokinen, welche beide den Abbau wichtiger Strukturproteine der Aortenwand begünstigen, sind entscheidende Abläufe an denen Entzündungsprozesse beteiligt sind. Solche Entzündungsreaktionen werden unter anderem durch die gegenseitige Bindung ko-stimulatorischer Moleküle, wie CD40 und CD40L, reguliert. Unter physiologischen Bedingungen soll diese Regulierung eine schädliche, fehlregulierte und langanhaltende Aktivierung von Immunzellen verhindern. Als Oberflächenproteine sind CD40 und CD40L auf hämatopoetischen Zellen wie Monozyten, Makrophagen, B-Zellen, T-Zellen und Thrombozyten, aber auch auf nicht-hämatopoetischen Zellen wie Fibroblasten, Endothelzellen und glatten Muskelzellen weit verbreitet. Die zugrundeliegenden Mechanismen dieser entzündlichen Prozesse, die zur Entstehung und zum Fortschreiten eines AAA beitragen, sind jedoch noch nicht vollständig geklärt.

Hypothese & Ziel: In dieser Arbeit wurde die Hypothese aufgestellt, dass im Rahmen der AAA-Pathologie die Aktivierung des CD40/CD40L-Signalwegs zu einer umfassenden Stimulierung von Immunzellen führt. Diese wiederum führt zur Freisetzung von Membran-abbauenden Enzymen und entzündungsfördernden Zytokinen, die die Entwicklung eines AAA weiter begünstigen. Daher wurde in dieser Studie die Inhibierung der CD40/CD40L-Achse als potenzielles therapeutisches Ziel zur Behandlung eines AAA in verschiedenen experimentellen Modellen untersucht.

Methoden: Um die Rolle des CD40/CD40L-Signalwegs in der AAA-Erkrankung zu entschlüsseln, wurden zwei unterschiedliche Mausmodelle verwendet. Entweder wurde der infrarenale Teil der Aorta von Mäuse mit C57BL/6J-Hintergrund vorübergehende mit Schweine-Pankreaselastase (PPE) perfundiert oder Mäusen mit einer Apolipoprotein E (*Apoe*$^{-/-}$) Defizienz wurde kontinuierlich eine subkutane Infusion mit Angiotensin (Ang) II verabreicht. C57BL/6J und *Apoe*$^{-/-}$ Mäuse erhielten Standardfutter oder eine Western Diät und wurden 28 Tage lang mit einem niedermolekularen Hemmstoff, der die Bindung zwischen CD40 und dem Tumornekrosefaktor rezeptor-assoziierten Faktor 6 (TRAF6) verhindert, weiterführend bezeichnet als TRAF-STOP, oder der Lösungsmittelkontrolle behandelt. Die Erweiterung der Aorta und das eventuelle Auftreten von Aneurysma-Rupturen, sowie die Degeneration von Strukturproteinen, die Expression und Aktivierung Membran-abbauender Enzyme, die Einwanderung von Immunzellen und das Vorkommen von entzündungsfördernden Zytokinen im AAA-Gewebe wurde mittels Ultraschalluntersuchungen, histologischer Färbungen, Durchflusszytometrie und Genexpressions-Analysen untersucht.
Darüber hinaus wurde eine Tamoxifen-induzierbare, globale genetische CD40-Defizienz sowie permanente zelltypspezifische CD40- oder CD40L-Defizienzen auf B-Zellen, myeloischen Zellen oder T-Zellen verwendet, um die Rolle des CD40/CD40L-Signalwegs bei einer AAA-Erkrankung weiter zu untersuchen. Hierbei wurden AAAs bei den Mäusen durch das oben beschriebene PPE-Model oder das AngII-Model ausgelöst. Ausdehnung oder Ruptur der Aorta wurde mittels Ultraschall untersucht.

Ergebnisse: Die Hemmung des CD40-TRAF6-Signalwegs führte zu einer signifikanten Verringerung des Aortendurchmessers und des Abbaus von Kollagen Typ IV, was vermutlich auf eine verringerte Expression der *Mmp2* mRNA im Aneurysmengewebe nach PPE-induzierter AAA-Bildung zurückzuführen ist. Darüber hinaus führte die Behandlung mit

TRAF-STOP zu einem signifikant reduzierten Anteil an myeloischen Zellen sowie zu einer signifikanten Verringerung der *Tnfa* mRNA Expression im Aneurysmengewebe. Zusätzlich konnte gezeigt werden, dass die Konzentration der entzündungsfördernden Zytokine, IL-12 und IL-17, im Plasma nach PPE-induzierter AAA-Bildung verringert war.
Bei *Apoe*$^{-/-}$ Mäusen, die Standardfutter oder eine Western Diät erhielten, zeigte die Hemmung des CD40-TRAF6-Signalweges eine nennenswerte protektive Wirkung vor AAA-Ruptur 28 Tage nach AngII-induzierter AAA-Bildung. Dies wurde deutlich durch die gesteigerten Überlebensraten der mit TRAF-STOP-behandelten Tiere. Zusätzlich zeigten *Apoe*$^{-/-}$ Mäuse mit einer Western Diät nach TRAF-STOP Gabe eine Verringerung des Aortenduchmessers 28 Tage nach AngII-induzierter AAA-Bildung.
Die Tamoxifen-induzierbare, globale genetische CD40-Defizienz verhinderte ebenfalls eine AAA Ruptur, reduzierte jedoch nicht die Ausdehnung der Aorta 28 Tage nach AngII-induzierter AAA-Bildung. Die permanente zelltypspezifische CD40-Defizienz auf B-Zellen und myeloischen Zellen hatte allerdings keinen Einfluss auf die Bildung und das Fortschreiten eines AAA 28 Tage nach AngII-induzierter AAA-Bildung. Auch die permanente CD40L-Defizienz auf T-Zellen zeigte 28 Tage nach PPE- und AngII-induzierter AAA-Bildung eine vergleichbare Sterblichkeit und eine ähnliche Aortenausdehnung verglichen mit ihren CD40L-exprimierenden Wurfgeschwistern.

Schlussfolgerung: Die Ergebnisse dieser Studie deuten darauf hin, dass eine pharmakologische Hemmung des CD40-TRAF6 Signalwegs die Ausdehnung des Bauchaneurysmas begrenzt, indem der Abbau von Strukturproteinen und die Entzündung im AAA-Gewebe nach PPE-induzierter AAA-Bildung teilweise vermindert wird. Die pharmakologische CD40-TRAF6 Hemmung und die Tamoxifen-induzierbare, globale genetische CD40-Defizienz nach AngII-induzierter AAA-Bildung scheinen die AAA-Ruptur, aber nicht die Ausdehnung der Aorta, ein wenig zu verhindern. Zudem liefert diese Studie Hinweise darauf, dass sowohl die permanente zelltypspezifische CD40-Defizienz auf B-Zellen und myeloischen Zellen, als auch die CD40L-Defizienz auf T-Zellen nicht wesentlich zur Bildung und Fortschreiten eines AAAs im AngII- sowie im PPE-induziertem experimentellem AAA-Modell beitragen.

Table of contents

List of figures

List of tables

List of abbreviations

AAA	*Abdominal aortic aneurysm*
AngII	*Angiotensin II*
ANOVA	*Analysis of variance*
APC	*Antigen-presenting cell*
Apoe	*Apolipoprotein E*
$CaCl_2$	*Calcium chloride*
CCL2	*Chemokine (C-C motif) ligand 2*
CD	*Cluster of differentiation*
CITE	*Cellular Indexing of Transcriptomes and Epitopes*
CVD	*Cardiovascular disease*
DAPI	*4', 6-Diamidino-2-phenylindole-dihydrochloride*
DC	*Dendritic cell*
DMSO	*Dimethyl sulfoxide*
DPBS	*Dulbecco's phosphate buffered saline*
EC	*Endothelial cell*
ECM	*Extracellular matrix*
EDTA	*Ethylenediaminetetraacetic*
ER	Estrogen receptor
EVAR	*Endovascular aneurysm repair*
EvG	*Elastica van Gieson*
FSC	*Forward scatter*
GM-CSF	*Granulocyte-macrophage colony-stimulating factor*
i.p.	*Intraperitoneal*
IFN	*Interferon*
Ig	*Immunoglobulin*
IL	*Interleukin*
ITI	inner to inner
JAK3	*Janus family kinase 3*
LTL	*Leading to leading*
Ly6C	*Lymphocyte antigen 6C*
MAPK	*Mitogen-activated protein kinase*
MFI	*Median fluorescent intensity*
MHC	*Major histocompatibility complex*
MI	*Myocardial infarction*
MMP	*Matrix metalloproteinase*
NaCl	*Sodium chloride*
NET	*Neutrophil extracellular trap*
NFκB	*Nuclear factor κB*
NK	*Natural killer*
OSR	*Open surgical repair*
OTO	outer to outer
PI-3K	*Phosphoinositide 3-kinase*
PMSF	*Phenylmethylsulfonyl fluoride*
PPE	*Porcine pancreatic elastase*
qPCR	*Quantitative polymerase chain reaction*
RT	*Room temperature*
s.c.	*Subcutaneous*
sCD40L	*Soluble CD40 Ligand*
SD	*Standard deviation*

SDS	*Sodium dodecyl sulphates*
SMC	*Smooth muscle cell*
SSC	*Side scatter*
STAT	*Signal transducer and activator of transcription*
TAA	*Thoracic aortic aneurysm*
TAM	*Tamoxifen*
TCR	*T cell receptor*
Th cells	*T helper cells*
TIMP	*Tissue inhibitors of matrix metalloproteinase*
TLR	*Toll-like receptors*
TNF	*Tumor necrosis factor*
TRAF	*TNF receptor-associated factor*
Treg cells	*Regulatory T cells*
WD	*Western diet*

Introduction

Clinical presentation and epidemiology of abdominal aortic aneurysm

Abdominal aortic aneurysm (AAA) is a progressive and life-threatening cardiovascular disease (CVD) that causes 150,000 to 200,000 deaths worldwide each year.[1, 2] Noteworthy, in 2019, the global prevalence of AAA in men over 60 years of age was approximately four times higher (2.45%) than in women of the same age (0.59%), whereby AAA incidence increases with age in both genders.[3]

Increased risk of AAA is mainly associated with male sex, smoking and age.[4, 5] Previous myocardial infarction (MI), coronary artery disease, peripheral vascular disease, hypertension, obesity, hypercholesterolemia and family history of aneurysms are also considered risk factors. However, no association was found between diabetes mellitus and AAA formation.[4]

An AAA is defined as a persistent dilation of the abdominal aorta exceeding the normal vessel diameter by 50%.[6] In clinical practice, an aortic diameter of 3 cm is considered as threshold for an AAA. AAAs are localized between the diaphragm and the aortic bifurcation[4] and more than 80% of AAA develop infrarenal.[7, 8] Aneurysms can also form above the renal arteries (suprarenal), around the renal arteries (pararenal) or reaching the renal arteries (juxtarenal).[6] In true aneurysm formation, all three layers of the aortic wall, the intima, the media and the adventitia are involved in the expansion.[7] Most AAAs dilate evenly in all directions (fusiform). If only some part of the circumference is involved, AAAs form saccular (Figure 1). By contrast, a dissection of the media, followed by an infiltration of blood, can also result in an enlargement of the aorta, forming a false aneurysm or pseudoaneurysm.

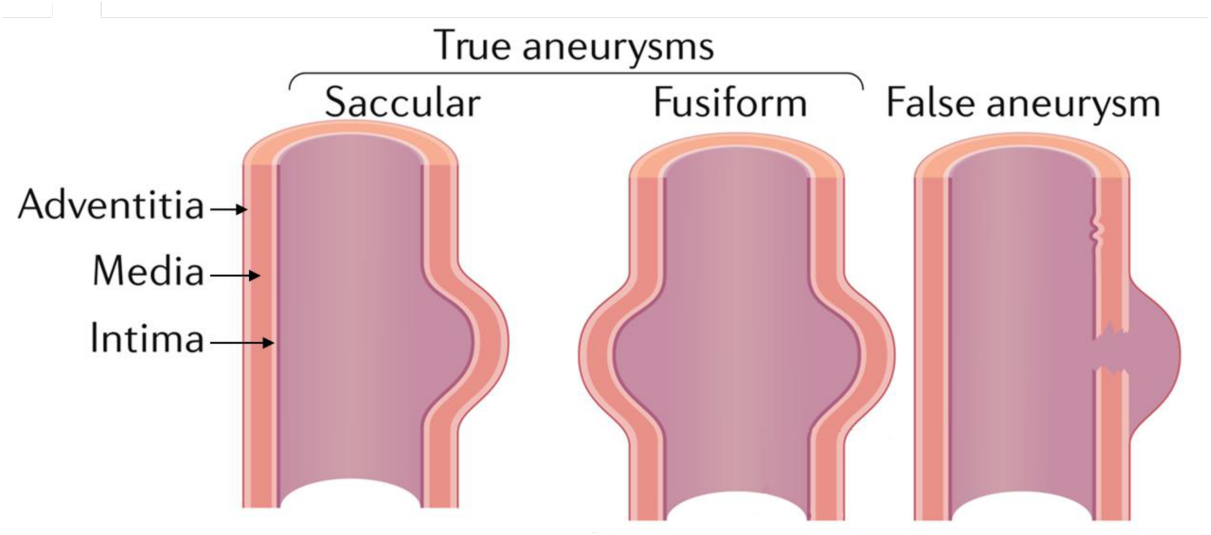

Figure 1: Outline of AAA types
The vascular wall consists of three layers; the intima, the media and the adventitia. True aneurysms involves the dilation of all three layers and form saccular or fusiform aortic expansions. False aneurysms develop due to arterial injury resulting in the dilation of the outer dimension of the aorta. Adapted from Sakalihasan et al..[7]

The intima is the innermost layer of the aorta, and comprises a single layer of endothelial cells (ECs), a basal membrane, and a subendothelial layer consisting of collagen and vascular smooth muscle cells (SMCs).[9, 10] The middle layer of the aorta, the media, consists of a network of SMCs, elastin and collagen fibrils forming a continuous, circumferential

orientated helix.[9] The adventitia is the outermost layer of arteries and mostly comprises fibroblasts and thick bundles of collagen fibres.[9]

AAA development is usually asymptomatic until abrupt aortic rupture, which is mostly fatal in 85 to 90% of cases.[11] Therefore, it is reasonable to screen patients at high risk of AAA using non-invasive ultrasound imaging to prevent possible rupture events. Ultrasonography was shown to be highly effective and sensitive, and it decreases lethal outcomes.[12, 13] Treatment of detected small aneurysms (4.0 - 5.4 cm) includes continued regular monitoring of AAA growth and, if necessary, cessation of smoking, as former and current smoking increases the risk of AAA by two to five times.[14] In addition, reducing cardiovascular risk factors by an antiplatelet therapy, lipid-lowering drugs and antihypertensive agents was shown to improve the survival of AAA patients.[15, 16] However, to date, there is no medical therapy that effectively limits AAA progression based on clinical trials.[16, 17] An aortic expansion of more than 5.5 cm in diameter in men and 5.0 cm in women is regarded as recommendation for elective surgery, as rupture risk increases with AAA size.[6] Open surgical repair (OSR) or endovascular aneurysm repair (EVAR) separates the AAA from blood circulation, thereby preventing further growth and rupture. A surgical intervention is only suitable for patients with less comorbidities and high life expectancy. Surgical risks are high, OSR carriers a 5% or greater risk for cardiovascular death or MI within 30 days after surgery and EVAR carries a cardiac risk of 1-5%.[16] EVAR is a less invasive approach and can be performed under local anaesthesia. Patients' full recovery takes only days to weeks, whereas patients after OSR fully recover within weeks to month.[6] The use of EVAR is staidly raising, but the aortic anatomy and the location of the AAA needs to be appropriate for EVAR. Both interventions have their benefits and disadvantages, but long-term mortality within 8-10 years were observed to be similar. To circumvent the risks of surgical interventions, medical treatment for AAA is necessary.

Pathophysiology of AAA

Main pathological hallmarks of AAA include vascular SMC apoptosis, oxidative stress, extracellular matrix (ECM) remodelling and proteolytic degradation, as well as immune cell-promoted inflammatory processes.[6]

ECM degradation

The ECM is a network consisting of several glycoproteins, proteoglycans, matrix proteins and their degradative matrix metalloproteinases (MMPs).[18, 19] It provides structure and mechanical properties of the vessel and is mainly organized and synthesised by vascular SMCs. One of the main matrix proteins is elastin. It is secreted as tropoelastin monomers and assembles into cross-linked elastic fibres, which contribute to the flexibility of the vessel.[20] The tensile characteristic of elastin mainly facilitates the distribution of stresses and loads evenly throughout the vascular wall.[19] Campa et al. showed a significantly decreased elastin amount in aneurysmal tissue of patients compared to healthy aorta.[21] In addition, elastase perfusion of an infrarenal aortic segment is used to cause aneurysm formation in rats and mice.[22, 23]

Different isoforms of collagens are also one of the most abundant components of the ECM, especially in the adventitia. McLean et al. identified 17 different types of collagens in the developing mouse aorta, whereby collagen types I, III, IV, V and VI were mostly expressed.[24] Collagen type I, III, and V assemble into large, organized fibrils and these collagens are the most abundant in the aortic vessel wall.[25] The high adventitial collagen

amount gives the aorta its stability and strength, hence, preventing aortic rupture.[9, 19] In aneurysmal disease collagen type I degradation was found to be increased in AAA patients.[26] Furthermore, genetic mutations of the collagen type III gene was associated with enhanced risk for aneurysm formation.[27] In contrast, collagen type IV is one of the main component of aortic basement membranes, which additionally provide adhesive substrates to encapsulate vascular SMCs.[28] Steffensen et al. showed that the collagen type IV amount in the aorta plays a crucial role in AAA disease, as a reduction resulted in augmented AAA formation.[29]

ECM proteins, such as elastin and collagens are proteolytically degraded by MMPs. Under physiological conditions MMPs contribute among others to angiogenesis, wound healing, embryonic development, morphogenesis and reproduction.[30] However, a dysregulation of MMP activity can result in pathological conditions such as aneurysm formation, arthritis, cancer, atherosclerosis and fibrosis.[31] The 26 human calcium-dependent zinc-containing endopeptidases known so far are originally classified into groups based on their substrate: collagenases, gelatinases, stromolysins, and matrilysins.[32] Activation of MMPs is dependent on the removal of a pro-domain, as each MMP is synthesised as inactive zymogen.[33] The pro-domain can either be cleaved by another endopeptidase, or allosteric re-conformation can occur or chemical modification leads to autoproteolysis. In addition, the activity of MMPs is regulated by the presence of tissue inhibitors of matrix metalloproteinases (TIMPs).[33] To date four members of TIMPs exists. TIMP-2, TIMP-3, and TIMP-4 are able to inhibit mostly all MMP members, whereas the MMP specificity of TIMP-1 differs. An imbalance of MMP and TIMP expression and activity in aortic tissue may lead to excessive ECM degradation and consequent dilation and thinning of the aortic wall, and thus, AAA formation and rupture.
Studies on human aneurysmal tissue revealed increased expression levels of MMP1, 2, 3, 9, 13 and 14.[20, 34] Of note, both gelatinases (MMP2 and MMP9) were described to mostly contribute to AAA development and progression, and MMP2- and MMP9-deficient mice were protected against calcium chloride ($CaCl_2$)-induced AAA formation.[35, 36] In addition, MMP9 plasma levels of AAA patients were associated with aneurysm size and dilation, and Wilson et al. described the increased MMP9 plasma levels as a potential biomarker for mortality of patients with AAA.[37, 38] MMP2 and MMP9 proteolytically degrade gelatin, elastin and fibronectin.[20] MMP2 was also found to cleave triple helical collagens, such as collagen type I and type III, whereas MMP9 has collagen types IV, V, VII, X and XIV as substrates. Gelatinases are expressed in various cell types, including ECs, vascular SMCs, fibroblasts, but also in immune cells like macrophages and neutrophils.[36, 39] Considering that, MMP-induced ECM degradation is a critical step in the development and progression of AAA, and that various cells are the source of MMPs, it is important to further understand the role of different cells in AAA disease.

Innate immune cells in the pathology of AAA

Recruitment and infiltration of different immune cells are critical steps in AAA formation and manifestation. During the course of AAA progression, distribution and activation status of immune cells in the aortic wall varies continuously.[40] First, cells of the innate immune system, including myeloid cells such as neutrophils, monocytes, macrophages, and dendritic cells (DCs), as well as lymphoid natural killer (NK) cells are recruited into the aortic wall.

Neutrophils belong to the class of polymorphonuclear leukocytes and are the most abundant type of granulocytes in the healthy human blood circulation.[41] They play a crucial role as patrolling effector cells as they can combat pathogens through phagocytosis,

degranulation or by release of neutrophil extracellular traps (NETs). In the context of AAA, neutrophils were found to accumulate mainly in the mural thrombus, and to store and release MMP9 in the thrombus.[42] Neutrophil-derived products such as neutrophil elastase or myeloperoxidase, which are released after activation, were found to be increased in plasma and aneurysmal tissue of AAA patients compared to healthy controls.[43] In addition, inhibition or deficiency of neutrophil elastase was shown to reduce experimental AAA formation. Eliason et al. showed that global neutrophil depletion protects against PPE-induced AAA formation in rats accompanied with reduced immune cell infiltration into the aneurysmal tissue.[44]

Monocytes derive from the bone marrow, patrol the blood circulation, and migrate into a tissue, where they differentiate into different types of macrophages.[45] In humans, monocytes are distinguished in three subtypes based on the expression of cluster of differentiation (CD) 14 and CD16 on their surface.[46] Classical monocytes ($CD14^{++}$ $CD16^{-}$) account for 90% of all monocytes in human blood, nonclassical monocytes ($CD14^{+}$ $CD16^{++}$) are the second most common subtype, whereas intermediate monocytes ($CD14^{++}$ $CD16^{+}$) are only present at low frequency. In mice, the surface marker CD11b identifies monocytes. Similar to humans, three subtypes of monocytes were found in mice that resemble human monocyte subsets in terms of chemokine receptor expression and function.[47] These $CD11b^{+}$ monocytes are subdivided based on the expression of lymphocyte antigen 6C (Ly6C) on their surface. $Ly6C^{high}$ monocytes are homologous to human classical monocytes, $Ly6C^{int}$ monocytes to human intermediate and $Ly6C^{low}$ monocytes to human nonclassical monocytes. In AAA patients, numbers of intermediate and nonclassical monocytes were increased, concomitant with a reduction in classical monocyte number.[48] An increase in classical and nonclassical circulatory monocytes was observed in experimental murine AAA models.[49, 50] This enhanced mobilization triggers recruitment of monocytes to the aneurysmal wall, and thus, promotes AAA progression.

Macrophages originate from three temporal successive sources, the yolk sac, the foetal liver and the bone marrow.[51] From there, macrophages develop common functions, such as phagocytosis and immune surveillance. They acquire F4/80, CD64 and proto-oncogene tyrosine-protein kinase MER as cell surface markers, and populate every tissue.[52] After migrating into a tissue, macrophages become resident and get their tissue-specific phenotype and function from the prevailing microenvironmental milieu, e.g. vascular macrophages maintain arterial homeostasis and mediate hypertension.[52] Due to this wide heterogeneity, macrophages have important functions in tissue homeostasis, development, repair, remodelling, and innate and adaptive immune response to pathogens. However, dysregulation of macrophage activity can contribute to diseases, such as cancer, fibrosis, Alzheimer's disease, and cardiovascular diseases.[53] Rateri et al. have shown a rapid accumulation of macrophages in a prolonged AngII-induced AAA formation model.[54] Of note, these macrophages were mostly present in the areas of medial disruption. In AAA patients, macrophages were found to be the most present inflammatory cell type in the media and adventitia of aneurysmal tissue.[55] This was accompanied by the finding, that macrophages promote AAA progression in humans and mice by releasing mediators such as cytokines, chemokines, nitric oxide, as well as MMPs such as MMP3, MMP9 and MMP12.[47, 56]

DCs play a crucial role in maintaining the immunological homeostasis.[57] On the one hand, mature DCs activate the adaptive immune system by presenting antigens to T cells and B cells, and on the other hand, immature DCs modulate immune tolerance. Krishna et al. has shown that systemic $CD11c^{+}$ dendritic cell depletion protects from AAA formation and growth, which was accompanied by a reduction in circulatory T and B cell numbers.[58]

Additionally, plasmacytoid DC recruitment and activation in aneurysmal tissue has been shown to be induced by neutrophilic NET release.[59]

NK cells belong to the family of innate lymphoid cells and 5-20% can be found in the blood circulation of humans.[60] Beside their cytotoxic functions, NK cells can differentiate into tolerant and regulatory NK cells depending on the present microenvironment.[61] Upon stimulation, human NK cells are known to be a source of high levels of interferon (IFN)-γ, and by releasing certain chemokines they actively recruit naïve and activated T cells.[60] In AAA pathogenesis NK cell numbers were shown to be increased in blood circulation as well as in aneurysmal tissue of patients.[40] Furthermore, studies from Hinterseher et al. showed evidence of an increase in NK cell-mediated cytotoxicity in human AAA tissue.[62]

Adaptive immune cells in the pathology of AAA

In addition to the contribution of innate immune cells to AAA, increased numbers of B and T cells have also been found in aneurysmal tissue of patients.[63]

B cells play important roles in immune responses by antibody and cytokine production as well as antigen presentation. To effectively fight against microbial infections, two major B cell lineages, B1 and B2, have developed.[64] B1 cells patrol the body, gather antigens and provide direct defence. In spleen and bone marrow, B1 cells produce large amounts of immunoglobulin (Ig) M antibodies. B2 cells originate from the bone marrow and differentiate into plasma cells, which cope with invading pathogens by massive production and release of IgG, IgA and IgE antibodies.[64] In the context of AAA, the role of B cells is controversial. On the one hand, B cell depletion with an anti-CD20 antibody in two different experimental models of AAA resulted in reduced AAA formation.[65] Mice deficient for membrane-bound IgM ($muMt^-$) showed reduced AAA development in a $CaCl_2$-induced experimental model of AAA.[66] In contrast, Meher et al. could not detect differences in AAA growth in $muMt^-$ mice when inducing AAA with elastase and adoptive transfer of B2 cells into muMT mice suppressed AAA development.[67]

T cells are composed of $CD4^+$ T helper cells (Th cells) and $CD8^+$ cytotoxic T cells.[68] Th cells recognize antigens presented by major histocompatibility complex (MHC) class II, and cytotoxic T cells spot antigens by MHC class I. Th cells can be further distinguished in Th1, Th2, Th17, Th22 and regulatory T cells (Treg cells), most of which have been found in human aneurysmal tissue.[40] Th17 cells are a well-known source of interleukin (IL)-17, which was shown to play an important role in AAA formation. Genetic IL-17 deficiency as well as inhibiting Th17 cell differentiation by digoxin resulted in reduced AAA development in different experimental murine models.[69, 70] In addition, Treg cells regulate and supress excessive immune responses and thus maintaining a balance in immunologic tolerance.[71] Dysregulation of Treg cell functions lead to autoimmune and inflammatory diseases. In the context of AAA, Yodoi et al. showed a protective role of Treg cell expansion on AAA formation and rupture as well as aggravated AAA development and mortality rate in Treg cell-deficient mice.[72]
Cytotoxic T cells play a crucial role in cell-mediated toxicity. Less is known about their contribution in AAA pathology. However, one study showed a detrimental role of cytotoxic T cells, as $CD8^+$ cytotoxic T cell deficiency resulted in reduced elastase-induced AAA formation.[73]

Cytokines and chemokines in the pathology of AAA

Hallmarks of AAA formation and development such as recruitment of immune cells into the vessel wall and further cell activation, apoptosis of vascular SMCs as well as release of proteases and associated ECM degradation are key events mediated by cytokines and chemokines.[74] Namely among others IL-1α, IL-1β, IL-6, IL-10, tumour necrosis factor (TNF) α and chemokine (C-C motif) ligand 2 (CCL2) were shown to be upregulated in human aneurysmal tissue compared to control samples.[75, 76]
IL-1β, IL-6 and TNFα plasma levels were shown to be highly increased in AAA patients compared to healthy controls.[77] These crucial pro-inflammatory cytokines induce the acute immune response and contribute to AAA development.[78-80] It has been shown that genetic depletion of IL-1β and TNFα as well as IL-6 inhibition resulted in reduced AAA expansion in experimental murine AAA models.[78-80]
Although IL-1β and IL-1α bind to the same receptor, referred to as IL-1R, their role in AAA pathology seems to be distinct. Salmon et al. have shown that IL-1α-deficient mice develop larger AAA after perivascular application of elastase.[79]
CCL2, also known as monocyte chemoattractant protein-1, is expressed and released by many different cell types to attract myeloid and lymphoid cells from the blood circulation via the endothelium to the site of inflammation.[81] Therefore, CCL2 might contribute to AAA pathology by promoting immune cell recruitment to the aneurysmal tissue. Moehle et al. has shown that genetic depletion of CCL2 protects against elastase-induced AAA formation in mice.[82]
In contrast, IL-10 was shown to alleviate inflammatory diseases and attenuate the release of pro-inflammatory cytokines.[74] In AAA disease, IL-10 decreases inflammatory responses, and upregulation of IL-10 resulted in reduced aneurysm dilation and incidence.[83]

The co-stimulatory dyad: CD40 and CD40L

Dysregulated and prolonged activation of immune cells can cause various diseases. To prevent this, the adaptive immune response upon stimulation is regulated by several coincident signals.[84] The recognition of an antigen presented by the MHC on the surface of an antigen-presenting cell (APC) by the T cell receptor (TCR) is the first signal. However, T cell activation is dependent on a second signal, which is the binding of a cell-surface co-signalling receptor to its ligand on both interacting cells.[84] The release of cytokines, which in turn enhance the signal, accompanies this process (Figure 2).[85] These co-signalling molecules can either modulate cell responses positively (co-stimulatory molecules) or negatively (co-inhibitory molecules).[84] Therefore, the second signal facilitates or restricts T cell activation and function. This whole process allows T cell priming and APC activation. One co-stimulatory dyad, consisting of CD40 and its ligand CD40L, is known to modulate multiple immune functions, and inhibition of this interaction was shown to be crucial for the development of an adaptive immune response.[86]

CD40 is a 48 kDa transmembrane receptor, which belongs to the TNF receptor family.[86] It was initially identified on the cell surface of B cells, but it is also expressed on DCs, monocytes, macrophages as well as on non-hematopoietic cells as fibroblasts, epithelial cells and ECs.[85] The DNA sequence of murine and human CD40 shares 62% homology.[87] CD40 binds to its ligand, CD40L, also known as CD154, a trimeric, type II transmembrane protein of the TNF receptor family. It is mainly expressed on activated T cells and platelets, but CD40L was shown to be also expressed on activated B cells as well as on monocytes, NK cells, ECs and SMCs under inflammatory conditions.[85, 86] CD40L can be cleaved from the cell surface resulting in smaller but biologically active soluble CD40L (sCD40L).[88] Its

DNA sequence is located on the X chromosome and shares a high sequence similarity between humans and mice (80%).[87]

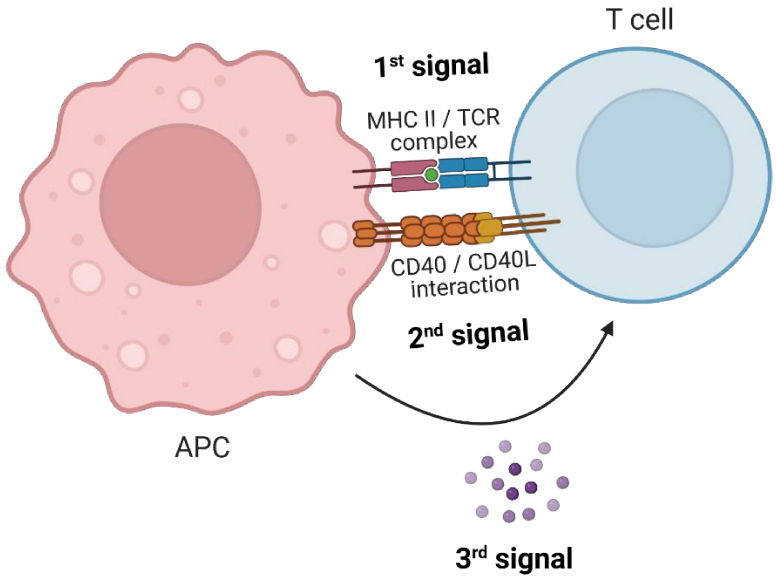

Figure 2: Initiation of an adaptive immune response
An adaptive immune response is initiated by three coincident signals. 1st, T cells recognize antigens presented by MHC on APCs with their TCR, forming a signalling complex. 2nd, co-signalling molecules such as CD40 and CD40L interact with each other. Released cytokines enhance the response, as a 3rd signal. APC = Antigen-presenting cell, MHC = Major histocompatibility complex, TCR = T cell receptor. Illustration based on Kambayashi et al.[89] and created with BioRender.com.

The CD40/CD40L signalling cascade

Binding of CD40L to its receptor CD40 promotes the recruitment of TNF receptor-associated factors (TRAFs) to the cytoplasmic domain of CD40 and initiates downstream signalling. To date, seven members of the TRAF family are known, whereby TRAF1, TRAF2, TRAF3, TRAF5, and TRAF6 directly bind to CD40.[90] TRAF1, TRAF2, and TRAF3 were shown to bind to the same part of the cytoplasmic domain, whereas TRAF6 interacts with a nonoverlapping proximal region.[91] As the binding affinity of TRAF proteins to CD40 vary depending on the cell type and predominant TRAF protein concentrations, activation of different signalling cascades can be induced.[91] After binding to CD40, TRAF proteins interact with several other downstream molecules and can activate the canonical or non-canonical nuclear factor κB (NFκB), the mitogen-activated protein kinase (MAPKs), or the phosphoinositide 3-kinase (PI-3K) signalling pathway (Figure 3).[92] Furthermore, it has been shown that CD40 signalling in DCs can also occur independent of TRAF proteins.[85] In this process, Janus family kinase 3 (JAK3) directly binds to the cytoplasmic domain of CD40 and further activates the signal transducer and activator of transcription (STAT) signalling pathway.[85] Important signalling events mediated by activation of these pathways include among others germinal centre formation, development of memory B cells, immunoglobulin gene switching, increased cytokine production and inhibited cell apoptosis.[90] In addition to that, TRAF proteins can also interact with other TNF receptors like CD30, CD134, Toll-like receptors (TLRs), or IL-1 receptors.[92]
The CD40/CD40L signalling cascade also promotes the functions of cytotoxic T cells by a feedback mechanism. Interaction of CD40 on DCs with CD40L regulates the expression of another co-stimulatory molecule, CD28, which in turn stimulates cytotoxic T cell activation.[93]

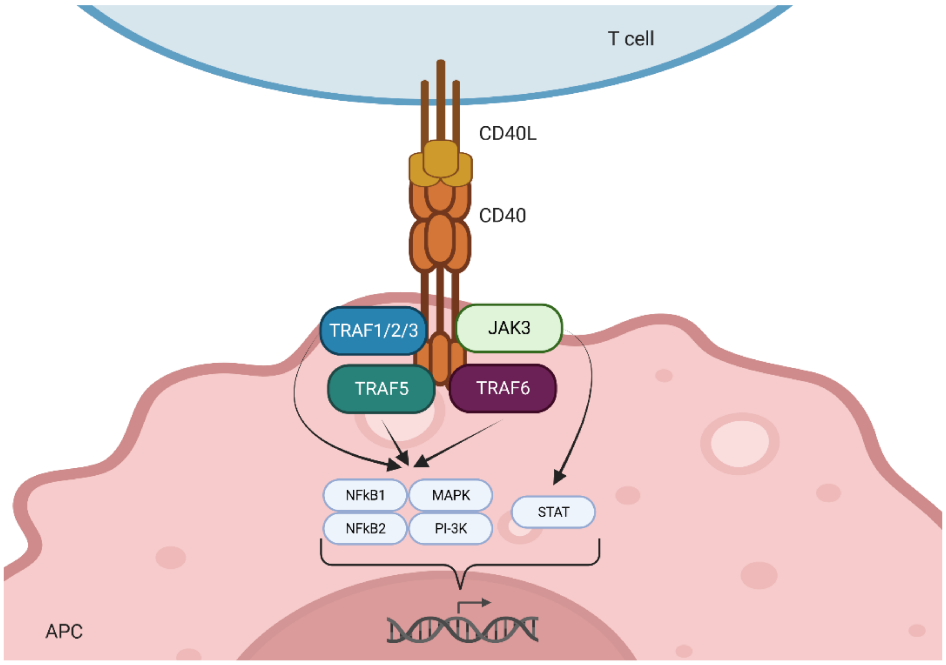

Figure 3: CD40 signalling pathway in APCs
After interaction of CD40L with CD40, various TRAF proteins or JAK3 can be recruited to the cytoplasmic domain of CD40. Thereby TRAF1, 2 and 3 can bind to the same part of the cytoplasmic domain of CD40, whereas TRAF5, TRAF6 and JAK3 interact with other receptor regions. Depending on the stimulus, TRAF proteins interact with different downstream kinases and thus can activate the NFκB1, NFκB2, MAPK or PI-3K signalling pathway. In addition, JAK3 can activate the STAT signalling pathway after binding to CD40. All of these pathways promote gene transcription in the cell nucleus. APC = Antigen-presenting cell, JAK3 = Janus family kinase 3, MAPK = Mitogen-activated protein kinase, NFκB1 = Canonical nuclear factor κB, NFκB2 = Non-canonical nuclear factor κB, PI-3K = Phosphoinositide 3-kinase, STAT = Signal transducer and activator of transcription, TRAF = TNF receptor-associated factors. Illustration based on Lai et al.[90] and created with BioRender.com.

The role of CD40/CD40L signalling in CVD

Initially, interaction of CD40 on B cells with CD40L on Th cells was found to be crucial for T cell-dependent B cell differentiation and activation as well as for the formation of memory B cells and germinal centres.[87] Blockage of this interaction causes an inhibition of the humoral immune response induced by T cells known as X-linked hyper-IgM syndrome.[94] In addition, to the contribution of CD40/CD40L signalling to diverse inflammatory and autoimmune diseases such as in inflammatory bowel disease, type 1 diabetes, rheumatoid arthritis and allograft rejection, this pathway plays a crucial role in CVD.[95]

CD40/CD40L signalling was found to facilitate the formation of atherosclerotic plaques by enhancing immune cell infiltration and by promoting the development of foam cells and the release of inflammatory cytokines.[95] This enhanced immune cell recruitment was shown to be triggered by an CD40L-induced increase in adhesion molecules on ECs as well as enhanced adhesion of monocytes to these cells.[96] CD40/CD40L signalling appears to contribute to the initiation of acute coronary events i.e. MI and sudden cardiac death as well as stroke, triggered by plaque rupture and thrombosis. Rupture is promoted by CD40L-induced macrophage activation, which was shown to enhance MMP expression and activation.[97] Furthermore, serum levels of sCD40L were found to be increased in MI or heart failure patients. In the context of MI, elevated sCD40L levels correlate with increased mortality.[95]

Targeting CD40/CD40L signalling with a global CD40L blockage in an experimental arterial hypertension model resulted in antithrombotic events and increased endothelial function. However, this was accompanied by extended bleeding and reduced leukocyte-platelet-aggregates.[95, 98]
In early and late disease stages of an atherosclerotic mouse model, studies by Mach et al. as well as Schönbeck et al. have shown reduced plaque formation, enhanced plaque stability as well as decreased macrophage and T cell infiltration into the atheroma following anti-CD40L treatment.[99, 100] However, it has been shown that sCD40L is crucial for thrombus formation and administration of anti-CD40L antibody into non-human primates and patients suffering from proliferative lupus nephritis caused thromboembolic events.[101] Therefore, novel approaches were developed to circumvent thromboembolic side effects by blocking CD40L. CD40-TRAF6 signalling was shown to play a crucial role in vascular biology, whereas interactions between CD40 and TRAF2/3/5 was not beneficial in a model for arterial neointima formation.[102] Lutgens et al. found that CD40-TRAF6 deficiency but not CD40-TRAF2/3/5 deficiency prevented atherosclerotic plaque development.[103] Small molecule inhibitors, termed TRAF-STOPs that specifically block the interaction between CD40 and TRAF6 and not between CD40 and TRAF2/3/5 were invented.[104] The administration of these inhibitors were shown to be beneficial in insulin sensitivity in a diet-induced obesity model, as well as in atherosclerotic plaque formation.[105, 106] In the context of AAA, Kusters et al. have already shown that CD40L deficiency protects against AAA formation and rupture.[107] This was accompanied by a reduction in infiltrating immune cells into aneurysmal tissue and decreased MMP activity.
Hence, it appears reasonable that inhibition of the CD40/CD40L signalling pathway is a potential therapeutic target for the treatment of cardiovascular diseases and AAA in particular.

Experimental murine models of AAA

AAA is a complex, multifactorial disease that causes approximately 200,000 deaths worldwide each year due to aortic rupture.[1, 2] However, currently there is no medical treatment available and only surgical repair can limit AAA progression.[17] This urges for translational research and the development of effective drug therapies. Experimental murine models are widely used to study AAA in *in vivo* research.
The four most often used experimental murine models for AAA based on the approximately numbers of publications are the angiotensin II (AngII) infusion model in hyperlipidaemic mice, the porcine pancreatic elastase (PPE) perfusion model, the $CaCl_2$ model and the external periadventitial PPE application (ePPE) model.[8] Daugherty et al. found in 2000 that continuous infusion with AngII for 28 days via a subcutaneously implanted pump induced AAA formation in mice deficient for apolipoprotein E (*Apoe*$^{-/-}$).[108] However, AngII treatment more likely lead to aortic dissection than AAA formation, accompanied by the development of intramural thrombi.[109] AAA induction via intraluminal or external periadventitial application of PPE was developed by Pyo et al. and Bhamidipati et al.[23, 110] In addition, $CaCl_2$ is also used to induced AAA by periadventitial application.[111] But the extent of aortic dilation induced by $CaCl_2$ is less distinct compared to the expansion caused by AngII or PPE.[109]
The induction of AAA using the AngII model can be carried out quickly and technically easily, whereas intraluminal or external periadventitial application of PPE or $CaCl_2$ requires a high level of operational skills and is more time-consuming.[109]
However, each model has its limitations and only partially mimics the human disease (Table 1). Therefore, it is advisable to investigate potential therapeutic targets in different experimental models to prove its effectiveness.

Table 1: Features of human AAA that are mimicked by different experimental murine models.
The AngII, PPE, CaCl2 and ePPE model are listed and it is indicated which features that are characteristic for human AAA pathology have also been described for the model (x) or have not yet been described (-). Table based on Busch et al.[8]

Feature of human AAA	**AngII**	**PPE**	**$CaCl_2$**	**ePPE**
Fibrosis	x	x	x	x
Fusiform aneurysm growth	-	x	x	x
Aortic dissection	x	-	-	-
Intraluminal thrombus formation	-	-	-	x
Intramural haemorrhage	x	-	-	-
Altered hemodynamic	x	x	-	x
Imbalanced proteolysis	x	x	x	x
Angiogenesis	x	x	x	-
Humoral immune response	x	x	-	-
Calcification	-	-	x	-
Rupture	x	-	-	-

Objectives of the study

AAA is a complex, multifactorial and life-threatening disease associated with SMC apoptosis, proteolytic ECM degradation, and extensive immune cell infiltration. The extensive activation of adaptive immune responses represents a main pathological aspect of AAA. Co-stimulatory molecules such as CD40 and CD40L enhance this activation and thus promote disease progression. This leads to the assumption that interfering with this signalling pathway will limit AAA growth and rupture. A previous study from Kusters et al. already showed a promising effect on AAA formation and fatal rupture in CD40L-deficient *Apoe*$^{-/-}$ mice. CD40L deficiency also led to reduced infiltration and activation of immune cells in aneurysmal tissue.[107] In addition, pharmacological inhibition of the CD40-TRAF6 signalling using TRAF-STOP showed beneficial effects in an experimental model of atherosclerosis by inhibiting plaque formation and progression.[106] In this model, the administration of TRAF-STOP also reduces infiltration of leukocytes and activation of macrophages.[106]

For this thesis, it was hypothesized that the activation of the CD40/CD40L signalling pathway in the context of AAA contributes to excessive immune cell stimulation. This results in the release and activation of proteolytic enzymes as well as the exposition of pro-inflammatory cytokines into the aneurysmal tissue that further promote AAA pathology. For this purpose, this study investigated the CD40/CD40L axis as potential therapeutic target in AAA disease. In detail:

1. The first aim was to examine the role of the selective inhibition of CD40-TRAF6 signalling by the small molecule inhibitor, TRAF-STOP, after PPE-induced AAA formation. Therefore, AAA development and growth were assessed using ultrasound imaging and analysis of macroscopic pictures. ECM proteins that maintain aortic structure as elastin and collagen and the expression and activation of proteolytic enzymes in aneurysmal tissue was investigated via histologic analyses and gene expression profiling. In addition, the immune cell infiltration, the inflammatory milieu and the systemic effect on blood pressure after CD40-TRAF6 signalling was determined by flow cytometric and gene expression analysis, as well as invasive blood pressure measurements.

2. The second aim was to evaluate the potential therapeutic effect of selective inhibition of CD40-TRAF6 signalling by TRAF-STOP after continuous AngII infusion to induce aortic expansion. In this model, mice were either fed a standard chow diet or a Western diet (WD). After AAA induction, aortic dilation, immune cell infiltration as well as cytokine release were investigated using ultrasound imaging and flow cytometric analysis.

3. The third aim focused on the circumstance that the co-stimulatory molecules, CD40 and CD40L, are widely expressed on various immune cells. Therefore, this study aimed to examine which cell type uses the CD40/CD40L signalling pathway and contributes to AAA formation and development. Ultrasound imaging was used to assess aortic dilation in mice with global, tamoxifen-inducible CD40 deficiency as well as with persistent B cell- or myeloid cell-specific CD40 deficiency after continuous AngII infusion. In addition, AAA development was examined in persistent T cell-specific CD40L-deficient mice after PPE and AngII-induced AAA formation.

Material and Methods

Mice

All animal studies and animal care were approved by the local ethics committee (LANUV; State Agency for Nature, Environment and Consumer Protection, NRW, Germany, file number AZ 81-02.04.2018.A408). Animal experiments were performed in accordance with the guidelines of the European convention on the protection of vertebrate animals used for scientific purposes as well as according to the Animal Research: Reporting of In Vivo Experiments (ARRIVE) II guidelines. Mice were maintained in a temperature-controlled room with a 12 h day-night cycle in the central facility premises for animal research and scientific animal protection tasks (ZETT) at the Heinrich-Heine-University Düsseldorf. All mice had ad libitum access to food and water. Male C57BL/6J mice were purchased from Janvier Labs (Saint-Berthevin, France) and male *Apoe*$^{-/-}$ mice were purchased from Taconic (Hudson, USA). Additional studies were performed on tamoxifen (TAM)- inducible, global CD40-deficient mice with *Apoe*$^{-/-}$ background(*Apoe*$^{-/-}$ *Cd40*$^{fl/fl}$ *CreER*^{tg}). Thereby, administered TAM binds to the estrogen receptor (ER), which induces Cre recombinase activity and translocation into the nucleus. Furthermore, cell-type specific CD40- and CD40L-deficient mice were generated by our group and used in this study. Thereby, the Cre recombinase is persistently expressed and active resulting in CD40 depletion on B cells (*Apoe*$^{-/-}$ *Cd40*$^{fl/fl}$ *Cd19 Cre*^{tg}) or myeloid cells (*Apoe*$^{-/-}$ *Cd40*$^{fl/fl}$ *Lyz2 Cre*^{tg}) or T cells (*Apoe*$^{-/-}$ *Cd40lg*$^{fl/fl}$ *Cd4 Cre*^{tg} and *Cd40lg*$^{fl/fl}$ *Cd4 Cre*^{tg}). Their Cre negative (*Cre*^{wt}) littermates were used as controls. All genotypes were confirmed through polymerase chain reaction using the listed primers (Table 2) performed by Transnetyx (Cordova, USA). C57BL/6J and CD40- or CD40L-deficient mice received a standard chow diet, whereas *Apoe*$^{-/-}$ mice were either fed a standard chow diet or a WD containing 21% fat and 0.15% cholesterol (cat# S8200-E010; EF NM TD.88137; Ssniff Spezialdiäten, Soest, Germany).

Table 2: List of primers used for genotype verification

Tested sequence	**Forward Primer**	**Reverse Primer**
Apoe$^{-/-}$	GGGAGAGCCGGAGGTGA	CCTGGGTGGAGAGGCTTTT
Cd40$^{fl/fl}$	AGAGAATAGGAACTTCGGAATAG GAACT	CTGCCATCTACCAAAGCAAGAAC
Cd40lg$^{fl/fl}$	GGAATGCTTAGCCCTGCAAATAA	AGTTCCTATTCCGAAGTTCCTAT TCTCT
Cre^{tg}	TTAATCCATATTGGCAGAACGAA AACG	CAGGCTAAGTGCCTTCTCTACA

Induction of abdominal aortic aneurysm formation

Experimental AAA was induced in eight- to twelve-week-old male mice using two different mouse models, continuous infusion with AngII into mice with *Apoe*$^{-/-}$ background or intraluminal aortic perfusion with PPE in C57BL/6J mice.

Angiotensin II model

Mice with *Apoe*$^{-/-}$ background were continuously infused with AngII via osmotic pumps (model 1004, Alzet, Cupertino, USA) at a rate of 1 µg/kg*min, previously described by Trachet et al.[112] This results in the formation of suprarenal true aneurysms or dissecting AAAs, as well as thoracic aortic aneurysms (TAA), developing mostly in the ascending aorta. One day prior to implantation, osmotic pumps were filled with AngII (cat# A9525, Sigma-Aldrich, Burlington, USA). Priming of pumps was ensured by incubating filled pumps in 0.9% sodium chloride (NaCl; cat# B101153, Fresenius Kabi, Bad Homburg, Germany) at 37°C. Mice received 0.1 mg/kg body weight buprenorphine (Buprenovet, Bayer, Leverkusen, Germany) subcutaneously (s.c.) via injection 30 min prior to surgery. Mice were anaesthetized with isoflurane (Piramal Critical Care) (initially 3 volume percent (vol%), continuous 1.5 vol% while surgery) and placed on a heated pad at 37°C. After lack of pedal responses was verified, a subcutaneous pocket was prepared on the right shoulder of the mouse and the pump was gently inserted with its moderator head positioned caudally. The incision was closed with an interrupted suture. Mice received buprenorphine (0.01 mg/ml) via the drinking water for at least two days post surgery and were monitored regularly until the end of the experiment. Male *Apoe*$^{-/-}$ mice were randomly divided into two groups. One group were fed a standard chow diet, the other group were fed a WD starting from the day of surgery as indicated. Any mouse that died prior to the experimental endpoint underwent autopsy to determine cause of death. Mice that died due to aneurysm rupture were included in assessment of AAA and TAA incidence.

Porcine pancreatic elastase perfusion model

C57BL/6J mice underwent aortic PPE perfusion to induce non-dissecting, infrarenal located AAAs as previously described by Pyo et al.[23] Thirty min prior to surgery, mice received (s.c.) 0.1 mg/kg body weight buprenorphine. Mice were initially anaesthetized with 3 vol% isoflurane and placed on a heated pad at 37°C while anaesthesia was maintained with continuous isoflurane exposure (1.5 vol%) during surgery. Lacking any pedal reflexes, mice underwent laparotomy. Thereafter, an infrarenal aortic segment was isolated, temporarily ligated and perfused with sterile isotonic saline containing type I porcine pancreatic elastase (2.15-3 U/ml, cat# E1250, Sigma-Aldrich) under pressure (120 mmHg) for 5 min using a catheter. Adjustment of elastase concentration was necessary, as different batches of elastase induced different AAA manifestations at the same concentration. After perfusion, the aortic puncture was sutured, ligations were removed and the abdomen was closed. Mice received buprenorphine (0.01 mg/ml) via the drinking water for three days post surgery and if required an additional injection of buprenorphine (0.1 mg/kg bw, s.c.) in the first eight hours after surgery. Close monitoring of mice was performed until the end of experiments. Mice were excluded from the study, if it was observed during surgery that the aorta was not properly inflated while perfusion. The PPE surgeries were performed by Julia Odendahl.

Induction of global CD40 deficiency with TAM administration

Activity and translocation of the Cre recombinase into the nucleus and thus CD40 deficiency, was induced by TAM administration in *Apoe*$^{-/-}$ *Cd40*$^{fl/fl}$ *CreER*^{tg} and their *Cre*^{wt} littermates. Mice were injected with 100 µl TAM (1 mg/injection; cat# T5648, Sigma-Aldrich) solved in peanut oil (cat# P2144, Sigma-Aldrich) intraperitoneal (i.p.) 14 days prior to AngII-induced AAA formation. Injections were repeated once a day for five consecutive days.

Pharmacological inhibitor treatment

CD40-TRAF6 signalling was inhibited using the small molecule TRAF-STOP 6860766, further referred to as TRAF-STOP, previously described by Zarzycka et al.[104] We received the TRAF-STOP compound from our cooperation partner MD, PhD Esther Lutgens (Cardiovascular Medicine, Experimental Cardio-Vascular Immunology Laboratory, Mayo Clinic, Rochester, USA). Mice were injected (i.p.) with TRAF-STOP (10 µmol/kg/injection) or 2.5% dimethyl sulfoxide (DMSO; cat# D8418, Sigma-Aldrich; in Dulbecco's phosphate buffered saline (DPBS); cat# D8537, Sigma-Aldrich) as solvent control. Injections started on the day of AAA induction and were carried on three times per week until mice were sacrificed.

Assessment of aortic diameter *in vivo*

Aortic diameter was examined prior to AAA induction and AAA development and progression was monitored weekly using non-invasive ultrasound technology. Images were captured with the Vevo 3100 high-resolution *in vivo* imaging system equipped with a 25-55 MHz - transducer (MX550D; VisualSonics Inc., FUJIFILM, Toronto, Canada). Briefly, mice were anaesthetized with isoflurane (initially 3 vol%, followed by 1.5 vol% while measurements) and placed on a heated pad at 37°C. Electrocardiogram, respiration rate and body temperature were continuously traced while measurements. Diameter of infrarenal (PPE model) or suprarenal (AngII model) abdominal aorta was assessed at the maximum dilation from leading to leading (LTL) edge in longitudinal B-Mode images (Figure 4). Additionally, in the AngII model the diameter of the thoracic aorta was examined at the site of middle ascending aorta in B-mode images in parasternal long-axis view only. The aortic diameter was analysed in three cardiac cycles at end-diastole using Vevo LAB 5.6.0 software. AAA and TAA incidence were defined as an increase in aortic diameter of at least 1.5-fold.

In addition, the abdominal aortic diameter was examined using macroscopic images of the aorta captured on the day of endpoint, if stated. A metric ruler served as scale reference. AA diameter was measured at the maximum dilation and was analysed using ImageJ Software (Fiji, version: 2.9.0/1.53t; Java 1.8.0_322 (64-bit)).

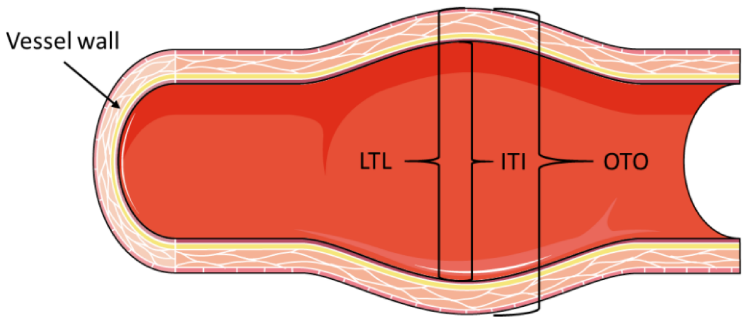

Figure 4: Schematic illustration of different methods to analyse the aortic diameter
The vessel diameter in ultrasound images can be measured from the outer to the inner vessel wall, which is referred to as leading to leading (LTL) edge. Additionally, the vessel diameter can be analysed from the inner to inner (ITI) and from the outer to outer (OTO) edges. Schema of dilated vessel is adapted from https://smart.servier.com/.

Blood pressure and heart rate measurements

The effect of CD40-TRAF6 signalling inhibition on arterial pressure and heart rate was invasively investigated in ten-week-old C57BL/6J mice. Therefore, mice received TRAF-STOP injections (10 µmol/kg/injection) three times per week until mice were sacrificed for blood pressure and heart rate measurements after three or seven days. Thirty min prior to measurements, mice received (s.c.) 0.1 mg/kg body weight buprenorphine. Thereafter, mice were initially anesthetized with 3 vol% isoflurane and placed in supine position on a heated pad at 37°C. Anaesthesia was maintained with continuous isoflurane exposure (1.5 vol%) during pressure measurements. The right common carotid artery was exposed and isolated from other neighbouring structures. The carotid artery was distally ligated and after arteriotomy a Millar pressure transducer (SPR-829 Mikro-Tip® Millar, Houston, USA) was introduced and advanced into the ascending aorta. Systolic and diastolic blood pressure, as well as heart rate were measured for 5 min using the PowerLab data acquisition system (AD Instruments, Sydney, Australia). Data was analysed using LabChart 7 software (AD Instruments). The measurements and data analysis were performed by Stefanie Becher.

Organ harvesting

At the endpoints (d7, d14, d28) mice were sacrificed after induction of deep anaesthesia with Ketamin (100 mg/kg; Ketaset®, Zoetis, Parsippany, USA) and Xylazin (10 mg/kg; Rompun™, Bayer). Blood was withdrawn from the heart and collected in heparinised centrifugation tubes. Additionally, 70 µl of whole blood was collected in EDTA tubes and analysed using an automated veterinary haematology analyser (VetScan® HM5, Zoetis). Plasma was collected after centrifugation of heparinised centrifugation tubes (1000 x g, 10 min, room temperature (RT)) and stored at -80°C. Blood cells were stored for further processing at RT. After thoracotomy, blood circulation of mice was perfused through the left ventricle with cold DPBS (cat# D8537, Sigma-Aldrich). Thereafter, spleen and aortic lymph nodes near the bifurcation were harvested and stored in DPBS on ice. Finally, the aorta was exposed, collected and stored in cold DPBS on ice for further investigations.

Histology

Sample preparation and embedding

For histological analyses, organs were fixed in 4% paraformaldehyde solution (cat# J61899.AP; ThermoFisher Scientific, Waltham, USA) for 1 h at RT. Afterwards organs were dehydrated in 30% sucrose (cat# 84097, Sigma-Aldrich) solution at 4°C until sample sank to the bottom. Samples were embedded in Tissue-Tek optimum cutting temperature (O.C.T.) freezing compound (Sakura Finetek, Amsterdam, the Netherlands) on dry ice. Serial sections of frozen tissue specimen were cut with 5-7 µm thickness using a cryostat (cat# CM3050S; Leica Biosystems, Wetzlar, Germany). Sections were collected on microscope slides (cat# J1800AMNZ, Menzel-Gläser, SuperFrost plus, Epredia, Kalamazoo, USA). Slides were stored at -20°C until further processing.

Elastica van Gieson staining

To evaluate elastic fibre degradation and aortic medial layer thickness Elastica van Gieson (EvG) staining of aortic cross-sections from DMSO- and TRAF-STOP-treated mice was

performed. Briefly, seven sequentially aortic cross-sections, using the cross-section with the largest aortic expansion as well as three sections before and three sections after, were incubated in Resorcinol-Fuchsine-solution (cat# X877.1, Carl Roth, Karlsruhe, Germany) for 10 min, followed by a 30 sec washing step under running tap water. Thereafter, staining with haematoxylin solution according to Gill II (cat# T864.2, Carl Roth) was performed for 30 sec, followed by a blueing step under running tap water for 1 min. Finally, aortic cross-sections were stained with Picrofuchsin using Van Gieson´s solution kit (cat# 3925.1, Carl Roth) for 2 min. After washing the sections with deionised water, they were mounted with VectaMount AQ Aqueous (cat# H-5501, Vector Laboratories, Newark, USA) and stored at 4°C until microscopy. Images were captured using a DMC4500 camera on a DM6B microscope (Leica Biosystems).
For determining elastin degradation, a grading system with four grades was established. Grade 1: completely intact elastin fibres to isolated elastic fibre breaks; grade 2: increased amount of elastic fibre breaks to area-wide absence (max. 30%) of 1 to 2 elastic fibres; grade 3: area-wide absence (30-50%) of 2 to 4 elastic fibres; grade 4: area-wide absence (more than 50%) of 2 to 4 elastic fibres or complete destruction of fibres. Elastin degradation of an AAA was presented as the average of grades from seven consecutive aortic cross-sections and was compared between treatment groups.
In addition, destruction of elastin fibres often results in increased enlargement of the aortic medial layer. Therefore, medial layer thickness was assessed in these EvG stained seven sequentially aortic cross-sections around the maximum diameter by determining the area of the medial layer and calculating the average for one AAA using ImageJ software (Fiji, version: 2.9.0/1.53t; Java 1.8.0_322 (64-bit)). Sarah Verheyen (B.Sc.) performed the staining and analysis of sections under my supervision.

Immunofluorescence staining

To determine collagen type IV amount in aneurysmal tissue of DMSO- and TRAF-STOP-treated mice, three consecutive aortic cross-sections around the maximum diameter from each mouse were used for immunofluorescence staining. Briefly, sections were incubated in DPBS supplemented with 0.1% Saponin Quillaja sp. (cat# S4521; Sigma-Aldrich), 0.5% Bovine Serum Albumin (BSA; fraction V; cat# 8076.3; Carl Roth) and 0.2% fish gelatine (cat# G7765; Sigma-Aldrich) at RT for 1 h to permeabilize the tissue and to block unspecific binding sites. Thereafter, sections were incubated with collagen type IV antibody (concentration: 5 µg/ml, polyclonal, cat# ab6586; abcam, Cambridge, United Kingdom) overnight at 4°C. The next day, sections were washed with DPBS three times. Afterwards, sections were incubated with a fluorescence labelled secondary antibody (Goat anti-Rat IgG (H+L) Cross-Adsorbed Secondary Antibody, Alexa Fluor™ 680, concentration: 2 µg/ml; cat# A-21096, ThermoFisher Scientific) at RT for 1 h. Afterwards, sections were again washed three times with DPBS. Followed by wheat germ agglutinin (WGA; dilution: 1:250, cat# W11261, ThermoFisher Scientific) staining. The WGA staining was used to generate an overview of the entire AAA, as WGA stains all glycoproteins of cell membranes. To diminish auto fluorescence of the aortic tissue, sections were treated with Vector TrueVIEW Autofluorescence Quenching Kit (cat# VEC-SP-8400, Vector Laboratories, Newark, USA) following the instructions of the manufacturer. Finally, cell nuclei were stained with 4', 6-Diamidino-2-phenylindole-dihydrochloride (DAPI, concentration: 1 ng/ml; cat# D1306, ThermoFisher Scientific) for 5 min at RT and aortic cross-sections were mounted with VectaMount AQ Aqueous (cat# H-5501, Vector Laboratories). Images were captured using a DFC9000GT camera on a DM6B microscope (Leica Biosystems).
The amount of collagen type IV in every cross-section was analysed using a semi-automated macro in ImageJ software (Fiji, version: 2.9.0/1.53t; Java 1.8.0_322 (64-bit)). In this, the area stained with collagen type IV is related to the total AAA area determined by WGA staining (Supplementary Figure 1). Collagen type IV amount per AAA was presented as the average of three sequentially aortic cross-sections. Sarah Verheyen (B.Sc.) performed the staining and analysis of sections under my supervision.

Spatial transcriptomics

To measure total mRNA expression in aortic tissue the Visium Spatial Gene Expression technology of 10X Genomics (Pleasanton, USA) was used (Figure 5). Therefore, aneurysmal cross-sections at their largest diameter of DMSO- and TRAF-STOP-treated mice were collected on Visium Spatial Gene Expression Slides (cat# PN-2000233, 10X Genomics). The slides were fixed with methanol (cat# 646377, Sigma-Aldrich) and afterwards stained with haematoxylin (Solution according to Gill II, cat# T864.2, Carl Roth) and eosin (cat# X883.2, Carl Roth) according to the manufactures Demonstrated Protocol CG000160 Rev C (10X Genomics). Afterwards, prepared Visium slides were further processed using the Visium Spatial Gene Expression workflow (10X Genomics) according to the manufacturer's instructions. Aneurysmal cross-sections were permeabilized for 12 min resulting in the release of mRNA. The mRNA was captured by spatially barcoded oligonucleotides present on the slide and cDNA was generated through a reverse transcription reaction. The barcoded cDNA was pooled and a cDNA library was generated. Thereafter, the cDNA was sequenced on a NextSeq 2000 system (Illumina Inc.; San Diego, USA) with a mean sequencing depth of approximately 120,000 reads/spot. The resulting raw sequencing data was further processed using the 10X Genomics spaceranger software (v2.0.0). Using the spaceranger count pipeline, the data was also processed by alignment of reads to the mm10 genome, unique molecular identifier (UMI) counting as well as tissue detection and fiducial detection. Lastly, the data of all cross-sections was combined and normalized for sequencing depth through the spaceranger aggr pipeline. Milena Feige (B. Sc.) prepared the Visium slides under my supervision. The cDNA library generation and sequencing was performed in cooperation with Dr. Tobias Lautwein at the Genomics & Transcriptomics Laboratory in Düsseldorf. Sarah Verheyen (B.Sc.) analysed the data under my supervision.

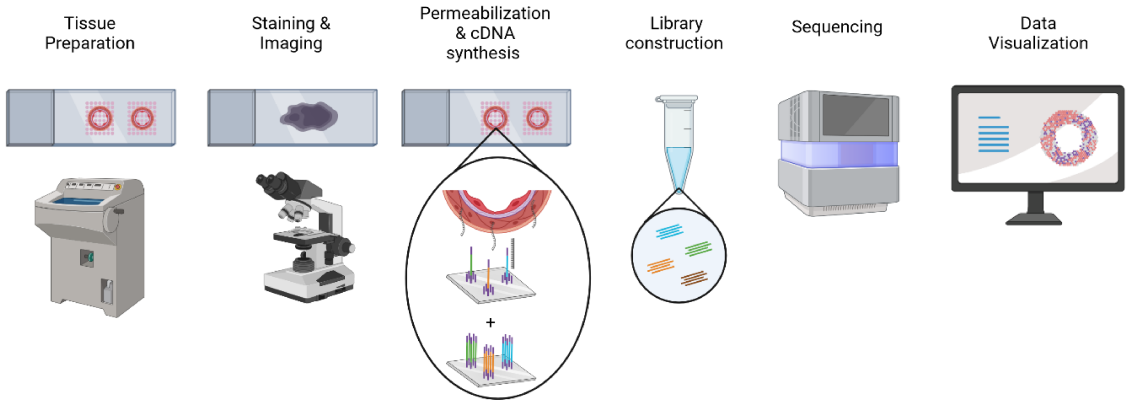

Figure 5: Spatial Transcriptomics workflow
Frozen aortic tissue is sectioned and placed onto the Capture Area on a gene expression slide. After tissue fixation, a staining with haematoxylin and eosin is performed and the stained sections are visualized using a brightfield microscope. In the next step, the tissue is permeabilized to release the mRNA that binds to the barcoded oligonucleotides on the Capture Area. The captured mRNA is processed to cDNA via reverse transcription. The barcoded cDNA is pooled to generate a library, which is further sequenced on an Illumina sequencer. Finally, the data is processed and analysed. Based on https://www.10xgenomics.com/products/spatial-gene-expression and created with BioRender.com.

Preparation of single cell suspensions

To further investigate the immune cells present in the collected tissues, single cell suspensions were prepared from aorta, blood, spleen, and aortic lymph nodes according to the following protocols.

Digestion of aortic tissue into single cell suspension

Preparation of single-cell suspension from harvested aortic tissue was performed as previously described by Hu et al.[113] Briefly, aneurysmal tissue was cut into 1-2 mm pieces and transferred into an enzyme digestion mixture containing 400 U/ml Collagenase I (cat# C0130, Sigma-Aldrich), 120 U/ml Collagenase XI (cat# C7657, Sigma-Aldrich), 60 U/ml Hyaluronidase I-S (cat# H3506, Sigma-Aldrich) and 60 U/ml Dnase I (cat# 11284932001, Sigma-Aldrich) in DPBS containing calcium and magnesium (DPBS++, cat# D8662, Sigma-Aldrich) supplemented with 20 mM HEPES (cat# 15630056, ThermoFisher Scientific). The tissue was digested in the enzyme mixture on a shaker (600 rpm) for 50 min at 37°C. Afterwards, cell suspension was poured onto a 100 µm cell strainer (cat# 43-50100-50, pluriSelect, Leipzig, Germany) and remaining tissue was mashed using a syringe plunger. After centrifugation (10 min, 450 x g, 4°C) supernatant was discarded. On the one hand, cells were resuspended in cold DPBS for further Cellular Indexing of Transcriptomes and Epitopes (CITE) by sequencing analysis. On the other hand, cells were resuspended in RPMI-1640 (cat# R7388; Sigma-Aldrich) supplemented with 10% foetal calf serum (cat# F9665; Sigma-Aldrich) for further flow cytometer analysis. For flow cytometric analysis, cells were incubated on a shaker (600 rpm) for 12 min at 37°C. Afterwards cell suspension was centrifuged (10 min, 450 x g, 4°C), resuspended in 500 µl DPBS and stored at 4°C until further processing.

Preparation of single-cell suspension from blood

After plasma was removed, blood cells were transferred into a tube containing 10 ml red blood cell (RBC) lysis buffer containing 8.29 mg/ml ammoniochloride, 1 mg/ml potassium bicarbonate and 0.0375 mg/ml sodium-ethylenediaminetetraacetic acid (Na-EDTA) (pH 7.4; central pharmacy, university hospital Düsseldorf, Germany). Cells were carefully vortexed for 5 sec and incubated for 15 min at RT. After centrifugation (7 min, 450 x g, RT), supernatant was discarded and an additional RBC lysis step was performed as described previously. Finally, cells were centrifuged (7 min, 450 x g, RT) and supernatant was discarded. Cells were resuspended in as much DPBS as the initial volume of blood collected, and stored at 4°C until further processing.

Preparation of single-cell suspension from splenic tissue

Harvested spleens were mashed using a syringe plunger through a 100 µm cell strainer (cat# 43-50100-50, pluriSelect), which was rinsed several times with cold DPBS. After centrifugation (450 x g, 5 min, 4°C), supernatant was discarded and cell pellet was resolved in DPBS. The cell suspension was transferred onto a 40 µm cell strainer (cat# 43-50040-50, pluriSelect), rinsed with cold DPBS, followed by another centrifugation step. Cells were resuspended in 5 ml RBC lysis buffer and incubated for 5 min at RT. Finally, cells were centrifuged (450 x g, 5 min, 4°C), supernatant was discarded and cell pellet was resuspended in 6 ml cold DPBS. Cell suspension was again poured over a 100 µm cell strainer and stored at 4°C until further processing.

Preparation of single-cell suspension from aortic lymph nodes

Harvested aortic lymph nodes were transferred onto a 100 µm cell strainer (cat# 43-50100-50, pluriSelect). Lymph nodes were mashed using a syringe plunger and the cell strainer was rinsed several times with cold DPBS to wash cells out. Collected cell suspension was centrifuged (450 x g, 5 min, 4°C), supernatant was discarded and cell pellet was resolved in 500 µl DPBS. Cell suspension was stored at 4°C until further processing.

Flow cytometry

Staining of single cells for flow cytometric analysis

For flow cytometric analysis, prepared single cell suspensions from aorta, spleen, lymph nodes or blood were stained with a CD16/32 antibody to avoid nonspecific binding and with a live/dead cell marker (Zombie AquaTM Fixable Viability Kit, 1:250, cat# 423102, BioLegend, San Diego, USA) for 10 min at RT in the dark. After centrifugation (450 x g, 5 min, 4°C), cells were stained with fluorochrome-labelled antibodies targeting different immune cell specific cell-surface receptors for 20 min at RT in the dark (Table 3). Finally, cells were centrifuged (450 x g, 5 min, 4°C), supernatant was discarded and cell pellet was resuspended in DPBS. Flow cytometric measurements were performed on the BD FACSVerse (BD; Franklin Lakes, USA). Flow cytometric data was analysed using the FlowJo™ V.10.5.3 software. To investigate the immune cell distribution in aneurysmal tissue the proportion of a target immune cell was indicated as percent of overall $CD45^+$ cells.

Determining CD40L expression on T cells

Cre recombinase activity in *Apoe*$^{-/-}$ *Cd40lg*$^{fl/fl}$ *Cd4 Cre*^{tg} mice should result in lack of CD40L on T cells, thus, the CD40L expression on T cells from aorta, aortic lymph nodes, spleen and blood from these mice and their Cre negative littermates was assessed. The number of cells from single cell suspensions were determined using a Neubauer cell-counting chamber with 0.1 mm depth and 0.0025 mm² area (cat# 0640110; Marienfeld superior, Lauda-Königshofen, Germany). One million cells were resuspended in RPMI-1640 (cat# R7388; Sigma-Aldrich) supplemented with 10% foetal calf serum (cat# F9665; Sigma-Aldrich) and fluorochrome-conjugated antibodies targeting CD45, CD3, CD8, CD4, and CD40L were added (Table 3). Thereafter, cells were stimulated with the eBioscience™ Cell Stimulation Cocktail (dilution: 1:500, cat# 00-4970-93, ThermoFisher Scientific) and incubated for 3 h at 37°C on a shaker. After centrifugation (500 x g, 5 min, 4°C), supernatant was discarded and cells were stained with the CD16/32 antibody and with a live/dead cell marker (Zombie AquaTM Fixable Viability Kit, dilution: 1:250, cat# 423102, BioLegend) for 10 min at RT in the dark. Cells were centrifuged, supernatant was discarded and cell pellet was resolved in DPBS. Flow cytometric measurements were performed on the BD FACSVerse (BD). Data of flow cytometric measurements was analysed using the FlowJo™ V.10.5.3 software. To examine the CD40L expression on different T cell populations the median fluorescent intensity (MFI) of CD40L was quantified.

Table 3: Fluorochrome-labelled antibodies used for flow cytometric analysis

Antibody	Clone	Dilution	cat#	Manufacturer
TruStain FcX™ anti-mouse CD16/32	93	1:50	101319	BioLegend
Brilliant Violet 421™ anti-mouse CD45	30-F11	1:200	103133	BioLegend
BD Pharmingen™ FITC Rat Anti-Mouse CD45	30-F11	1:200	553079	BD Biosciences
FITC anti-mouse CD19	MB19-1	1:100	101505	BioLegend
PE anti-mouse Ly6C	HK1.4	1:133.3	128007	BioLegend
PerCP/Cyanine5.5 anti-mouse Ly6G	1A8	1:100	127615	BioLegend
PE/Cyanine7 anti-mouse NK1.1	PK136	1:200	108713	BioLegend
APC/Cyanine7 anti-mouse/human CD11b	M1/70	1:200	101225	BioLegend
BD Horizon™ V450 Rat Anti-Mouse CD3 Molecular Complex	17A2	1:100	561389	BD Biosciences
APC/Fire™ 750 anti-mouse CD4	GK1.5	1:200	100459	BioLegend
PerCP/Cyanine5.5 anti-mouse CD8a	53-6.7	1:200	100734	BioLegend
APC anti-mouse CD40	3/23	1:80	124611	BioLegend
APC anti-mouse CD154 (CD40L)	SA047C3	1:40	157009	BioLegend

Staining and sorting of cells for CITE sequencing

For CITE sequencing, two aneurysms of each treatment group 7 days after PPE-induced AAA formation were collected and pooled to prepare a single cell suspension as described in Digestion of aortic tissue into single cell suspension. Cells were stained with a CD16/32 antibody to avoid nonspecific bindings for 10 min at RT. Afterwards, cells were incubated with a fluorochrome-labelled CD45 antibody (Clone: 30-F11; cat# 103115, BioLegend), a TotalSeq™-A Mouse Universal Cocktail V1.0 (dilution: 1:1200; cat# 199901; BioLegend), and individual Hashtag antibodies (TotalSeq™-B0303 and TotalSeq™-B0304; Biolegend) for 20 min at RT. Centrifugation (5 min, 500 x g, 4°C) was performed and supernatant was discarded. Thereafter, cells were resuspended in MACS buffer (cat# 130-091-221; Miltenyi Biotec, Bergisch Gladbach, Germany). After adding DAPI (concentration: 1 ng/ml), cells were sorted using a MoFlo XDP (Beckman Coulter, Krefeld, Germany) and viable $CD45^+$ cells were collected. Sorting of the cells was performed by Dr. Alexander Lang in cooperation with Dipl. Ing. Katarina Raba at the Core Flow Cytometry Facility at the Institute for Transplantation Diagnostics and Cell Therapeutics at the University hospital Düsseldorf.

Single Cell Library Generation

Collected viable $CD45^+$ cells were used to generate single cell libraries using the 10X Chromium Controller system utilizing the Chromium Next GEM Single Cell 5' Kit v2 (10X Genomics) according to manufacturer's instructions. Sequencing was carried out on a NextSeq 550 system (Illumina Inc.) with a mean sequencing depth of ~50,000 reads/cell for gene expression, ~20,000 reads/cell for the TotalSeq-ADT library and ~5,000 reads/cell for the HashTag library. To generate the TotalSeq-ADT library, the TotalSeq™-A Mouse Universal Cocktail, V1.0 was used following the manufacturer's instructions. For the

HashTag library, cells from the DMSO-treated mice were tagged using the TotalSeq™-B0303 anti-mouse Hashtag 3 Antibody (Clone: 30-F11; cat# 155835; BioLegend). In addition, cells from the TRAF-STOP-treated mice were marked with the TotalSeq™-B0304 anti-mouse Hashtag 4 Antibody (Clone: 30-F11; cat# 155837; BioLegend). The library generation was performed in cooperation with Dr. Tobias Lautwein at the Genomics & Transcriptomics Laboratory in Düsseldorf.

Processing of 10X Genomics single cell data

Bioinformatic demultiplexing was performed with R using the package Seurat (v4.02) with the protocol “Demultiplexing with hashtag oligos” v. 2022-01-11 described by Hao et al.[114] The generated raw sequencing data was further processed using the 10X Genomics CellRanger software (v6.0.2). Raw BCL-files were demultiplexed and processed to Fastq-files using the CellRanger mkfastq pipeline. A gene-barcode matrix was generated by performing an alignment of reads to the mm10 genome and UMI counting via the CellRanger multi pipeline. The analysis of data was performed by Sarah Verheyen (B.Sc.) under my supervision.

Multiplex Assay

Concentrations of inflammatory markers were measured in plasma samples and aneurysmal tissue of DMSO- and TRAF-STOP-treated mice using the LEGENDplex™ bead-based immunoassay (LEGENDplex™ Mouse Inflammation Panel Standard, cat# 740446, BioLegend). This assay allows the simultaneous quantification of multiple soluble analytes by flow cytometry.
Aneurysmal tissue lysates were prepared using the Bio-Plex® Cell Lysis Kit (cat# 171304011; Batch number: 64433112, BIO-RAD, Hercules, USA). Briefly, AAAs were collected and rinsed with wash buffer. Afterwards, the tissue was cut into several 1-2 mm pieces. The AAA pieces were transferred into a 2 ml tissue grinder out of glass. 250 µl lysis buffer, including factor 1, factor 2, and phenylmethylsulfonyl fluoride (PMSF), was added following the manufacturer’s instructions. Thereafter, the tissue pieces were mashed by rotating and pressing the pestle into the grinder about 20 times. The resulting cell lysate was snap-frozen in liquid nitrogen and stored at -80°C until further processing.
LEGENDplex™ bead-based immunoassay was performed according to the manufacturer’s instructions. The assay is based on the principles of a sandwich immunoassay, in which a soluble target analyte is captured between two antibodies. The beads conjugated to the capture antibody differ in sizes and intensity of APC fluorescence, allowing a distinguished detection of IL-1α, IL-1β, IL-6, IL-10, IL-12p70, IL-23, IL-27, IL-17A, CCL2, Granulocyte-macrophage colony-stimulating factor (GM-CSF), IFNβ, TNFα, and IFNγ. Briefly, plasma samples and aortic lysates were thawed and centrifuged (4°C, 1 min, 500 x g) prior to the assay. Plasma samples were diluted 1:1 in assay buffer, whereas aortic lysates were not diluted. The assay
was performed in a 96 well plate with V-bottom (cat# 651201; Greiner Bio-One, Kremsmünster, Austria) and 12.5 µl of each sample as well as standard was used. A serial dilution of the cytokine standard resulted in a concentration curve with a logarithmic scale, which was used to determine the concentration of a target analyte using the LEGENDplex™ data analysis software (BioLegend).

Gelatin Zymography

Activity of gelatinases, MMP2 and MMP9, was determined in aneurysmal tissue of DMSO- and TRAF-STOP-treated mice. AAA samples were extracted in lysis buffer containing 0.1% Sodium dodecyl sulphates (SDS; cat# 2326.2, Carl Roth), 0.5% Triton X-100 (cat# T8787, Sigma-Aldrich), and 0.5% Sodium deoxycholate (cat# 30970, Sigma-Aldrich) in DPBS. First, AAA tissue was minced without lysis buffer for 40 s at a frequency of 20 Hz using an oscillating mill MM 400 (Retsch, Haan, Germany). Afterwards, 50 µl lysis buffer was added and the tissue was homogenized for 2 min at a frequency of 30 Hz using the oscillating mill MM 400. Finally, after 10 min at 4°C in an ultrasonic bath, the aortic extracts were centrifuged at 4°C and 17,000 x g for 15 min.
Thereafter, protein concentration was determined in a microplate (F-Bottom, cat# 655101, Greiner BioOne) using the DC™ Protein Assay (cat# 5000116, BioRad) following the manufacturer's instructions. BSA was used to generate a serial dilution series, whose concentration ranged from 10,000 µg/ml to 78.125 µg/ml to produce a standard curve. The absorbance of standards and samples were measured at 750 nm using a microplate reader (FLUOstar Omega; BMG Labtech, Ortenberg, Germany).
MMP2 and MMP9 activities were detected in Novex™ 10% Zymogram Plus (Gelatin) gels (cat# ZY00102BOX, ThermoFisher Scientific). Briefly, 20 µg protein of each aortic extract was loaded into the zymogram gel positioned in a XCell SureLock™ Mini-Cell (cat# EI0001, ThermoFisher Scientific). Samples were electrophoresed in the presence of non-reducing buffers at RT for 2 h. Tris-Glycin SD-sample buffer (cat# LC2676, ThermoFisher Scientific) and a running buffer that contains 1% SDS were used in this experiment. After electrophoresis, the gel was incubated in Renaturing Buffer (1X; cat# LC2670, ThermoFisher Scientific) at RT with gentle agitation for 30 min. Gelatinase activity was then elicited by first equilibrating the gel in Developing Buffer (1X; cat# LC2671, ThermoFisher Scientific) at RT with gentle agitation for 30 min and then incubating the gel in fresh Developing Buffer at 37°C for 40 h. Subsequently, proteolytic activity in the gel was detected by staining the gel with the Colloidal Blue Staining Kit (cat# LC6025, ThermoFisher Scientific) following the manufacturer's instructions by performing 6 h of staining followed by overnight incubation in deionized water. PageRuler™ Plus Prestained Protein Ladder (3 µl; cat# 26619, ThermoFisher Scientific) was used as protein size standard. Image acquisition was performed with the Odyssey Fc Imager (LI-COR, Lincoln, USA) using channel 700 for 2 min. Scanned zymogram was quantified by measuring the signal intensity of the bands with the Image Studio™ Software.

Statistics

Data are presented as mean ± standard deviation (SD) and *n* refers to biologically independent animals. Statistical analysis and graphical illustrations were performed using GraphPad Prism 8 (Graphpad Prism Inc., La Jolla, USA). Data was tested for normal distribution using Shapiro-Wilk test. If data passed normality test, data was analysed for significant differences between two groups using unpaired Student's t test (two-tailed). If data was not normally distributed the unpaired Mann-Whitney (two-tailed) test was used to compare two groups. Two-way repeated measures analysis of variance (ANOVA) with Sidak's multiple comparisons post test was used to examine the influence of two different categorical independent variables on a continuous dependent variable. The Log-rank (Mantel-Cox) test was performed to compare the distributions of survival of two groups. Contingency of AAA development was tested using the two-sided Fisher's exact test. The incidence of an AAA/TAA or no AAA/TAA was expressed and presented as percentage. $P<0.05$ was considered as statistically significant and further significance levels were stated

as *p≤0.05, **p≤0.01, ***p≤0.001, ****p≤0.0001. P-values above 0.100 were not considered in this work and were not included in the graphs.

Results

Pharmacological inhibition of CD40-TRAF6 signalling in AAA formation and progression

In this study the potential of TRAF-STOP 6860766, further referred to as TRAF-STOP, a small molecule inhibitor, that blocks the signal transduction from CD40 to TRAF6, was evaluated in abdominal aortic aneurysm formation. Mice received DMSO (2.5% in DPBS) as solvent control or TRAF-STOP (10 µmol/kg) three times per week starting on the day of surgery until the endpoint. Organs were harvested and further analysed 7, 14 and 28 days after PPE-induced AAA formation. Non-invasive ultrasound imaging was used to assess the development of AAA weekly (Figure 6 A). The small molecule inhibitor was developed by Zarzycka et al. and contains a linker including a Michael acceptor functionality and an N-H group, that connects one benzene and one 3-Bromochlorobenzene (Figure 6B).[104] The inhibitor was designed to bind in a TRAF6 pocket at its C-domain and thereby inhibiting the binding of TRAF6 to the CD40 receptor.

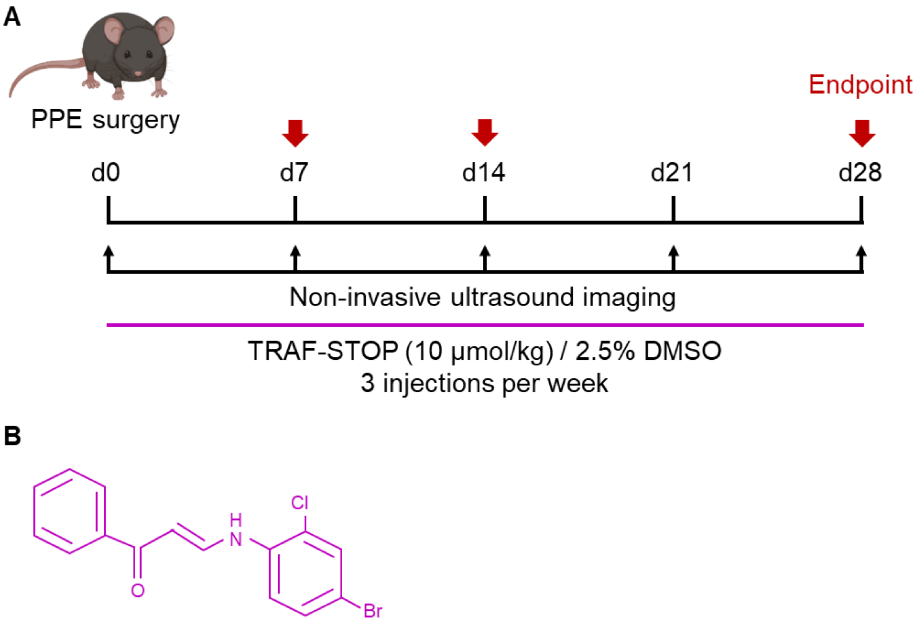

Figure 6: Experimental design to investigate the inhibition of CD40-TRAF6 signalling after PPE-induced AAA formation
(A) *Experimental setup. AAA was induced in mice via intraluminal PPE perfusion of the infrarenal aorta. Mice were treated with 2.5% DMSO or 10 µmol/kg TRAF-STOP three times per week. Non-invasive ultrasound imaging was used to assess the dilation of the aorta weekly. After 7, 14 or 28 days post surgery mice were sacrificed and organs were harvested (red arrows). (B) Chemical structure of the small molecule inhibitor, referred to as TRAF-STOP that specifically binds to the TRAF6 protein and thereby blocks the interaction between TRAF6 and the CD40 receptor. PPE = Porcine pancreatic elastase.*

Pharmacological inhibition of CD40-TRAF6 signalling by TRAF-STOP attenuated elastase-induced AAA formation and progression

Following PPE perfusion, the aortic diameter was assessed weekly via non-invasive ultrasound imaging, showing a progressive increase in both treatment groups. Representative ultrasound images of DMSO- and TRAF-STOP-treated mice before surgery and 7, 14, 21 and 28 days after AAA induction are shown in Figure 7 A. Assessment of the aortic dilation revealed a significant less aortic expansion in TRAF-STOP-treated mice

compared to DMSO-treated mice 14 and 28 days after AAA induction (Figure 7 B). In detail, medial aortic diameter was 1.42 mm and 1.58 mm in DMSO-treated mice, whereas TRAF-STOP treatment inhibited aortic expansion with a reduced medial aortic diameter of 1.06 mm and 1.25 mm two and four weeks after PPE surgery. In addition to the assessment of the aortic diameter using non-invasive ultrasound imaging, the reduction in aortic expansion upon TRAF-STOP treatment could be confirmed by the analysis of macroscopic pictures captured of harvested aortae. Representative macroscopic images of aortae from DMSO- and TRAF-STOP-treated mice 28 days after AAA induction are shown in Figure 7 C. Analysis of aortic diameter using macroscopic images revealed a significant reduction in aortic dilation after TRAF-STOP treatment (Figure 7 D). Summarized, CD40-TRAF6 inhibition led to a reduced AAA expansion, shown by the analysis of ultrasound images and macroscopic pictures.

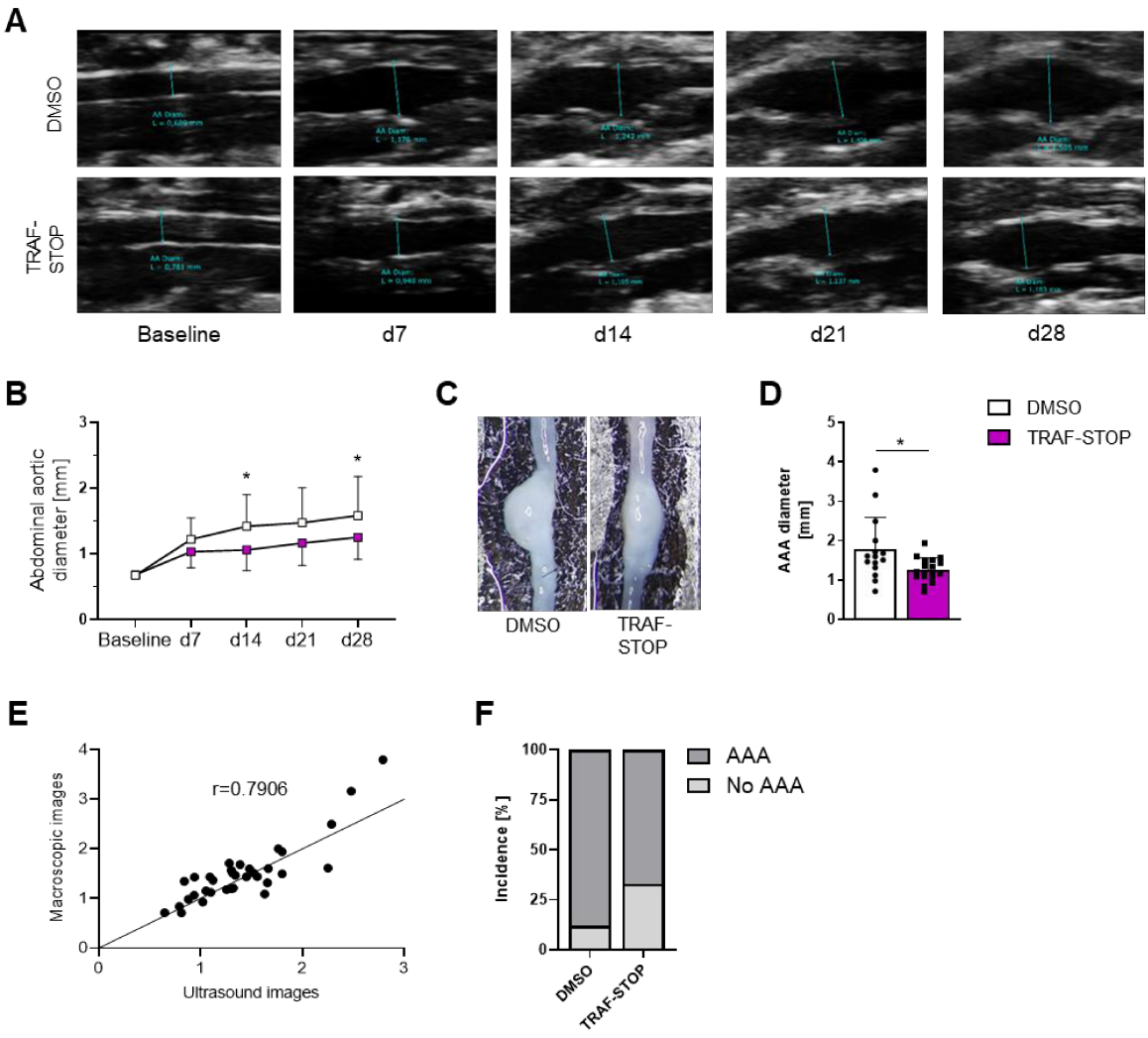

Figure 7: Reduced aortic dilation upon TRAF-STOP treatment 28 days after PPE-induced AAA formation (A) *Representative ultrasound images of the infrarenal aorta from mice treated with DMSO or TRAF-STOP prior to surgery (Baseline) and 7, 14, 21 and 28 days post surgery. (B) Analysis of abdominal aortic diameter using ultrasound images before and 7, 14, 21 and 28 after AAA induction. Two-way ANOVA with Sidak's multiple comparisons post test; *p<0.05. (C) Representative macroscopic images of the infrarenal aortic segment harvested from DMSO- or TRAF-STOP-treated mice 28 days post PPE-induced AAA formation. (D) Quantification of abdominal aortic diameter using macroscopic images 28 days after AAA induction. Unpaired Mann-Whitney test (two-tailed); *p<0.05. (E) Two-tailed nonparametric Spearman Correlation of analysis methods for the assessment of abdominal aortic dilation using ultrasound images or macroscopic images. (F) Incidence of AAA formation upon DMSO or TRAF-STOP treatment 28 days after AAA induction. DMSO treatment led to an AAA incidence of 87.5%, whereas 66.67% of TRAF-STOP-treated mice developed an AAA. Two-sided Fisher's exact test; p=0.2327. Mean ± SD; DMSO n=16, TRAF-STOP n=18.*

Two-tailed nonparametric Spearman correlation indicated that both analysing methods correlated with each other (r=0.7906) and thus non-invasive ultrasound imaging as well as the analysis of macroscopic images can be used to assess AAA formation (Figure 7 E). An AAA was defined as an increase in aortic diameter of at least 1.5-fold. In this study, 14 out of 16 DMSO-treated mice developed an AAA, corresponding to an AAA incidence of 87.5%. In contrast, 12 out of 18 mice developed an AAA in the TRAF-STOP-treated group, corresponding to a reduced AAA incidence of 66.67% 28 days after PPE-induced AAA induction (Two-sided Fisher's exact test; p=0.2327) (Figure 7 F).

CD40-TRAF6 signalling inhibition led to limited collagen degradation in aneurysmal tissue

AAA formation is among others characterized by degradation and remodelling of ECM proteins. Hence, loss of elastin and collagen was examined in aneurysmal tissue of DMSO- and TRAF-STOP-treated mice 28 days after PPE-induced AAA formation. Based on an EvG staining a grading system for elastic fibre destruction was established. Four grades categorize elastin degradation in aortic cross-sections: from intact elastin structures (Grade 1) to complete destruction of elastin fibres (Grade 4) (Figure 8 A). Elastin degradation in aneurysmal tissue was slightly decreased in TRAF-STOP-treated mice 28 days after AAA induction (Figure 8 B). Specifically, CD40-TRAF6 inhibition resulted in an average grade of elastic fibre destruction of 3.3 compared to an average grade of 3.6 in DMSO-treated mice. In addition, elastic fibre destruction often causes expansion of the medial layer, thus, medial layer thickness of aortic cross-sections of DMSO- and TRAF-STOP-treated mice was determined after staining of elastic fibres using EvG staining. Inhibition of CD40-TRAF6 signalling resulted in a 5-fold decreased medial layer thickness in aortic cross-sections compared to that of DMSO-treated mice, but the change did not rise to the level of statistical significance (Unpaired Mann-Whitney test (two-tailed); p=0.1135) (Figure 8 C).

Furthermore, collagen type IV content was histologically examined in aneurysmal cross-sections of DMSO- and TRAF-STOP-treated mice 28 days after PPE-induced AAA formation. Immunofluorescence staining of collagen type IV revealed a significantly greater amount of collagen type IV in aneurysmal tissue of TRAF-STOP-treated mice. Specifically, 42% collagen type IV positive area per AAA area was determined in mice treated with TRAF-STOP, whereas only 18% collagen type IV positive area per AAA area was detected in aneurysmal cross-sections of DMSO-treated mice (Figure 8 D, E).

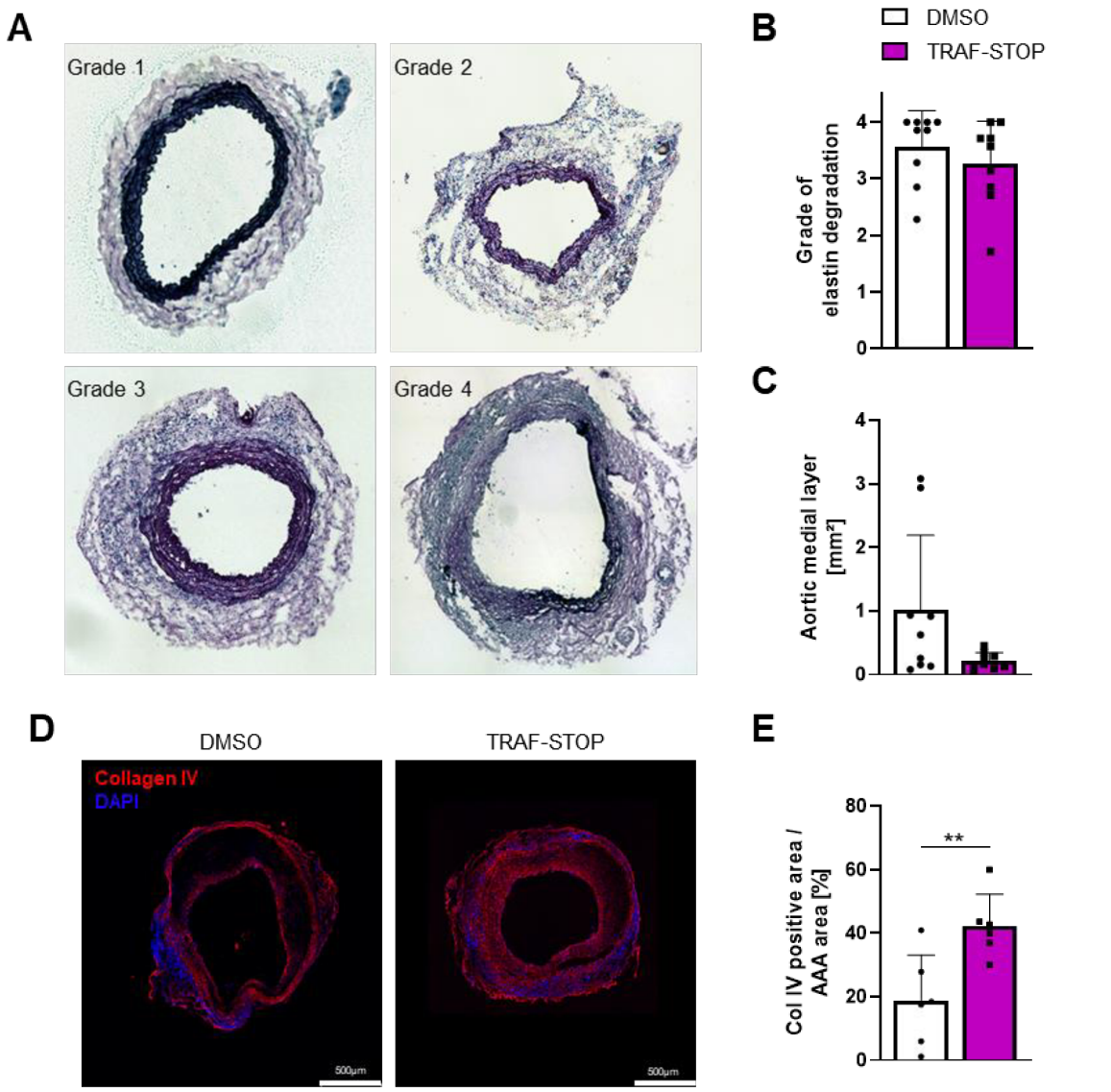

Figure 8: TRAF-STOP treatment led to reduced collagen type IV degradation 28 days after PPE-induced AAA formation

*EvG and collagen type IV staining was performed to evaluate ECM degradation and medial aortic wall thickness in AAA cross-sections from DMSO- and TRAF-STOP-treated mice 28 days after PPE-induced AAA formation. (A) Representative EvG staining of aortic cross-sections, indicating an established grading system used for quantification of elastic fibre degradation. Grade 1: completely intact elastin fibres to isolated elastic fibre breaks; Grade 2: increased amount of elastic fibre breaks to area-wide absence (max 30%) of 1 to 2 elastic fibres; Grade 3: area-wide absence (30-50%) of 2 to 4 elastic fibres; Grade 4: area-wide absence (more than 50%) of 2 to 4 elastic fibres or complete destruction of fibres. (B) Quantification of medial elastic fibre destruction using the established grading system as a mean of grades from 7 sequentially AAA cross-sections from DMSO- and TRAF-STOP-treated mice 28 days after PPE surgery. Unpaired Mann-Whitney test (two-tailed); p=0.2570. Mean ± SD. DMSO n=9, TRAF-STOP n=9. (C) Quantification of medial layer area in aneurysmal tissue as an average of 7 consecutive AAA cross-sections from DMSO- and TRAF-STOP-treated mice 28 days after PPE surgery. Unpaired Mann-Whitney test (two-tailed); p=0.1135. Mean ± SD. DMSO n=9, TRAF-STOP n=9. (D) Representative collagen type IV (red) and cell nuclei (blue) staining in aortic cross-sections from DMSO- and TRAF-STOP-treated mice 28 days after AAA induction. Scale bar = 500 µm. (E) Quantification of collagen type IV positive stained area normalized to whole AAA area as an average of 3 sequentially cross-sections. Unpaired Student's t test (two-tailed), **p<0.01. Mean ± SD. DMSO n=6, TRAF-STOP n=6.*

CD40-TRAF6 inhibition led to reduced *Mmp2* expression in aneurysmal tissue 7 and 14 days after AAA induction

Degradation of the ECM by MMPs is a hallmark of AAA progression. Therefore, the effect of CD40-TRAF6 signalling inhibition by TRAF-STOP on MMP expression levels in aneurysmal tissue was examined by gene expression profiling using Spatial Transcriptomics and CITE sequencing data. *Mmp9* and *Mmp2* mRNA expression was determined using Spatial Transcriptomic technology in aneurysmal cross-sections from DMSO- and TRAF-STOP-treated mice 7 and 14 days after PPE-induced AAA formation. CD40-TRAF6 inhibition led to reduced *Mmp2* mRNA expression in two individual experiments at both endpoints (Figure 9 A). *Mmp9* mRNA expression was decreased in aneurysmal tissue from TRAF-STOP-treated mice 14 days after AAA induction. However, the expression of *Mmp9* varied between the two experiments 7 days after PPE surgery (Figure 9 A).
In addition, CITE sequencing data was generated from collected $CD45^+$ immune cells in single-cell suspension from infrarenal aortic segments from DMSO- and TRAF-STOP-treated mice 7 days after PPE-induced AAA formation. Data analysis of the expression levels of proteolytic MMPs revealed a reduction in *Mmp2* mRNA expression and an increase in *Mmp9* mRNA expression in mice after TRAF-STOP administration (Figure 9 B).

MMPs are synthesised as inactive zymogen[33], thus, MMP expression is not sufficient to state about the proteolytic activity in aneurysmal tissue. Therefore, proteolytic activity of gelatinases, MMP9 and MMP2, was determined in aneurysmal tissue of DMSO- and TRAF-STOP-treated mice 14 days after PPE-induced AAA formation by gelatin gel zymography. Proteolytic activity of MMP9, pro-MMP2 and MMP2 in aortic lysates was detected in zymogram as cleared, white bands (Figure 10 A). Quantification of signal intensity of the bands revealed no changes in the activity of MMP9, pro-MMP2 and MMP2 in aortic lysates upon TRAF-STOP treatment 14 days after AAA induction (Figure 10 B). Analysis of signal intensity of every band is shown in Supplementary Figure 2.

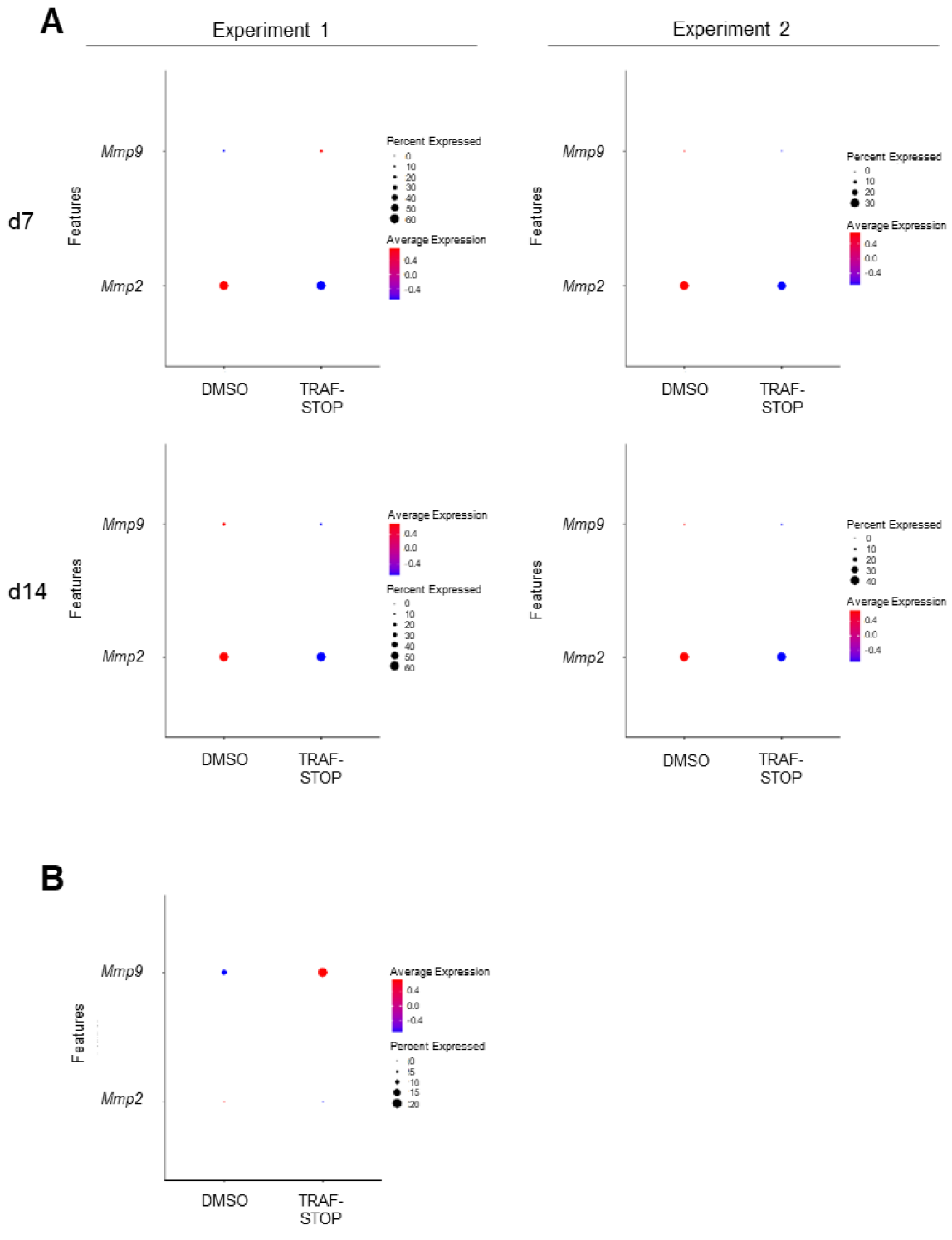

Figure 9: Reduced Mmp2 mRNA expression in aneurysmal tissue after CD40-TRAF6 inhibition
Analysis of Mmp9 und Mmp2 mRNA expression in aneurysmal tissue of DMSO- and TRAF-STOP-treated mice 7 and 14 days after PPE-induced AAA formation. (A) Mmp9 und Mmp2 mRNA expression in aneurysmal cross-sections from two independent experiments each 7 and 14 days after AAA induction revealed by Spatial Transcriptomic data analysis. Analysis of gene expression in one AAA cross-section per independent experiment and per treatment group. DMSO n=2, TRAF-STOP n=2 per endpoint. (B) Mmp9 und Mmp2 mRNA expression in collected CD45⁺ immune cells from digested AAA tissue from DMSO- and TRAF-STOP-treated mice 7 days after PPE surgery determined by CITE sequencing data analysis. DMSO n=1 (two pooled AAA), TRAF-STOP n=1 (two pooled AAA).

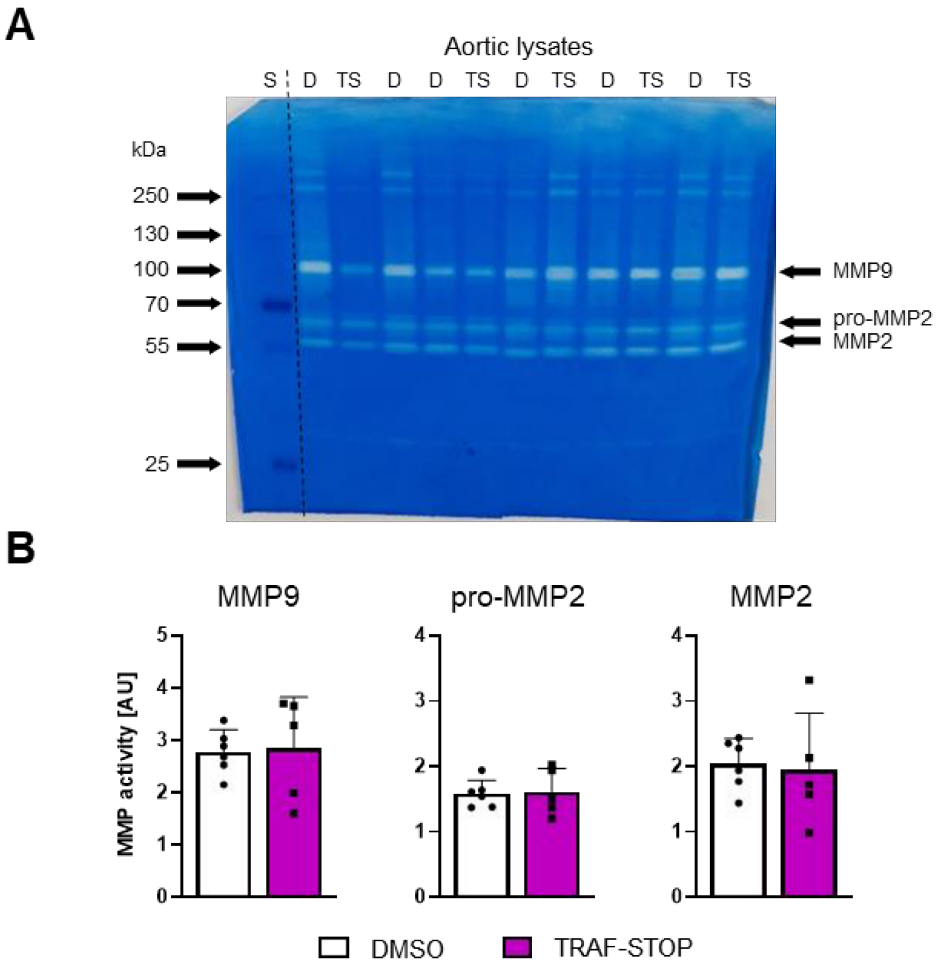

Figure 10: No changes in MMP9, pro-MMP2 and MMP2 activity in aortic lysates after CD40-TRAF6 inhibition
(A) Gelatin gel zymography of aortic lysates from DMSO- and TRAF-STOP-treated mice 14 days after PPE-induced AAA formation. White bands are the result of proteolytic activity. 20 µg of total aortic protein lysate was loaded into every lane. Protein size standard was loaded into the first lane, followed by aortic lysates of treated mice. S = Size standard, D = DMSO, TS = TRAF-STOP (B) Quantification of MMP9, pro-MMP2 and MMP2 activities detected in zymogram by analysing the signal intensity of the bands. Mean ± SD. DMSO n=6, TRAF-STOP n=5.

Flow cytometry revealed a reduction in the proportion of macrophages in aneurysmal tissue after CD40-TRAF6 inhibition

The infiltration of inflammatory cells is a hallmark of AAA formation and development. Therefore, this study examined the distribution of immune cells in aneurysmal tissue as well as in blood circulation of DMSO- compared to TRAF-STOP-treated mice. Flow cytometric analysis was performed of digested aneurysmal tissue 7 and 28 days after PPE-induced AAA formation. For the analysis, side scatter (SSC) and forward scatter (FSC) were used to exclude cell debris and erythrocytes followed by a singlet gate to exclude cell doublets. Next, a gate was applied to identify all viable $CD45^+$ leukocytes. Afterwards $CD11b^+$ $Ly6G^-$ macrophages and $NK1.1^+$ $CD3^-$ $CD19^-$ natural killer cells could be identified. $CD11b^+$ cells were further used to identify $CD11b^+$ $Ly6G^+$ neutrophils. Finally, cells that were negative for CD11b and NK1.1 were used to identify $CD19^+$ B cells (Figure 11 A). Additionally, $CD3^+$ T cells were identified from viable $CD45^+$ leukocytes after excluding any cell debris, erythrocytes and cell doublets. $CD3^+$ T cells were then categorized in $CD4^+$ Th cells and $CD8^+$ cytotoxic T cells (Figure 11 B).

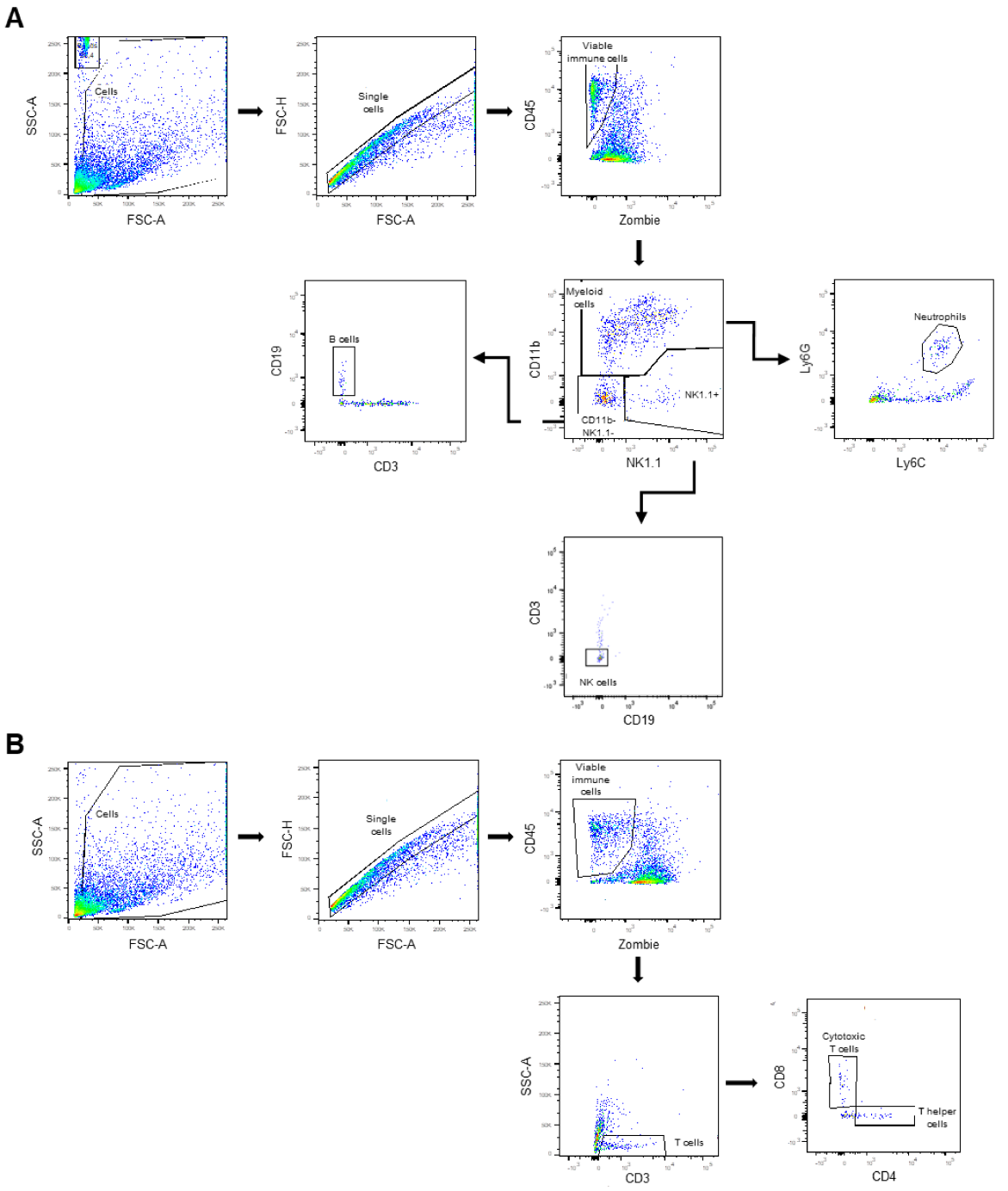

Figure 11: Flow cytometric gating strategies used to identify different immune cell populations in aneurysmal tissue
(A) *Representative gating strategy for identifying distributions of overall immune cells (viable CD45⁺), myeloid cells (CD11b⁺, Ly6G⁻), neutrophils (CD11b⁺, Ly6G⁺), natural killer cells (NK1.1⁺, CD3⁻, CD19⁻) and B cells (CD19⁺) in aneurysmal tissue after AAA induction. (B) Representative gating strategy for identifying overall T cells (CD3⁺), T helper cells (CD3⁺,CD4⁺), and cytotoxic T cells (CD3⁺,CD8⁺) in aneurysmal tissue after AAA induction.*

Flow cytometric analysis of aneurysmal tissue revealed a significant decrease in the CD11b⁺ macrophage proportion in TRAF-STOP-treated mice 28 days after AAA induction, whereas the proportion of macrophages was not altered 7 days after PPE-induced AAA formation (Figure 12 B). This was accompanied by an increase in the proportions of CD19⁺ B cells after inhibition of CD40-TRAF6 signalling 28 days after AAA induction but the change did not rise to the level of statistical significance (Two-way ANOVA with Sidak's multiple

comparisons post test p=0.0897) (Figure 12 E and G). The percentage of $CD3^+$ $CD4^+$ Th cells in aneurysmal tissue of TRAF-STOP-treated mice tend to be enhanced 28 days after AAA induction, although the change did not rise to the level of statistical significance (Two-way ANOVA with Sidak's multiple comparisons post test p=0.3163). The proportions of overall $CD45^+$ immune cells, $CD11b^+$, $Ly6G^+$ neutrophils, $NK1.1^+$ natural killer cells, $CD3^+$ T cells and $CD3^+$ $CD8^+$ cytotoxic T cells were not changed in TRAF-STOP-treated mice compared to DMSO control group 7 and 28 days after PPE-induced AAA formation (Figure 12 A, C, D, F, H).

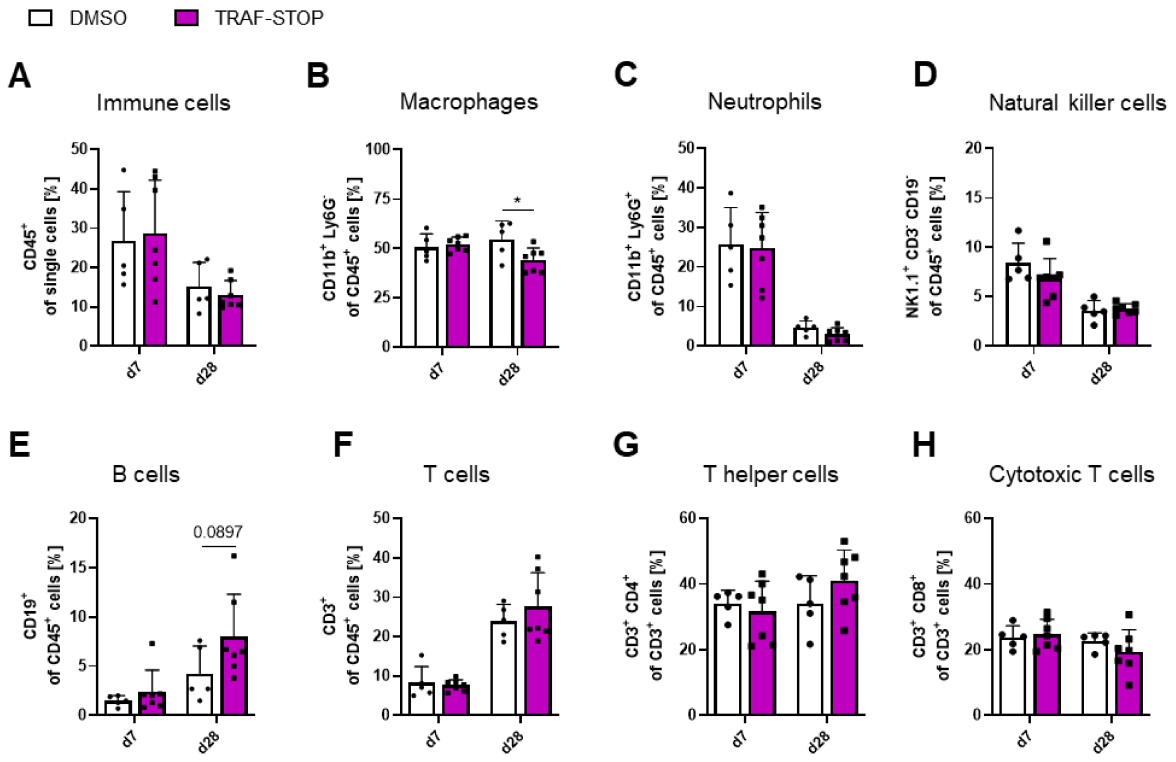

Figure 12: Decreased proportion of macrophages in aneurysmal tissue of TRAF-STOP-treated mice 28 days after PPE-induced AAA formation

*Flow cytometric analysis of different immune cell populations from single cell suspension of aneurysmal tissue from mice treated with DMSO or TRAF-STOP 7 and 28 days after PPE surgery. Proportions of overall $CD45^+$ immune cells (A), $CD11b^+$ $Ly6G^+$ neutrophils (C), $NK1.1^+$ $CD3^-$ $CD19^-$ natural killer cells (D), $CD3^+$ T cells (F) and $CD3^+$ $CD8^+$ cytotoxic T cells (H) were not altered in mice upon TRAF-STOP treatment after AAA induction. The amount of $CD11b^+$ $Ly6G^-$ macrophages (B) was significantly reduced in AAA tissue from TRAF-STOP-treated mice 28 days post PPE-surgery. The percentage of $CD19^+$ B cells (E) and $CD3^+$ $CD4^+$ T helper cells (G) was slightly increased in AAA tissue from TRAF-STOP-treated mice 28 days after AAA induction. Two-way ANOVA with Sidak's multiple comparisons post test; *p<0.05. Mean ± SD. DMSO n=5, TRAF-STOP n=7.*

To assess the accompanying systemic inflammation, whole blood samples after DMSO and TRAF-STOP administration were analysed using an automated haematology analyser. Measurements showed no differences in the numbers of circulating leukocytes, lymphocytes, monocytes and neutrophils in TRAF-STOP-treated mice compared to DMSO-treated mice 7 and 28 days after AAA induction (Figure 13 A-D).

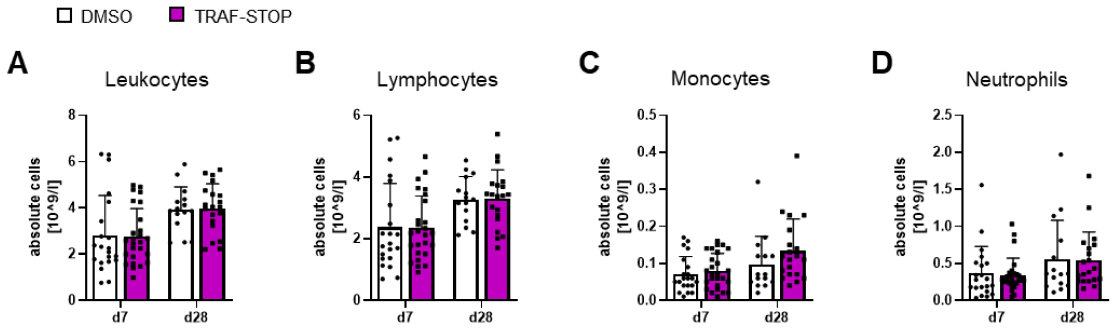

Figure 13: Numbers of circulatory immune cells were not affected after CD40-TRAF6 inhibition
Absolute cell numbers of leukocytes (A), lymphocytes (B), monocytes (C) and neutrophils (D) were measured using an automated haematology analyser in whole blood samples from DMSO- and TRAF-STOP-treated mice 7 and 28 days after PPE-induced AAA formation. Haematology analysis revealed no differences between treatment groups. Mean ± SD. DMSO n=21 (d7), n = 15 (d28), TRAF-STOP n=26 (d7), n = 20 (d28).

Reduced *Tnfa* expression in aneurysmal tissue upon CD40-TRAF6 inhibition 14 days after PPE-induced AAA formation

The inflammatory response leading to AAA development and progression is driven by the release of several cytokines and chemokines. Therefore, the expression of different cytokines and chemokines contributing to inflammatory processes were investigated in aneurysmal tissue as well as in blood circulation of DMSO- and TRAF-STOP-treated mice 7 and 14 days after PPE-induced AAA formation.

Cytokine mRNA expression levels of *Ccl2*, *Tnfa*, *Il6*, *Il1b* und *Il1a* were analysed in Spatial Transcriptomic data of AAA cross-sections from two DMSO- and TRAF-STOP-treated mice 7 and 14 days after AAA induction. Spatial Transcriptomic analysis revealed a reduced *Tnfa* mRNA expression after CD40-TRAF6 signalling inhibition at both time points. *Ccl2* mRNA expression differed between the two experiments 7 days after PPE surgery, but higher expression levels were detected in TRAF-STOP-treated mice 14 days after AAA induction. The expression levels of *Il6* and *Il1b* varied between the two experiments 7 and 14 days after PPE surgery. *Il1a* expression was only detectable in one out of two treated mice at each endpoint. However, AAA cross-sections of TRAF-STOP-treated mice showed higher expression levels of *Il1a* at both time points compared to DMSO-treated ones (Figure 14 A, B).

Furthermore, changes in cytokine mRNA expression were examined in collected viable $CD45^+$ cells from aneurysmal tissue of DMSO- and TRAF-STOP-treated mice 7 days post PPE surgery using CITE sequencing data analysis. CD40-TRAF6 inhibition resulted in increased *Tnfa, Il1b* und *Il1a* expression, whereas *Ccl2* and *Il6* expression levels were reduced in immune cells of aneurysmal tissue from TRAF-STOP-treated mice compared to DMSO-treated ones (Figure 15).

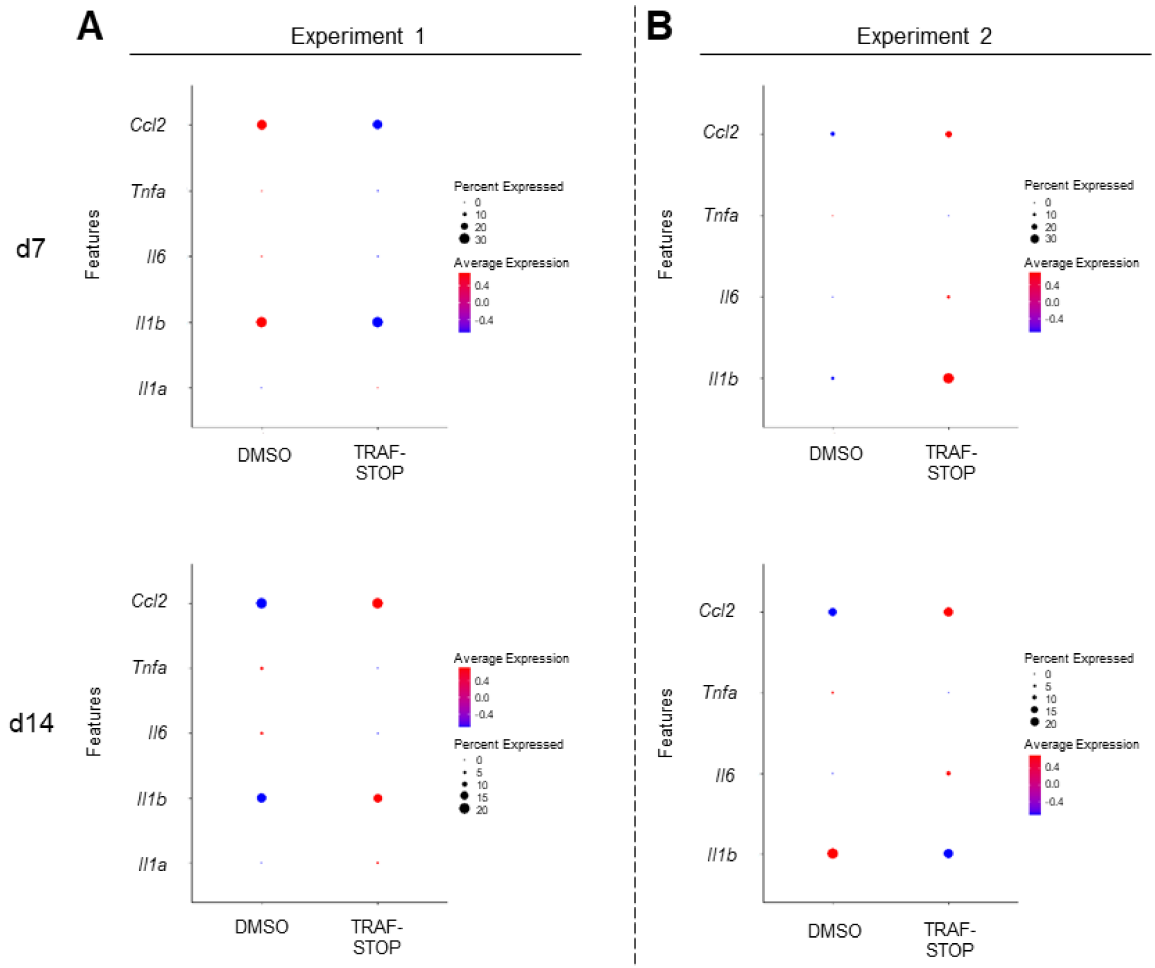

Figure 14: Altered cytokine mRNA expression in aneurysmal tissue after CD40-TRAF6 inhibition
Analysis of Ccl2, Tnfa, Il6, Il1b und Il1a mRNA expression in aneurysmal cross-sections of DMSO- and TRAF-STOP-treated mice 7 and 14 days after PPE-induced AAA formation using Spatial Transcriptomics technology. Analysis of gene expression was performed in one AAA cross-section per independent experiment per endpoint. (A, B) Dot plots of data analysis from individual experiments at both time points. Tnfa mRNA expression was reduced in TRAF-STOP-treated mice at both time points. No consistent mRNA expression of Ccl2, Il6, Il1b und Il1a between both analysed time points. Il1a expression was only detectable in one experiment.

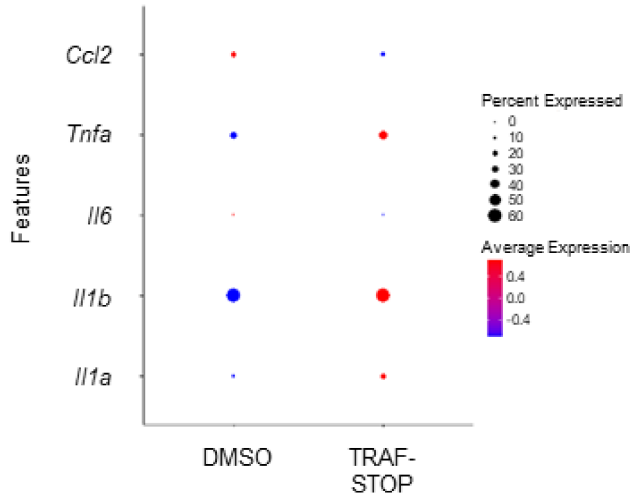

Figure 15: Cytokine mRNA expression in immune cells from aneurysmal tissue after CD40-TRAF6 inhibition
Dot plot of Ccl2, Tnfa, Il6, Il1b und Il1a mRNA expression in collected CD45⁺ cells from AAA tissue from DMSO- and TRAF-STOP-treated mice 7 days after PPE-induced AAA formation generated by CITE sequencing data

analysis. Ccl2 and Il6 mRNA expression was higher in DMSO-treated mice compared to TRAF-STOP-treated ones, whereas Tnfa, Il1b and Il1a mRNA expression was increased in TRAF-STOP-treated mice. DMSO n=1 (two pooled AAA), TRAF-STOP n=1 (two pooled AAA).

Since mRNA expression and concentration of one secreted cytokine can differ in physiologic conditions, the effect of CD40-TRAF6 signalling inhibition was examined on cytokine levels in aneurysmal lysates 7 days after PPE-induced AAA formation using a bead-based immunoassay and flow cytometry. Protein concentration of IL-1α, IL-1β, IL-6, TNFα and CCL2 was measurable in AAA tissue of DMSO- and TRAF-STOP-treated mice. However, protein concentrations of these cytokines normalized to the weight of analysed aneurysmal tissue was similar between both treatment groups (Figure 16 A-E).

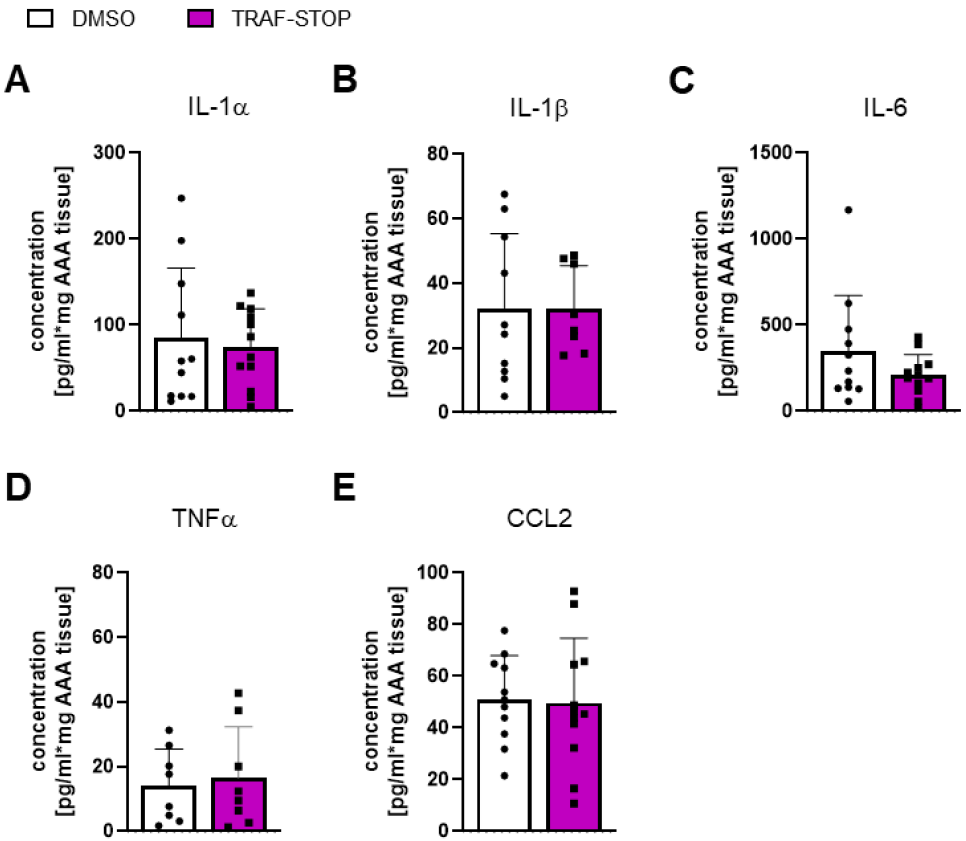

Figure 16: Pro-inflammatory cytokine concentrations in aneurysmal tissue were not altered after CD40-TRAF6 inhibition
Quantification of cytokine concentration of IL-1α (A), IL-1β (B), IL-6 (C), TNFα (D) and CCL2 (E) in aortic lysates of DMSO- and TRAF-STOP-treated mice 7 days post PPE-induced AAA formation normalized to AAA weight and measured by a bead-based immunoassay. Mean ± SD. DMSO n=8-11, TRAF-STOP n=8-12.

CD40-TRAF6 inhibition led to decreased plasma levels of IL-12 and IL-17 28 days after PPE-induced AAA formation

Puchenkova et al. reported that in human AAA patients, blood levels of various cytokines were changed compared to controls.[74] Therefore, the systemic effect of the inhibition of CD40-TRAF6 signalling on plasma concentration of several cytokines was analysed in DMSO- and TRAF-STOP-treated mice 28 days after PPE-induced AAA formation. Analysis of a bead-based immunoassay revealed that TRAF-STOP treatment led to significantly reduced plasma concentrations of IL-12 and IL-17 compared to DMSO-treated controls (Figure 17 E, F). In addition, IL-1β as well as IFN-β concentrations in plasma of mice after TRAF-STOP administration were decreased compared to DMSO-treated mice, but the

change did not rise to the level of statistical significance (unpaired Mann-Whitney test (two-tailed); both p=0.0952) (Figure 17 B, J). However, plasma concentrations of IL-1α, IL-6, IL-10, IL-23, IL-27, TNFα, IFN-γ, CCL2 and GM-CSF were similar in both treatment groups (Figure 17 A, C, D, G, H, I, K, L and M).

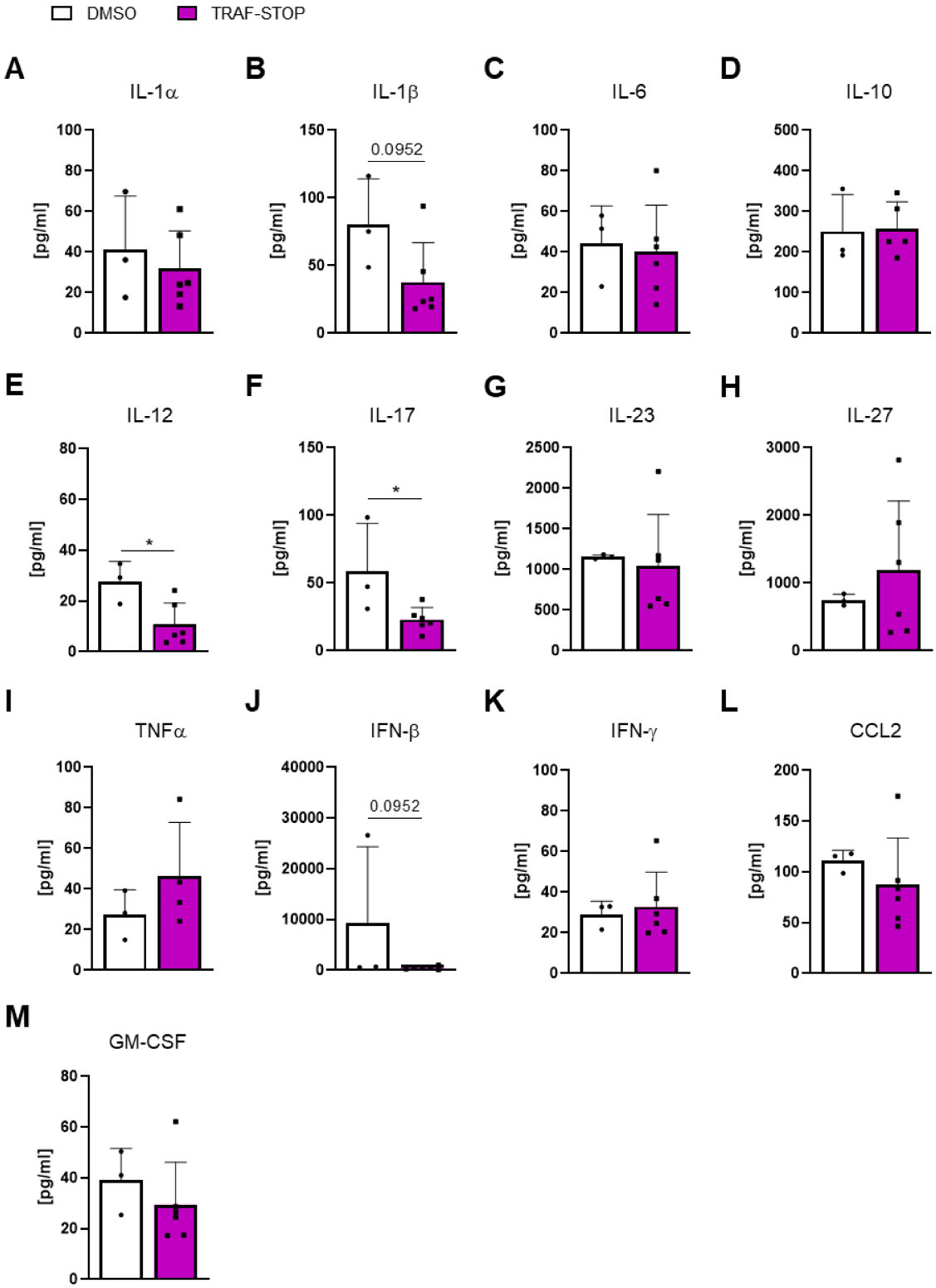

Figure 17: Reduced IL-12 and IL-17 concentration in plasma after CD40-TRAF6 inhibition
Quantification of cytokine concentrations in plasma from mice treated with DMSO or TRAF-STOP 28 days after PPE-induced AAA formation measured by a bead-based immunoassay. Plasma concentration of IL-12 (E) and IL-17 (F) was decreased upon TRAF-STOP treatment. Unpaired Student's t test (two-tailed) (A, C, D, E, F, G,

*H, I, L) and unpaired Mann-Whitney test (two-tailed) (B, J, K, M); *p<0.05. Mean ± SD. DMSO n=2-3, TRAF-STOP n=4-6.*

Inhibition of CD40-TRAF6 signalling did not alter diastolic blood pressure

Hypertension has been associated with a higher risk of AAA.[115] Therefore, this study investigated the systemic effect on systolic and diastolic blood pressure, heart rate and body weight after three and seven days of DMSO and TRAF-STOP administration without AAA induction using invasive blood pressure measurements. Systolic blood pressure was significantly increased in TRAF-STOP-treated mice compared to DMSO-treated ones after three days of administration. However, this effect was abrogated after seven days of treatment (Figure 18 A). Diastolic blood pressure, heart rate and body weight were similar in both treatment groups after three and seven days of treatment (Figure 18 B-D).

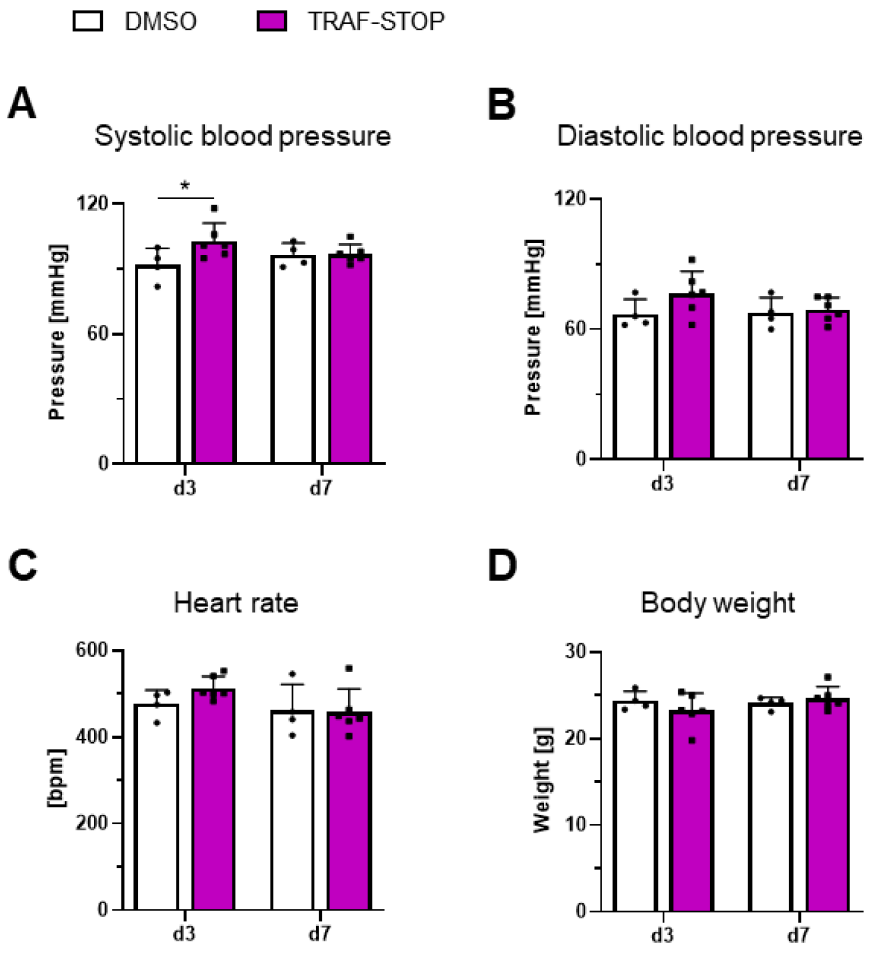

Figure 18: Blood pressure, heart rate and body weight of mice were not altered after CD40-TRAF6 inhibition after 7 days of treatment

*Analysis of systolic blood pressure (A), diastolic blood pressure (B), heart rate (C) and body weight (D) of C57BL/6J mice treated with DMSO and TRAF-STOP for three and seven days (every second day) without prior AAA induction. Inhibition of CD40-TRAF6 signalling for three days led to higher systolic blood pressure. However, after seven days of administration systolic blood pressure was restored and similar in treatment groups. Diastolic blood pressure, heart rate and body weight of mice were also similar in treatment groups after three and seven days of administration. Two-way ANOVA with Sidak's multiple comparison post test; *p<0.05. Mean ± SD. DMSO n=4, TRAF-STOP n=6.*

Inhibition of CD40-TRAF6 signalling protected against aneurysmal rupture in *Apoe*$^{-/-}$ mice on standard chow diet after AngII-induced AAA formation

Different experimental mouse models are well established to study AAA pathology and identify potential therapeutic targets in *in vivo* research. Nevertheless, each model has its limitations and can only partially mimic processes of human AAA development.[8] This study addresses this issue by investigating CD40-TRAF6 signalling inhibition in the PPE-induced as well as in the AngII-induced AAA model.
Therefore, *Apoe*$^{-/-}$ mice were continuously infused with 1 µg/kg*min AngII by subcutaneously implanted osmotic pumps. These mice received DMSO (2.5%) as solvent control or TRAF-STOP (10 µmol/kg) three times per week starting on day of implantation for 28 days after AAA induction. In this experimental part of the study, *Apoe*$^{-/-}$ mice were fed a standard chow diet and aortic dilation was assessed weekly by ultrasound imaging (Figure 19).

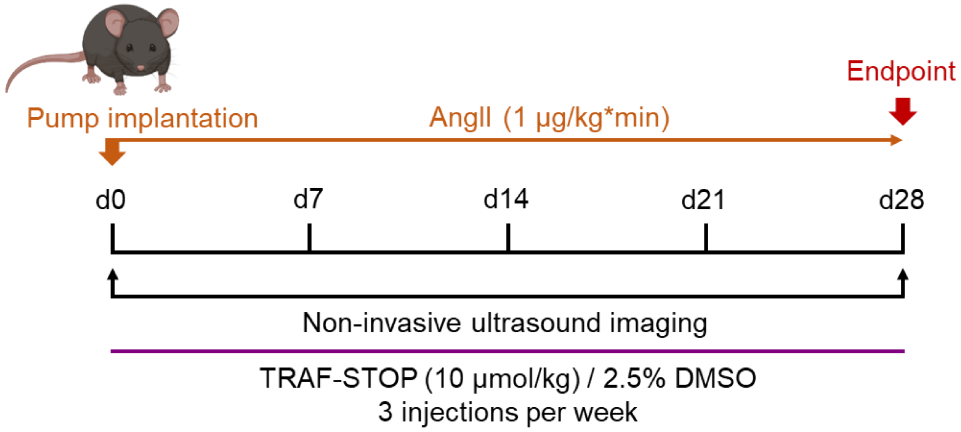

Figure 19: Experimental design to investigate the effects of CD40-TRAF6 inhibition in the AngII model with mice on standard chow diet
*Experimental setup. Aneurysms were induced by continuous infusion of Angiotensin (Ang) II (1 µg/kg*min) through subcutaneously implanted osmotic pumps into hyperlipidaemic Apoe*$^{-/-}$ *mice. From the day of surgery, mice were treated with 2.5% DMSO or 10 µmol/kg TRAF-STOP three times per week. Over the whole experimental period, mice were fed a standard chow diet. Prior to surgery and on the day of organ harvesting, non-invasive ultrasound imaging was used to assess aortic dilation. Mice were sacrificed and organs were harvested 28 days post surgery.*

Observations showed, that CD40-TRAF6 blockage by TRAF-STOP remarkably protected against AAA rupture. Specifically, 8 out of 22 DMSO-treated *Apoe*$^{-/-}$ mice died from aortic rupture, corresponding to a survival rate of 63.6%, whereas, only 6 out of 25 TRAF-STOP-treated mice died, resulting in a survival rate of 76%, but the change did not rise to the level of statistical significance (Log-rank (Mantel-Cox) test p=0.2860) (Figure 20 A). Analysis of ultrasound images revealed a similar abdominal aortic expansion as well as ascending aortic dilation in both treatment groups 28 days after AngII-induced AAA formation (Figure 20 B, D). As in the PPE model, the formation of an aortic aneurysm was defined by a 1.5-fold increase in aortic diameter. An AAA was developed by 16 out of 22 DMSO-treated and 16 out of 25 TRAF-STOP-treated *Apoe*$^{-/-}$ mice 28 days after pump implantation. Thus, AAA incidence was similar in both treatment groups, 73% to 64% (Figure 20 C). Assessment of TAA incidence in the ascending aorta showed that 10 out of 21 DMSO-treated and 6 out of 23 TRAF-STOP-treated *Apoe*$^{-/-}$ mice developed a TAA 28 days after AAA induction, corresponding to TAA incidences of 48% and 26%, but this change did not rise to the level of statistical significance (Two-sided Fisher's exact test; p=0.2106) (Figure 20 E). In this experimental set-up, *Apoe*$^{-/-}$ mice were more prone to develop AAA than TAA (Figure 20 C, E).

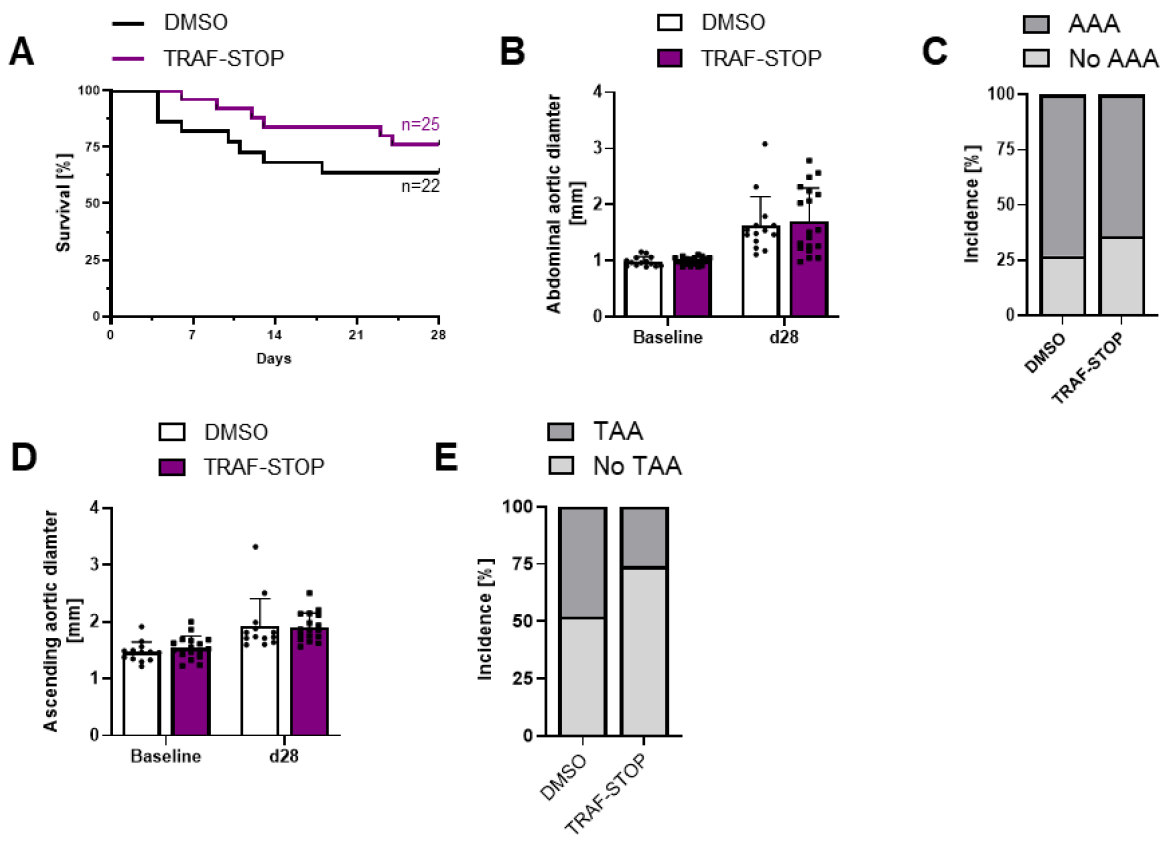

Figure 20: CD40-TRAF6 inhibition led to a slightly improved survival rate after AngII-induced AAA formation
AAAs were induced by continuous AngII infusion of Apoe$^{-/-}$ mice on standard chow diet. (A) Kaplan-Meier curve displayed the percentage of survival of DMSO- and TRAF-STOP-treated Apoe$^{-/-}$ mice 28 days after AngII-induced AAA formation. Log-rank (Mantel-Cox) test p=0.2860. DMSO n=22, TRAF-STOP n=25. (B) Analysis of abdominal aortic diameter using ultrasound images before (Baseline) and 28 days after pump implantation. Mean ± SD. DMSO n=14, TRAF-STOP n=19. (C) Percentage of AAA or no AAA incidence in Apoe$^{-/-}$ mice on standard chow diet treated with DMSO or TRAF-STOP 28 days after AAA induction. DMSO n=22, TRAF-STOP n=25. (D) Analysis of ascending aortic diameter using ultrasound images prior to (Baseline) and 28 days after AngII pump implantation. Mean ± SD. DMSO n=13, TRAF-STOP n=17. (E) Incidence of TAA or no TAA in Apoe$^{-/-}$ mice on standard chow diet upon DMSO or TRAF-STOP treatment 28 days after AAA induction. DMSO n=21, TRAF-STOP n=23. AAA and TAA were defined as an increase in aortic diameter of at least 1.5-fold. Animals that died due to AAA or TAA rupture were included in determination of incidences. AAA = Abdominal aortic aneurysm, TAA = Thoracic aortic aneurysm.

CD40-TRAF6 inhibition led to a noticeable reduction in the T cell proportion of AAA tissue from *Apoe*$^{-/-}$ mice

Immune cells play a crucial role in promoting AAA formation and progression, thus, the distribution of different immune cells in digested AAA tissue and in blood circulation of DMSO- and TRAF-STOP-treated *Apoe*$^{-/-}$ mice on standard chow diet was investigated 28 days after AngII-induced AAA formation. Flow cytometric analysis revealed no changes in the proportion of overall CD45$^+$ immune cells, CD11b$^+$ Ly6G$^-$ macrophages, CD11b$^+$ Ly6G$^+$ neutrophils, NK1.1$^+$ CD3$^-$ CD19$^-$ natural killer cells, CD19$^+$ B cells, CD3$^+$ CD4$^+$ Th cells and CD3$^+$ CD8$^+$ cytotoxic T cells in aneurysmal tissue of TRAF-STOP-treated *Apoe*$^{-/-}$ mice compared to DMSO- treated ones (Figure 21). However, the proportion of CD3$^+$ T cells in AAA tissue after TRAF-STOP administration was reduced by 4.2% compared to DMSO treatment 28 days after AngII-induced AAA formation, but the change did not rise to the level of statistical significance (p=0.0752; unpaired Student's t test (two-tailed)) (Figure 21F).

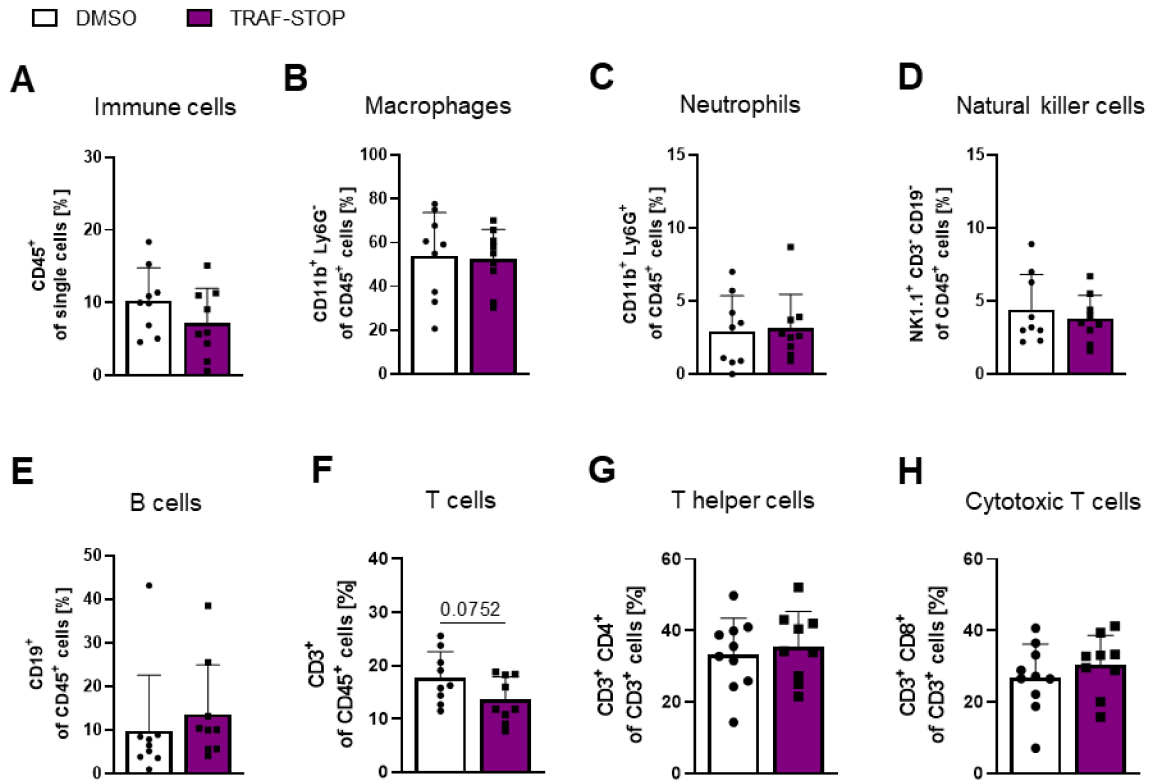

Figure 21: CD40-TRAF6 inhibition led to no significant changes in immune cell proportions in aneurysmal tissue of Apoe$^{-/-}$ mice after AAA induction

Flow cytometric analysis of different immune cell populations in digested AAA tissue from Apoe$^{-/-}$ mice on standard chow diet treated with DMSO or TRAF-STOP 28 days after AngII-induced AAA formation. The CD3^{+} T cell proportion (F) was slightly decreased in AAA tissue from TRAF-STOP-treated mice compared to DMSO-treated ones. Whereas the proportions of overall CD45^{+} immune cells (A), CD11b^{+} Ly6G^{-} macrophages (B), CD11b^{+} Ly6G^{+} neutrophils (C), NK1.1^{+} CD3^{-} CD19^{-} natural killer cells (D), CD19^{+} B cells (E) and CD3^{+} CD4^{+} T helper cells (G) and CD3^{+} CD8^{+} cytotoxic T cells (H) were similar in aneurysmal tissue from both treatment groups. Unpaired Student's t test (two-tailed). Mean ± SD. DMSO n=9-10, TRAF-STOP n=9.

Moreover, the systemic effect of inhibiting the CD40-TRAF6 signalling on circulatory immune cell numbers in whole blood samples was examined using an automated haematology analyser. Numbers of circulatory leukocytes, lymphocytes, monocytes as well as neutrophils were similar in DMSO- and TRAF-STOP-treated *Apoe$^{-/-}$* mice on standard chow diet 28 days after AngII-induced AAA formation (Figure 22).

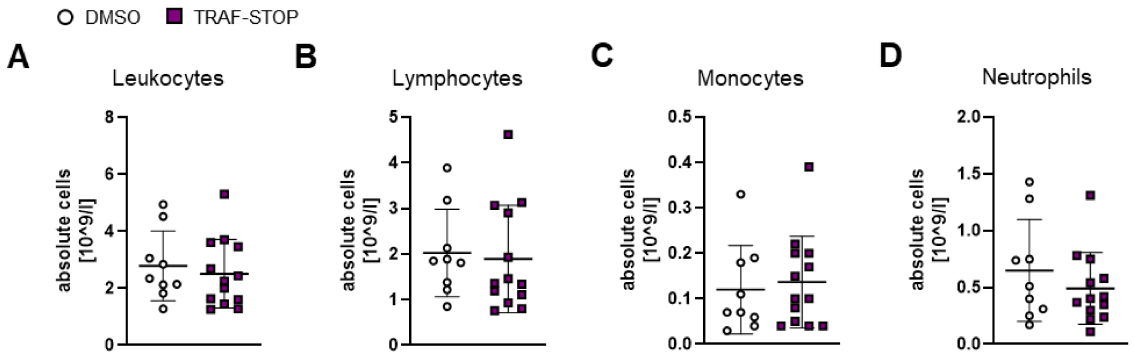

Figure 22: CD40-TRAF6 inhibition did not affect numbers of circulatory immune cells after AAA induction

Absolute cell numbers of leukocytes (A), lymphocytes (B), monocytes (C) and neutrophils (D) were determined in whole blood samples from DMSO- and TRAF-STOP-treated Apoe$^{-/-}$ mice on standard chow diet 28 days after AngII-induced AAA formation using an automated haematology analyser. Similar immune cell numbers were detected in both treatment groups. Mean ± SD. DMSO n=9, TRAF-STOP n=13.

CD40-TRAF6 inhibition resulted in a noticeable decrease of TNFα plasma concentration in *Apoe*$^{-/-}$ mice 28 days after AAA induction

Additionally, the systemic effect of CD40-TRAF6 inhibition on plasma concentrations of several cytokines was investigated in DMSO- and TRAF-STOP-treated *Apoe*$^{-/-}$ mice on standard chow diet 28 days after AngII-induced AAA formation. Analysis of bead-based immunoassay revealed similar concentrations of IL-1α, IL-1β, IL-6, IL-10, IL-12, IL-17, IL-23, IL-27, IFN-β, IFN-γ, CCL2 and GM-CSF in plasma from both treatment groups (Figure 23 A-H, J-M). However, CD40-TRAF6 signalling inhibition resulted in a reduction of TNFα plasma concentration compared to DMSO-treated *Apoe*$^{-/-}$ mice, but the change did not rise to the level of statistical significance (unpaired Student's t test (two-tailed); p=0.0803) ((Figure 23 I).

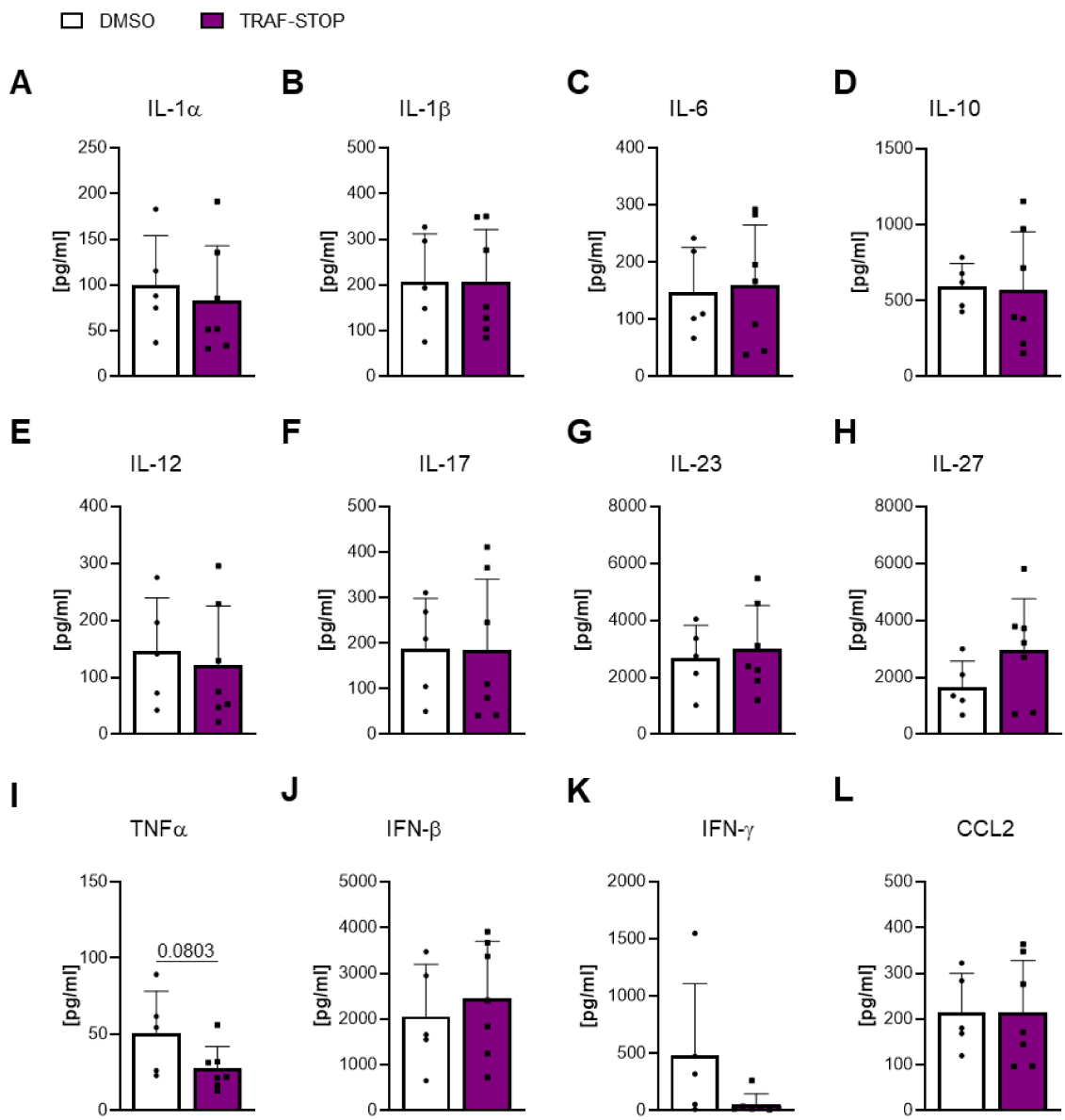

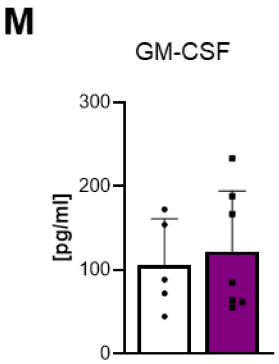

Figure 23: No significant changes in plasma cytokine concentrations after CD40-TRAF6 inhibition in Apoe$^{-/-}$ mice 28 days after AAA induction

Cytokine concentrations in plasma from Apoe$^{-/-}$ mice on standard chow diet treated with DMSO or TRAF-STOP 28 days after AngII-induced AAA formation measured by a bead-based immunoassay. TRAF-STOP treatment led to a slight reduction in TNFα (I) plasma concentration, whereas cytokine concentrations of IL-1α, IL-1β, IL-6, IL-10, IL-12, IL-17, IL-23, IL-27, IFN-β, IFN-γ, CCL2 and GM-CSF were similar in both treatment groups (A-H, J-M). Unpaired Student's t test (two-tailed). Mean ± SD. DMSO n=5, TRAF-STOP n=7.

CD40-TRAF6 signalling inhibition resulted in a remarkably reduction in aortic dilation using a more severe AngII model

This study showed a potential protective effect after pharmacological CD40-TRAF6 inhibition using TRAF-STOP on AAA formation in the PPE model and minor evidence regarding survival rate after AAA rupture in the AngII model. Therefore, the impact of inhibiting the CD40-TRAF6 signalling on AAA development and rupture was confirmed using a more severe AngII model. In this experimental setup, male *Apoe*$^{-/-}$ mice were continuously infused with AngII at a rate of 1 µg/kg*min using subcutaneously implanted osmotic pumps. Additionally, these mice received DMSO (2.5%) or TRAF-STOP (10 µmol/kg) three times per week starting on the day of implantation over the entire experimental period of 28 days. Commencing with pump implantation *Apoe*$^{-/-}$ mice were fed a WD and aortic dilation was assessed prior to and 28 days after pump implantation by ultrasound imaging (Figure 24).

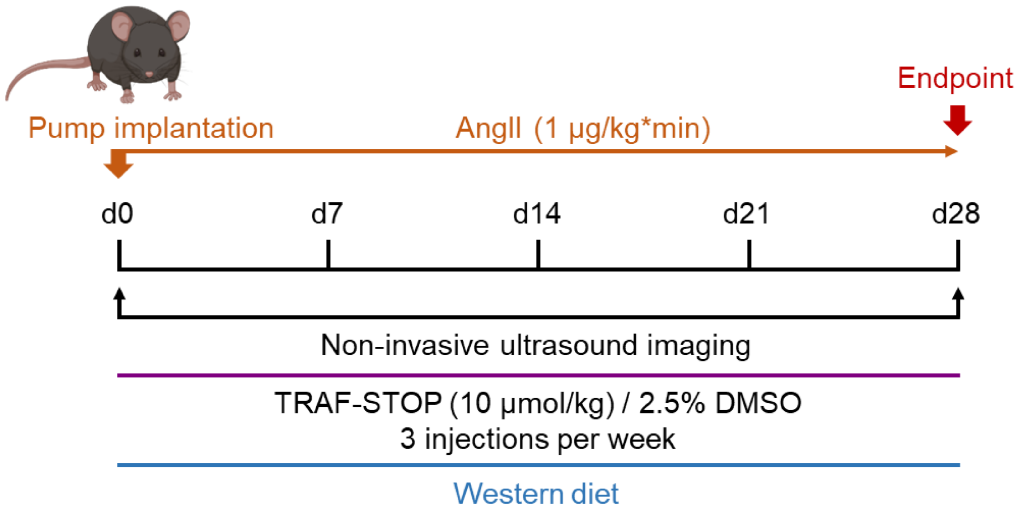

Figure 24: Experimental design to investigate inhibition of CD40-TRAF6 signalling in a severe AngII model
*Experimental setup. Aneurysms were induced by continuous infusion of Angiotensin (Ang) II at a rate of 1 µg/kg*min through subcutaneously implanted osmotic pumps into hyperlipidaemic Apoe*$^{-/-}$ *mice. From the day of surgery, mice were fed a WD and treated with 2.5% DMSO or 10 µmol/kg TRAF-STOP three times per week. Prior to surgery and on the day of organ harvesting, non-invasive ultrasound imaging was performed to assess aortic dilation. Mice were sacrificed and organs were harvested 28 days post surgery.*

The effects of CD40-TRAF6 signalling blockage by TRAF-STOP were investigated in a more severe AngII model on 25 *Apoe*$^{-/-}$ mice, which were implanted an osmotic pump filled with AngII and which were fed a WD. Of these animals, 13 were treated with DMSO and 12 with TRAF-STOP. DMSO administration led to a mortality rate of 53.85% in *Apoe*$^{-/-}$ mice, whereas only one third (33.33%) of the TRAF-STOP-treated mice died due to aortic rupture 28 days after AAA induction (Log-rank (Mantel-Cox) test p=0.4102) (Figure 25 A). Abdominal aortic dilation was assessed using non-invasive ultrasound imaging prior to and 28 days after pump implantation. DMSO-treated mice developed greater AAA compared to TRAF-STOP-treated *Apoe*$^{-/-}$ mice. Mean AAA diameter was 2.1 mm in DMSO-treated mice, and 1.6 mm in TRAF-STOP-treated mice, but the change did not rise to the level of statistical significance (Two-way ANOVA with Sidak's multiple comparisons post test; p=0.1435) (Figure 25 B). In this set-up, 12 out of 13 DMSO-treated *Apoe*$^{-/-}$ mice developed an AAA, corresponding to an AAA incidence of 92.3%. In contrast, 8 out of 12 mice

developed an AAA after TRAF-STOP administration, corresponding to a noticeable reduction in AAA incidence of 66.67% 28 days after AngII-induced AAA induction (Two-sided Fisher's exact test; p=0.1602) (Figure 25 C). Continuous infusion with AngII can also lead to the development of TAAs, thus, ascending aortic diameter was also assessed using ultrasound imaging. However, the expansion of ascending aortic diameter was similar in both treatment groups 28 days after pump implantation (Figure 25 D). TAA incidence was slightly reduced in TRAF-STOP-treated mice compared to the DMSO-treated ones 28 days after pump implantation, corresponding to TAA incidences of 41.67% and 61.5% respectively (Two-sided Fisher's exact test; p=0.4338) (Figure 25 E). It could be observed that *Apoe*$^{-/-}$ mice continuously infused with AngII and on WD diet were more susceptible to develop AAA than TAA regardless of treatment. An AAA incidence of 92.3% and 66.67% was observed compared to a TAA incidence of 61.5% and 41.67% in DMSO- and TRAF-STOP-treated mice, respectively (Figure 25 C, E).

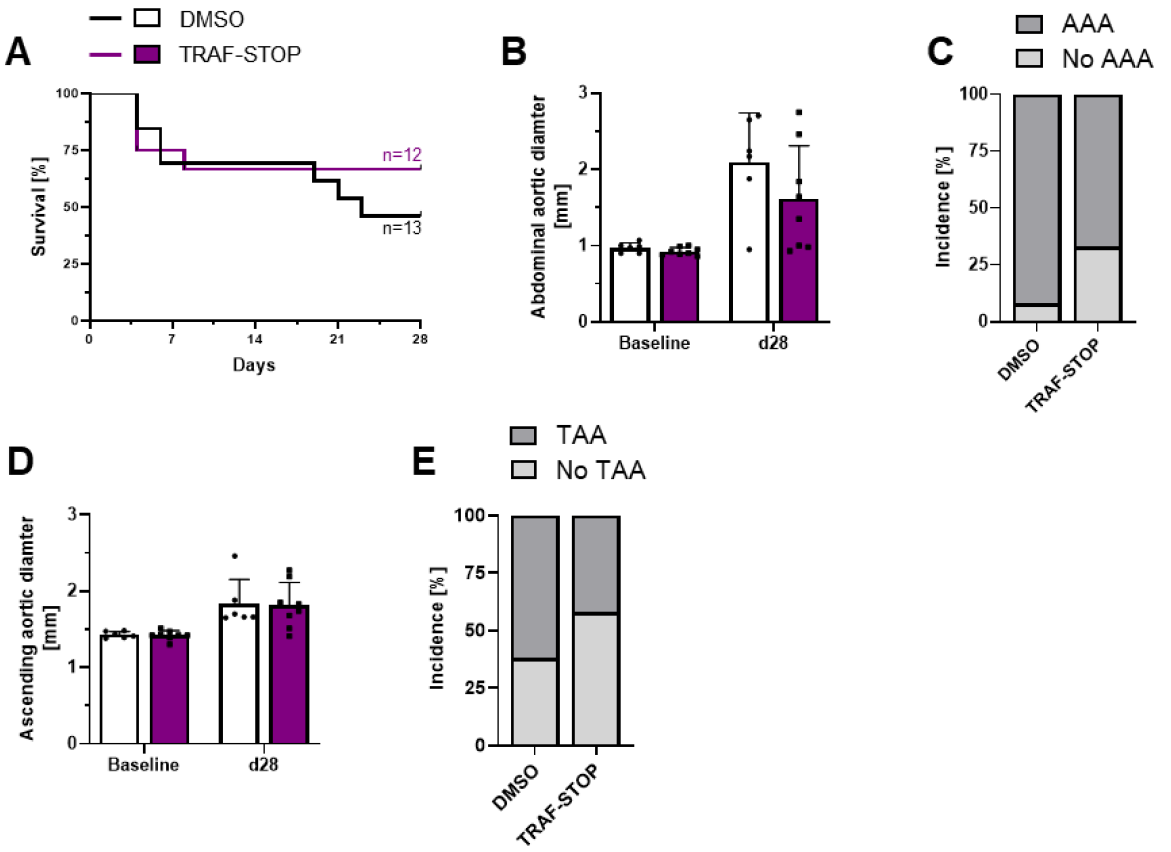

Figure 25: Remarkably reduction of mortality rate and aortic dilation in Apoe$^{-/-}$ mice after CD40-TRAF6 inhibition and AAA induction

AAAs were induced by continuous AngII infusion of Apoe$^{-/-}$ mice on WD diet. (A) *Kaplan-Meier curve shows the percentage survival of DMSO- and TRAF-STOP-treated Apoe$^{-/-}$ mice 28 days after AngII-induced AAA formation. Log-rank (Mantel-Cox) test p=0.4102. DMSO n=13, TRAF-STOP n=12. (B) Analysis of abdominal aortic diameter using ultrasound images before pump implantation (Baseline) and 28 days after AAA induction. Two-way ANOVA with Sidak's multiple comparisons post test; p=0.1435. Mean ± SD. DMSO n=6, TRAF-STOP n=8. (C) Incidence of AAA or no AAA upon DMSO and TRAF-STOP treatment 28 days after AAA induction. Animals that died due to AAA rupture were included. Two-sided Fisher's exact test; p=0.1602. DMSO n=13, TRAF-STOP n=12. (D) Analysis of ascending aortic diameter using ultrasound images before (Baseline) and 28 days after pump implantation. Mean ± SD. DMSO n=6, TRAF-STOP n=8. (E) Incidence of TAA or no TAA after DMSO and TRAF-STOP administration 28 days after AAA induction. Animals that died due to TAA rupture were included. Two-sided Fisher's exact test; p=0.4338. DMSO n=13, TRAF-STOP n=12. AAA and TAA were defined as an increase in aortic diameter of at least 1.5-fold. AAA = Abdominal aortic aneurysm, TAA = Thoracic aortic aneurysm.*

Decreased proportion of neutrophils and enhanced T cell proportion in AAA tissue of *Apoe*$^{-/-}$ mice after CD40-TRAF6 inhibition and AngII-induced AAA formation

AAA development and progression are crucially driven by the infiltration of various immune cells into the aneurysmal tissue. Therefore, the levels of several immune cell populations in AAA tissue as well as in blood circulation of DMSO- and TRAF-STOP-treated *Apoe*$^{-/-}$ mice on WD diet were examined 28 days after AngII-induced AAA formation. Flow cytometric analysis of digested AAA tissue revealed a significant reduction of the CD11b^{+} Ly6G^{+} neutrophil proportion after TRAF-STOP administration. Neutrophil proportions in DMSO- and TRAF-STOP-treated mice were 13.05% and 5.58% (Figure 26 C). CD40-TRAF6 inhibition led to a significant increase in CD3^{+} T cell frequency in AAA tissue (Figure 26 F). Furthermore, the proportion of CD3^{+} CD8^{+} cytotoxic T cells was 1.5-fold higher in mice after TRAF-STOP administration compared to DMSO treatment, but the change did not rise to the level of statistical significance (unpaired Mann-Whitney test (two-tailed); p=0.1658) (Figure 26 H). The percentage of overall CD45^{+} immune cells, CD11b^{+} Ly6G^{-} macrophages, NK1.1^{+} CD3^{-} CD19^{-} natural killer cells, CD19^{+} B cells and CD3^{+} CD4^{+} Th cells in AAA tissue was similar in both treatment groups 28 days after AAA induction (Figure 26 A, B, D, E, G).

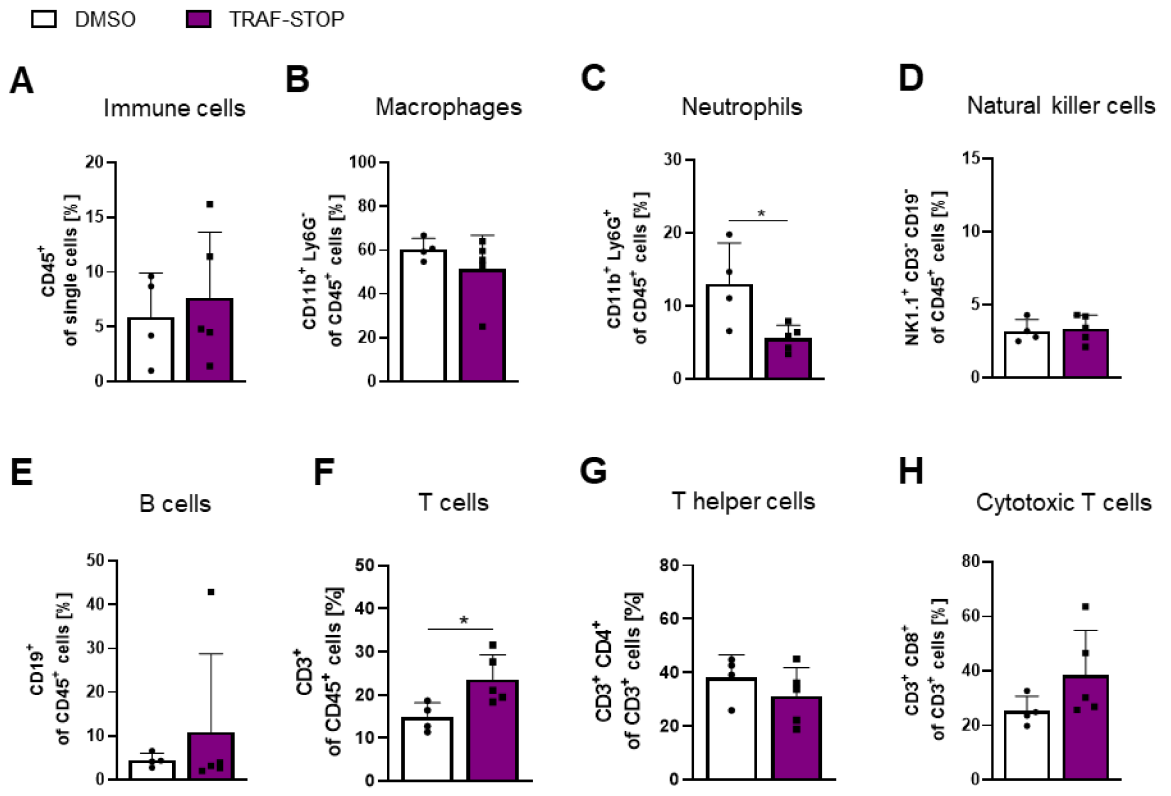

Figure 26: Decreased proportion of neutrophils and increased proportion of T cells in AAA tissue after CD40-TRAF6 inhibition in a severe AngII model

*Flow cytometric analysis of different immune cell populations in AAA tissue from Apoe$^{-/-}$ mice on WD diet treated with DMSO or TRAF-STOP 28 days after AngII-induced AAA formation. Proportions of overall CD45^{+} immune cells (A), CD11b^{+} Ly6G^{-} macrophages (B), NK1.1^{+} CD3^{-} CD19^{-} natural killer cells (D), CD19^{+} B cells (E) and CD3^{+} CD4^{+} T helper cells (G) CD8^{+} cytotoxic T cells (H) were not significantly altered in mice upon TRAF-STOP treatment. Whereas the percentage of CD11b^{+} Ly6G^{+} neutrophils (C) was significantly reduced and the percentage of CD3^{+} T cells (F) was significantly increased in aneurysmal tissue from TRAF-STOP-treated mice 28 days post AAA induction. Unpaired Student's t test (two-tailed) (A, B, C, D, F, H) or unpaired Mann-Whitney test (two-tailed) (E, G); *p<0.05. Mean ± SD. DMSO n=4, TRAF-STOP n=5.*

In addition, the systemic effect of inhibiting the CD40-TRAF6 signalling on absolute circulatory immune cell numbers in whole blood of *Apoe*$^{-/-}$ mice on WD diet 28 days after AngII-induced AAA formation was examined using an automated haematology analyser. This analysis revealed similar absolute numbers of circulatory leukocytes, lymphocytes, monocytes and neutrophils in both treatment groups 28 days after pump implantation (Figure 27).

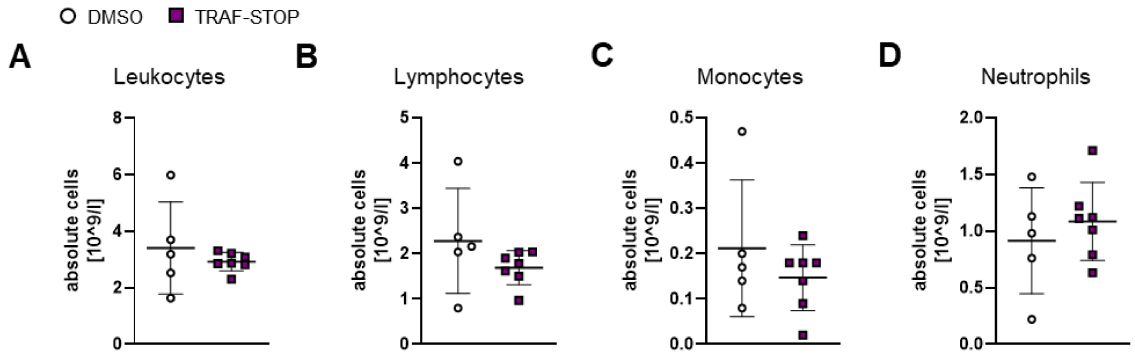

Figure 27: Number of circulatory immune cells was not altered after CD40-TRAF6 inhibition in a severe AngII model
Absolute cell numbers of leukocytes (A), lymphocytes (B), monocytes (C) and neutrophils (D) was determined using an automated haematology analyser in whole blood samples from DMSO- and TRAF-STOP-treated Apoe$^{-/-}$ mice on WD diet 28 days after AngII-induced AAA formation. Haematology analysis revealed no differences between treatment groups. Mean ± SD. DMSO n=5, TRAF-STOP n=7.

CD40-TRAF6 inhibition led to increased plasma concentrations of several pro-inflammatory cytokines in *Apoe*$^{-/-}$ mice on WD diet

Cytokines play an important role in the activation and infiltration of immune cells, and thus in AAA pathology. Therefore, the systemic effect of CD40-TRAF6 inhibition on cytokine concentrations of plasma samples from DMSO- and TRAF-STOP-treated *Apoe*$^{-/-}$ mice fed a WD diet 28 days after AngII-induced AAA formation were examined using a bead-based immunoassay and flow cytometry. Analysis revealed a significant increase in plasma concentrations of IL-1β, IL-10, IL-12 and GM-CSF (Figure 28 B, D, E, M). However, plasma concentrations of IL-1α, IL-6, IL-17, IL-23, IL-27, TNFα, IFN-β, IFN-γ and CCL2 were similar in both treatment groups (Figure 28 A, C, F, G, H, I, J, K, L).

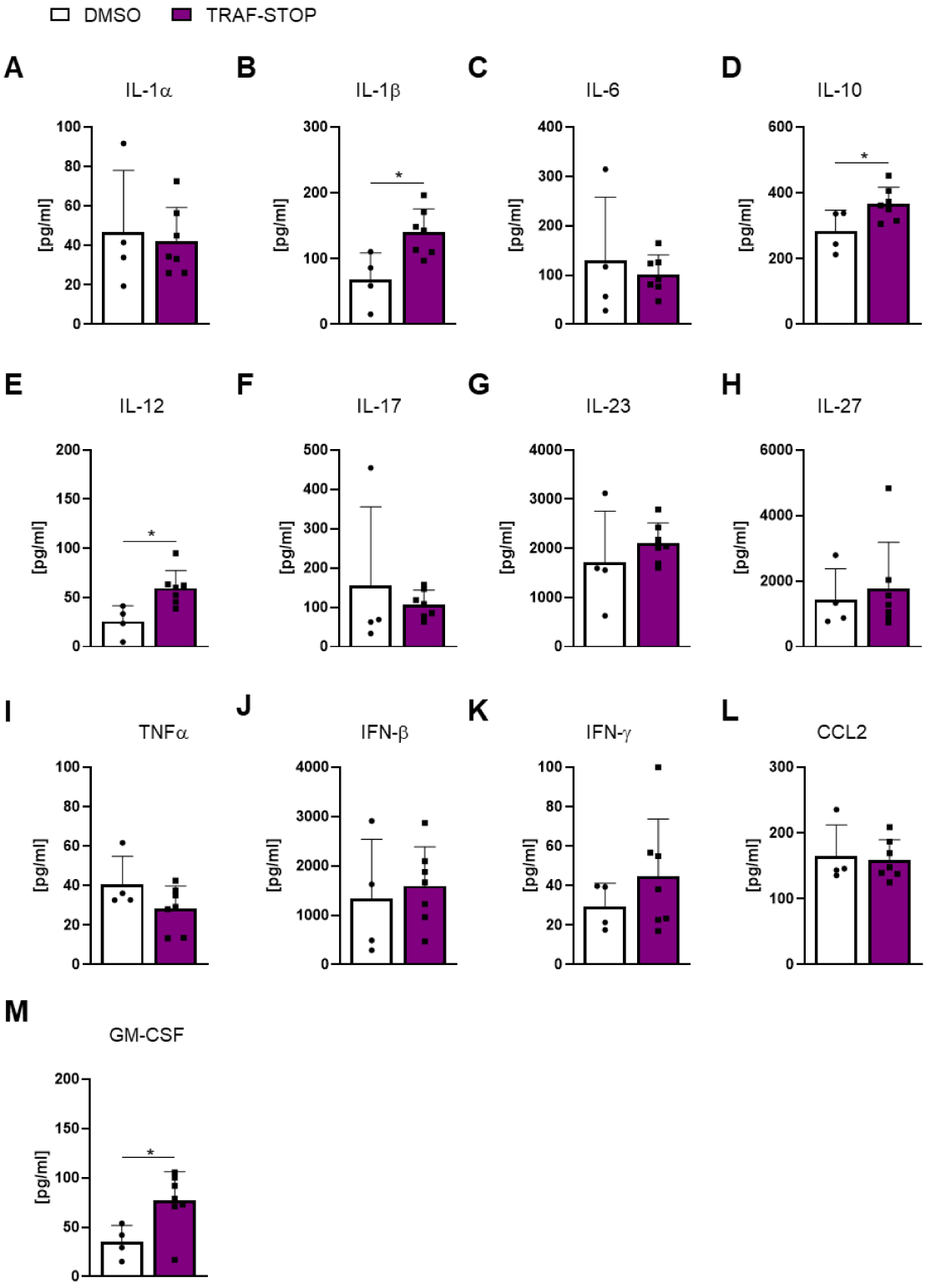

Figure 28: Increased IL-1β, IL-10, IL-12 and GM-CSF plasma concentration after CD40-TRAF6 inhibition in a severe AngII model

*Cytokine concentrations in plasma from Apoe$^{-/-}$ mice on WD diet treated with DMSO or TRAF-STOP 28 days after AngII-induced AAA formation measured by a bead-based immunoassay. TRAF-STOP treatment led to increased plasma concentration of IL-1β (B), IL-10 (D), IL-12 (E) and GM-CSF (M). Plasma concentrations of other cytokines were not altered upon TRAF-STOP treatment. Unpaired Student's t test (two-tailed) (A, B, C, D, E, G, J, K, M) or unpaired Mann-Whitney test (two-tailed) (F, H, I, L). *p<0.05. Mean ± SD. DMSO n=4, TRAF-STOP n=7.*

Tamoxifen-induced CD40 deficiency protects against AngII-induced AAA rupture

To strengthen the potential beneficial effects of the pharmacological inhibition of CD40-TRAF6 signalling using the small molecule inhibitor, TRAF-STOP, in the context of AAA formation and progression, shown in the PPE model, a genetically modified mouse model was established. Hereby, TAM injections were used for global Cre recombinase-induced CD40 depletion in *Apoe*$^{-/-}$ mice. *Apoe*$^{-/-}$ *Cd40*$^{fl/fl}$ *CreER*^{tg} and *Apoe*$^{-/-}$ *Cd40*$^{fl/fl}$ *CreER*^{wt} mice received 100 µl TAM (1 mg/injection) on five consecutive days. AAA was induced 14 days after the first TAM administration via continuous infusion with AngII at a rate of 1 µg/kg*min for 28 days using subcutaneously implanted osmotic pumps. Aortic diameter was assessed prior to the implantation and on the endpoint (Figure 29).

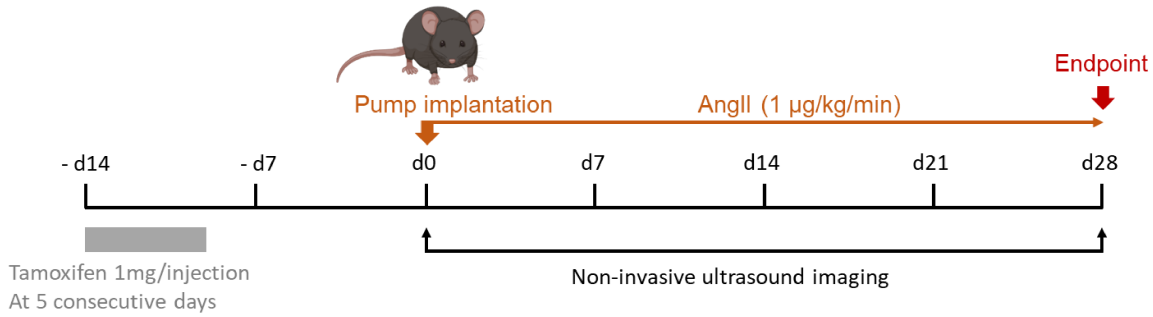

Figure 29: Experimental design to investigate tamoxifen-induced CD40 deficiency in AAA pathology
Experimental setup. Apoe$^{-/-}$ *Cd40*$^{fl/fl}$ *CreER*^{tg} *and their Cre negative littermates were treated with 1 mg/injection tamoxifen at five consecutive days. Two weeks after the first injection, AAA was induced by continuous infusion of Angiotensin (Ang) II (1 µg/kg*min) through subcutaneously implanted osmotic pumps. Prior to surgery and on the day of organ harvesting, non-invasive ultrasound imaging was used to assess AAA formation. Mice were sacrificed and organs were harvested 28 days post AAA induction.*

After 28 days of AngII infusion, 60% of the *Apoe*$^{-/-}$ *Cd40*$^{fl/fl}$ *CreER*^{wt} mice and only one third of the global CD40-deficient CreER^{tg} littermates died due to aortic rupture, corresponding to survival rates of 40% and 72.7%, but the change did not rise to the level of statistical significance (Log-rank (Mantel-Cox) test p=0.0665) (Figure 30 A). Analysis of non-invasive ultrasound images revealed no differences in the expansion of abdominal aortic diameter in mice that lack CD40 compared to *Apoe*$^{-/-}$ *Cd40*$^{fl/fl}$ *CreER*^{wt} mice 28 days after pump implantation (Figure 30 B). In this set-up, 4 out of 5 *Apoe*$^{-/-}$ *Cd40*$^{fl/fl}$ *CreER*^{wt} mice developed an AAA, corresponding to an AAA incidence of 80%, whereas 7 out of 11 *Apoe*$^{-/-}$ *Cd40*$^{fl/fl}$ *CreER*^{tg} mice developed an AAA, corresponding to an AAA incidence of 63.6% (Figure 30 C). In this experimental model, continuous AngII infusion can also lead to TAA formation, thus, ascending aortic diameter was also examined using ultrasound imaging. However, ascending aortic expansion was similar in both genetic strains (Figure 30 D). Three out of five *Apoe*$^{-/-}$ *Cd40*$^{fl/fl}$ *CreER*^{wt} mice, whereas only three out of 11 *Apoe*$^{-/-}$ *Cd40*$^{fl/fl}$ *CreER*^{tg} mice developed a TAA 28 days after pump implantation (Two-sided Fisher's exact test; p=0.2995) (Figure 30 E). Mice were more prone to develop AAA than TAA regardless of Cre recombinase expression. An AAA incidence of 80% and 63.6% could be shown 28 days after pump implantation compared to a TAA incidence of 60% in Cre negative and 27.3% in Cre positive mice (Figure 30 C, E).

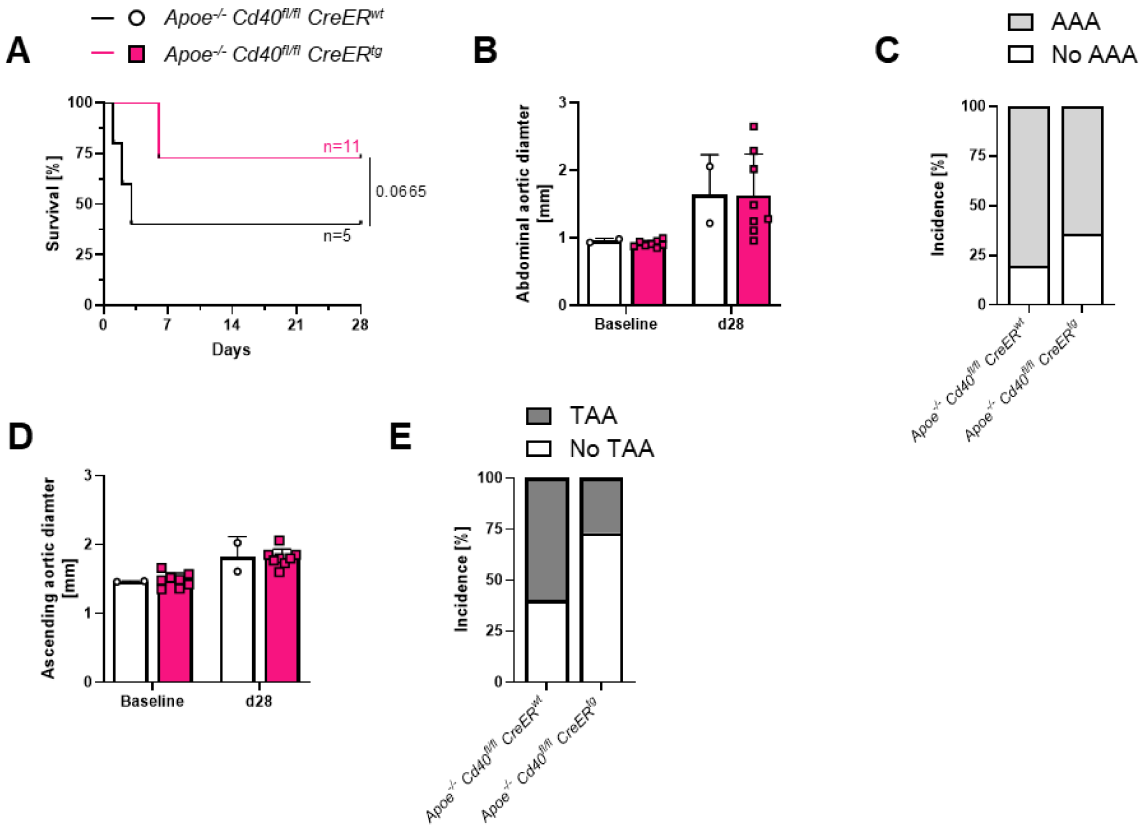

Figure 30: Global CD40 deficiency led to enhanced survival after AngII-induced AAA formation
Global CD40 deficiency was induced by tamoxifen injections two weeks prior to AngII-induced AAA formation in Apoe$^{-/-}$ Cd40$^{fl/fl}$ CreER^{wt} and their Cre-expressing littermates Apoe$^{-/-}$ Cd40$^{fl/fl}$ CreER^{tg} (A) Kaplan-Meier curve shows the percentage survival of CD40-expressing and global CD40 deficient Apoe$^{-/-}$ mice 28 days after AngII-induced AAA formation. Log-rank (Mantel-Cox) test; p=0.0665. Apoe$^{-/-}$ Cd40$^{fl/fl}$ CreER^{wt} n=5, Apoe$^{-/-}$ Cd40$^{fl/fl}$ CreER^{tg} n=11 (B) Analysis of abdominal aortic diameter using ultrasound images prior to pump implantation (baseline) and 28 days after AAA induction. Mean ± SD. Apoe$^{-/-}$ Cd40$^{fl/fl}$ CreER^{wt} n=2, Apoe$^{-/-}$ Cd40$^{fl/fl}$ CreER^{tg} n=8. (C) Incidence of AAA or no AAA in CD40-expressing and global CD40 deficient Apoe$^{-/-}$ mice 28 days after AAA induction. Two-sided Fisher's exact test; p>0.9999. Apoe$^{-/-}$ Cd40$^{fl/fl}$ CreER^{wt} n=5, Apoe$^{-/-}$ Cd40$^{fl/fl}$ CreER^{tg} n=11. (D) Analysis of ascending aortic diameter using ultrasound images prior to (baseline) and 28 days after pump implantation. Mean ± SD. Apoe$^{-/-}$ Cd40$^{fl/fl}$ CreER^{wt} n=2, Apoe$^{-/-}$ Cd40$^{fl/fl}$ CreER^{tg} n=8. (E) Incidence of TAA or no TAA in Apoe$^{-/-}$ Cd40$^{fl/fl}$ CreER^{wt} and Apoe$^{-/-}$ Cd40$^{fl/fl}$ CreER^{tg} 28 days after pump implantation. Two-sided Fisher's exact test; p=0.2995. Apoe$^{-/-}$ Cd40$^{fl/fl}$ CreER^{wt} n=5, Apoe$^{-/-}$ Cd40$^{fl/fl}$ CreER^{tg} n=11. Animals that died due to AAA or TAA rupture were included in incidence determinations. AAA and TAA were defined as an increase in aortic diameter of at least 1.5-fold. AAA = Abdominal aortic aneurysm, TAA = Thoracic aortic aneurysm.

Reduced CD40 expression on overall immune cells and B cells of *Apoe$^{-/-}$ Cd40$^{fl/fl}$ CreER^{tg}* mice

The effectiveness of global CD40 deficiency on different CD40-expressing immune cells in *Apoe$^{-/-}$ Cd40$^{fl/fl}$ CreER^{tg}* compared to their Cre negative *Apoe$^{-/-}$ Cd40$^{fl/fl}$ CreER^{wt}* littermates after TAM administration and AAA-induction was examined using flow cytometric analysis. Single cell suspensions from blood, aortic lymph nodes and spleen was used, to investigate CD40 expression. Flow cytometric analysis was performed using a gating strategy that excluded any cell debris as well as erythrocytes (SSC-A versus FSC-A) followed by a singlet gate excluding any cell doublets (FSC-H versus FSC-A). Viable CD45^{+} immune cells were identified and further used to determine CD40 expression on these (Figure 31 A). In addition, viable CD45^{+} immune cells were used to identify CD11b^{+} myeloid cells and CD3^{+} T cells. Further, CD40 expression on myeloid cells was determined (Figure 31 B) and CD11b^{+} Ly6G^{+} neutrophils and their CD40 expression were examined (Figure 31 D). CD19^{+}

B cells were identified out of the CD11b$^-$ CD3$^-$ population and their CD40 expression was determined (Figure 31 C).

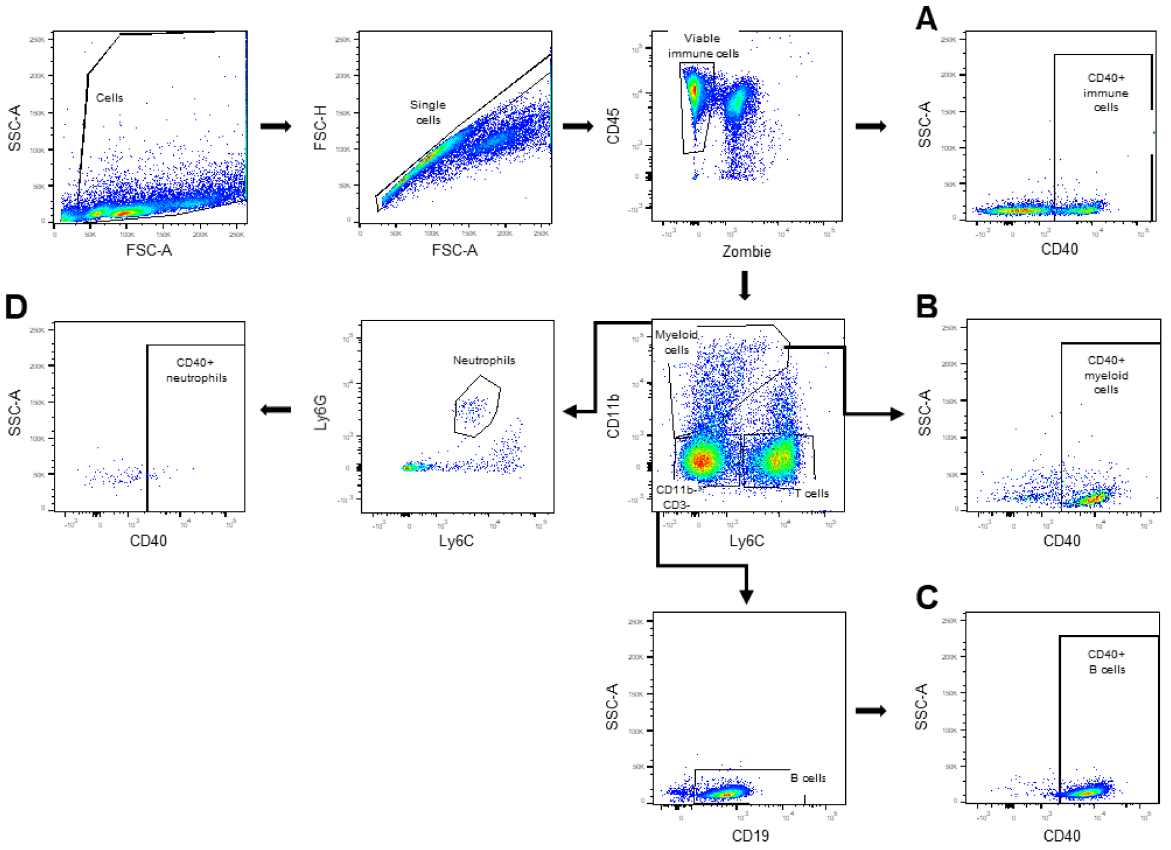

Figure 31: Flow cytometric gating strategy used to assess CD40 expression on overall immune cells, myeloid cells, neutrophils and B cells
Gating strategy to examine CD40 expression on overall immune cells (CD45$^+$), myeloid cells (CD11b$^+$), B cells (CD19$^+$) and neutrophils (CD11b$^+$ Ly6G$^+$) in blood circulation as well as in lymphatic and renal tissue. Exemplary dot plots from flow cytometric analysis of aortic lymph nodes from an Apoe$^{-/-}$ Cd40$^{fl/fl}$ CreER^{wt} mice showing CD40 expression on (A) overall immune cells, (B) myeloid cells, (C) B cells and (D) neutrophils. A = Area, FSC = forward scatter, H = Height, SSC = side scatter.

CD40 expression on CD45$^+$ overall immune cells, CD19$^+$ B cells, and CD11b$^+$ myeloid cells in blood circulation, aortic lymph nodes and spleen was determined in *Apoe$^{-/-}$ Cd40$^{fl/fl}$ CreER^{wt}* and their Cre-expressing littermates *Apoe$^{-/-}$ Cd40$^{fl/fl}$ CreER^{tg}* after TAM administration and AngII-induced AAA formation. Flow cytometric analysis revealed a decrease in median fluorescent intensity (MFI) of CD40 of approximately 50% or less on overall immune cells as well as on B cells from blood, aortic lymph nodes and spleen (Figure 32 A, B, D, E, G, H). However, MFI of CD40 on myeloid cells was only reduced in tissue of aortic lymph nodes, whereas in blood and spleen the MFI of CD40 was similar in both genetic strains (Figure 32 C, F, I). Furthermore, MFI determination of CD40 on these cells showed that CD40 was mostly expressed on B cells, whereas the MFI of CD40 was the lowest on myeloid cells from blood and splenic tissue (Figure 32).

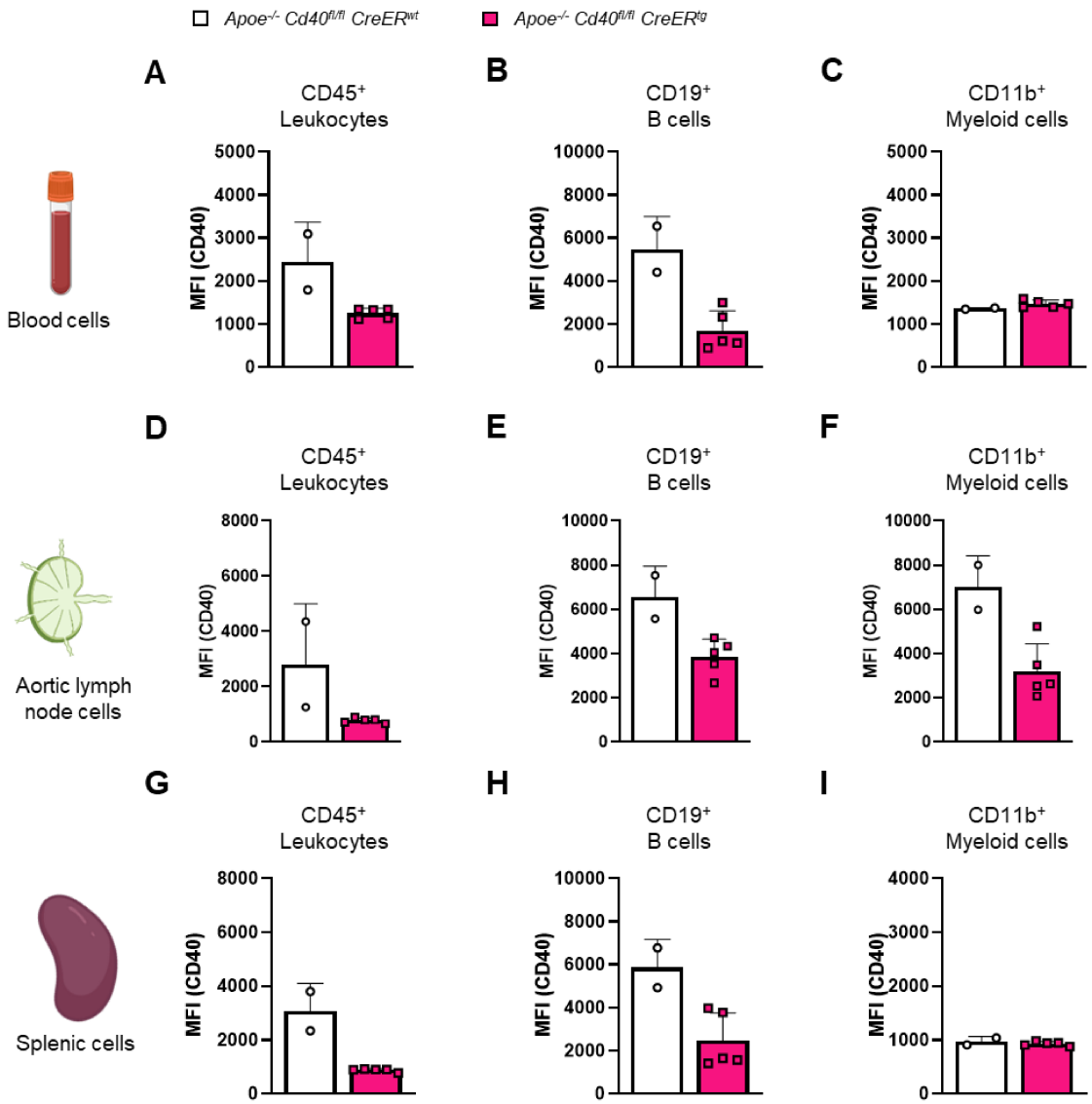

Figure 32: Reduced CD40 expression on overall immune cells and B cells after TAM-induced Cre activity in Apoe$^{-/-}$ Cd40$^{fl/fl}$ CreER^{tg} mice

CD40 deficiency was examined in Apoe$^{-/-}$ Cd40$^{fl/fl}$ CreER^{wt} and their Cre-expressing littermates Apoe$^{-/-}$ Cd40$^{fl/fl}$ CreER^{tg} after tamoxifen injections two weeks prior to AngII-induced AAA formation using flow cytometry. MFI of CD40 was determined in circulatory (A-C), lymphatic (D-F) and splenic (G-I) on CD45^{+} overall immune cells, CD19^{+} B cells and CD11b^{+} myeloid cells. Mean ± SD. Apoe$^{-/-}$ Cd40$^{fl/fl}$ CreER^{wt} n=2, Apoe$^{-/-}$ Cd40$^{fl/fl}$ CreER^{tg} n=5. Reduced MFI of CD40 on overall immune cells and B cells in all tested tissues after TAM administration and 28 days after AngII-induced AAA formation. MFI = median fluorescence intensity. Icons of tissues from BioRender.com.

Effects of cell type-specific CD40 deficiency on AAA formation

The first part of this study showed a potential protective role of pharmacologically inhibiting CD40-TRAF6 signalling using TRAF-STOP in the context of AAA pathology in the PPE model as well as evidence of reduced mortality rate due to decreased aortic rupture in the AngII model (Pharmacological inhibition of CD40-TRAF6 signalling in AAA formation and progression). However, CD40 is widely expressed on several hematopoietic cells, like B cells, monocytes and macrophages as well as on non-hematopoietic cells.[85] To further investigate which cell type-specific CD40 signalling contributes to the potential beneficial effects on AAA formation and progression, cell-type specific CD40-deficient mouse strains were generated. In this part of this study, mice deficient for CD40 on B cells (*Apoe*$^{-/-}$ *Cd40*$^{fl/fl}$ *Cd19 Cre*^{tg}) and on myeloid cells (*Apoe*$^{-/-}$ *Cd40*$^{fl/fl}$ *Lyz2 Cre*^{tg}) and their Cre negative littermates (Cre^{wt}) were examined.

CD40 deficiency on B cells did not affect AAA formation and rupture

Apoe$^{-/-}$ *Cd40*$^{fl/fl}$ *Cd19 Cre*^{tg} and *Apoe*$^{-/-}$ *Cd40*$^{fl/fl}$ *Cd19* Cre^{wt} mice were continuously infused with AngII at a rate of 1 µg/kg*min for 28 days via subcutaneously implanted osmotic pumps. Aortic diameter was assessed using non-invasive ultrasound imaging prior to and 28 days after the pump implantation. Four weeks of AngII treatment led to a slightly increased survival rate in B cell-specific CD40 lacking mice compared to their Cre^{wt} littermates 45% and 33.3% respectively (Log-rank (Mantel-Cox) test p=0.3147) (Figure 33 A). However, abdominal aortic dilation and AAA incidence was similar in both genetic strains. Specifically, medial diameter of suprarenal aorta was 1.9 mm in *Apoe*$^{-/-}$ *Cd40*$^{fl/fl}$ *Cd19 Cre*^{wt} mice and 2.1 mm in their Cre-expressing littermates (Figure 33 B). Furthermore, 13 out of 15 *Apoe*$^{-/-}$ *Cd40*$^{fl/fl}$ *Cd19 Cre*^{wt} mice and 17 out of 20 *Apoe*$^{-/-}$ *Cd40*$^{fl/fl}$ *Cd19 Cre*^{tg} mice developed an AAA, corresponding to similar AAA incidences of 86.6% and 85% (Figure 33 C).

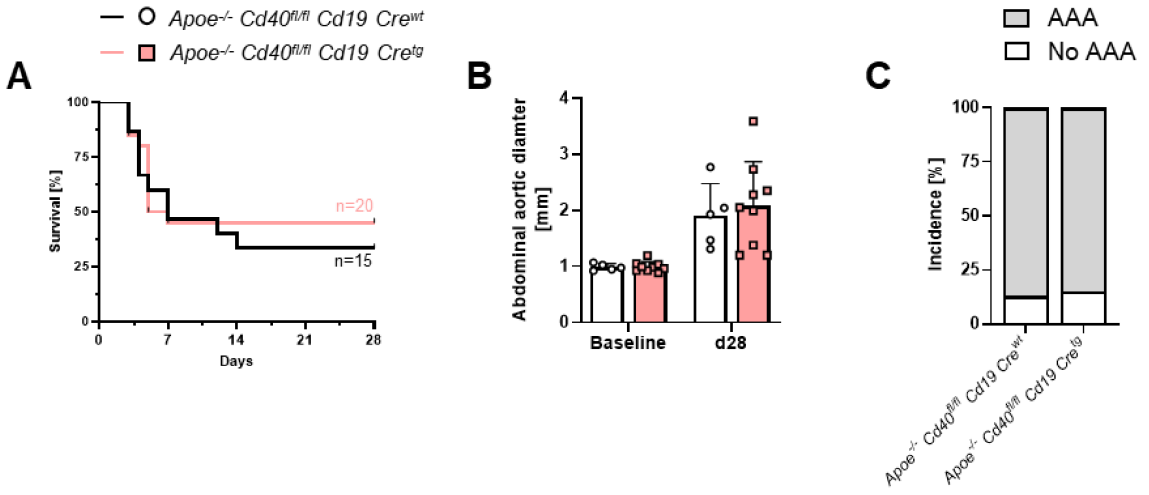

Figure 33: Lack of CD40 on B cells did not affect survival rate, AAA expansion and incidence after AngII-induced AAA formation

AAAs were induced by continuous AngII infusion in Apoe$^{-/-}$ *Cd40*$^{fl/fl}$ *Cd19 Cre*^{wt} *and Apoe*$^{-/-}$ *Cd40*$^{fl/fl}$ *Cd19 Cre*^{tg} *mice.* (A) *Kaplan-Meier curve shows the percentage survival B cell-specific CD40-deficient mice and their Cre*^{wt} *littermates 28 days after pump implantation. Log-rank (Mantel-Cox) test p=0.3147. Apoe*$^{-/-}$ *Cd40*$^{fl/fl}$ *Cd19 Cre*^{wt} *n=15, Apoe*$^{-/-}$ *Cd40*$^{fl/fl}$ *Cd19 Cre*^{tg} *n=20. (B) Analysis of abdominal aortic diameter using ultrasound images before the pump implantation (baseline) and 28 days after AAA induction. Mean ± SD. Apoe*$^{-/-}$ *Cd40*$^{fl/fl}$ *Cd19 Cre*^{wt} *n=5, Apoe*$^{-/-}$ *Cd40*$^{fl/fl}$ *Cd19 Cre*^{tg} *n=9. (C) Incidence of AAA or no AAA in Apoe*$^{-/-}$ *Cd40*$^{fl/fl}$ *Cd19 Cre*^{wt} *and B cell-specific CD40-deficient mice 28 days after AAA induction. Apoe*$^{-/-}$ *Cd40*$^{fl/fl}$ *Cd19 Cre*^{wt} *n=15, Apoe*$^{-/-}$ *Cd40*$^{fl/fl}$ *Cd19 Cre*^{tg} *n=20. Animals that died due to AAA rupture were included. AAA formation was defined as an increase in aortic diameter of at least 1.5-fold.*

Lack of CD40 on B cells did not affect the number of circulatory immune cells 28 days after AngII-induced AAA formation

The potential systemic effect on circulating immune cells of 28-day AngII-treated B cell-specific CD40-deficient mice compared to their Cre^{wt} littermates was examined using an automated haematology analyser. This analysis revealed similar absolute numbers of circulatory leukocytes, lymphocytes, monocytes and neutrophils in both genetic strains (Figure 34).

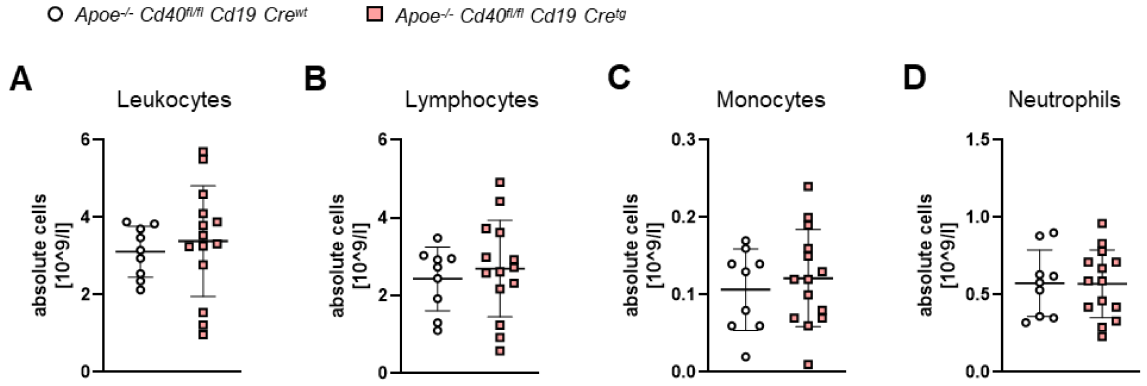

Figure 34: Lack of CD40 on B cells did not affect the numbers of circulatory immune cells
Absolute cell numbers of leukocytes (A), lymphocytes (B), monocytes (C) and neutrophils (D) were determined in whole blood samples from Apoe$^{-/-}$ Cd40$^{fl/fl}$ Cd19 Cre^{wt} mice and their Cre-expressing littermates mice 28 days after AngII-induced AAA formation using an automated haematology analyser. Unpaired Student's t test (two-tailed). Mean ± SD. Apoe$^{-/-}$ Cd40$^{fl/fl}$ Cd19 Cre^{wt} n=9, Apoe$^{-/-}$ Cd40$^{fl/fl}$ Cd19 Cre^{tg} n=14.

CD40 expression on B cells of *Apoe$^{-/-}$ Cd40$^{fl/fl}$ Cd19 Cre^{tg}* mice was significantly reduced in several tissues

Flow cytometric analysis was used to validate CD40 deficiency on B cells in different tissues of *Apoe$^{-/-}$ Cd40$^{fl/fl}$ Cd19 Cre^{wt}* and *Apoe$^{-/-}$ Cd40$^{fl/fl}$ Cd19 Cre^{tg}* mice. CD40 expression on $CD19^+$ B cells, $CD11b^+$ myeloid cells and $CD11b^+$ $Ly6G^+$ neutrophils was determined in aorta, blood, aortic lymph nodes and spleen using the previously described gating strategy (Figure 31).
A representative dot plot showed a reduced amount of CD40-expressing B cells in aortic lymph nodes from *Apoe$^{-/-}$ Cd40$^{fl/fl}$ Cd19 Cre^{tg}* compared to their Cre^{wt} littermates. Specifically, the percentage of B cells expressing CD40 was 99% in *Apoe$^{-/-}$ Cd40$^{fl/fl}$ Cd19 Cre^{wt}* mice (Figure 35 A), whereas only 6.81% of B cells from Cre positive mice expressed CD40 on their surface (Figure 35 B).

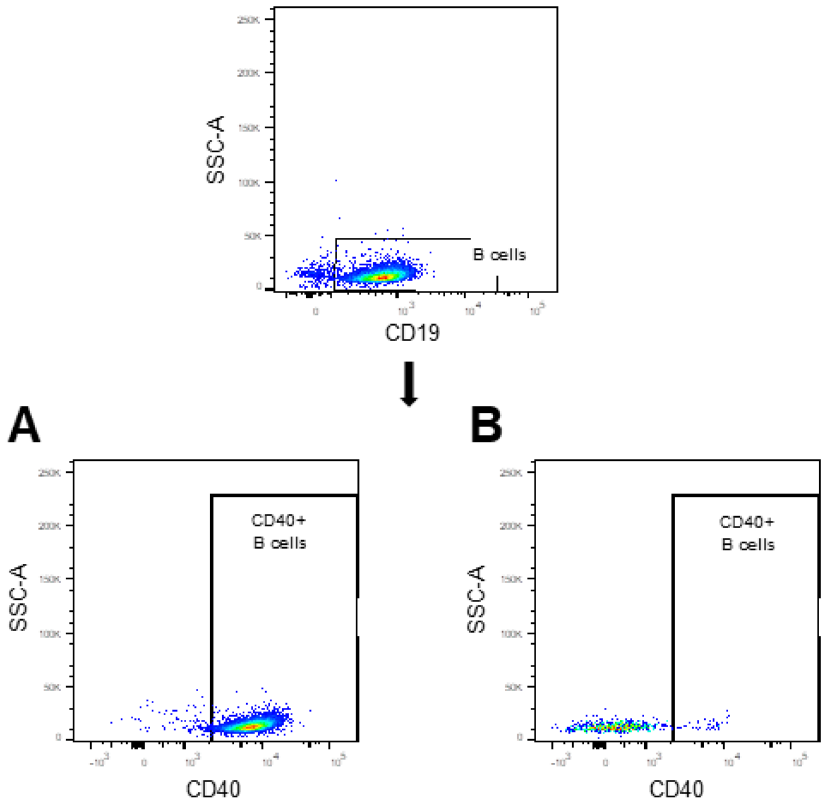

Figure 35: CD40 expression on B cells was reduced in Apoe$^{-/-}$ Cd40$^{fl/fl}$ Cd19 Cre^{tg} mice
Exemplary dot plots from flow cytometric analysis showing CD40-expressing B cells in tissue of aortic lymph nodes from Apoe$^{-/-}$ Cd40$^{fl/fl}$ Cd19 Cre^{wt} mice (A) and from an Apoe$^{-/-}$ Cd40$^{fl/fl}$ Cd19 Cre^{tg} mice (B).

MFI of CD40 was determined to evaluate the CD40 expression on CD19^{+} B cells, CD11b^{+} myeloid cells and CD11b^{+} Ly6G^{+} neutrophils in aorta, blood, aortic lymph nodes and spleen 28 days after AngII-induced AAA formation in both genetic strains. MFI of CD40 on B cells was significantly decreased in all tested tissues and in blood circulation from *Apoe$^{-/-}$ Cd40$^{fl/fl}$ Cd19 Cre^{tg}* mice (Figure 36 A, D, G, J). In addition, MFI of CD40 was significantly reduced on myeloid cells in aorta and aortic lymph nodes from *Apoe$^{-/-}$ Cd40$^{fl/fl}$ Cd19 Cre^{tg}* mice compared to their Cre^{wt} littermates (Figure 36 B, H). However, MFI of CD40 from myeloid cells in blood circulation and spleen was similar in both genetic strains (Figure 36 E, K). Highest MFI of CD40 in *Apoe$^{-/-}$ Cd40$^{fl/fl}$ Cd19 Cre^{wt}* mice was detected on B cells independent of tested tissue, whereas MFI of CD40 on myeloid cells and neutrophils was lower than that of B cells but mostly similar in tested tissues (Figure 36).

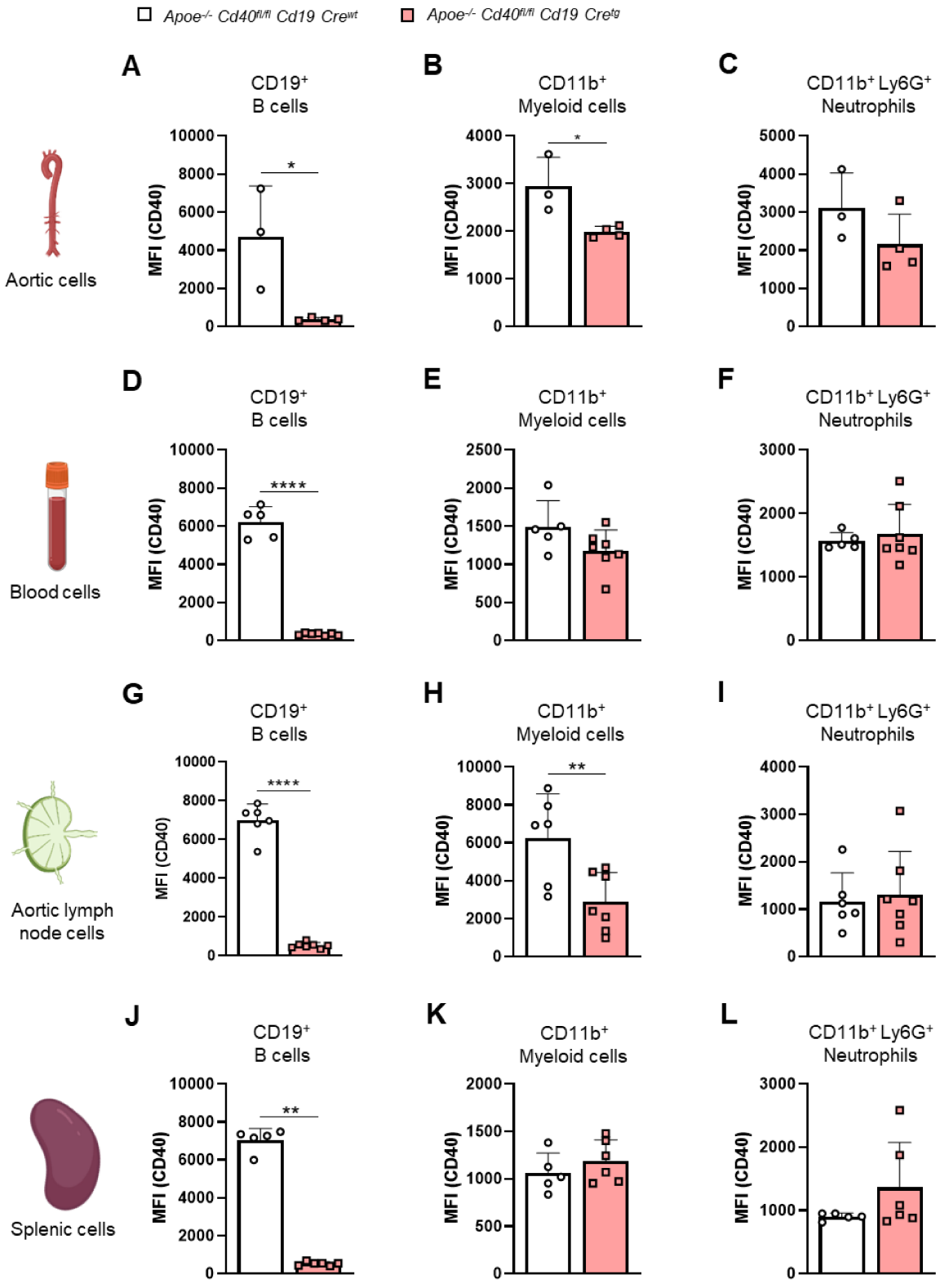

Figure 36: Flow cytometric analysis of CD40 expression on B cells, myeloid cells and neutrophils
*MFI of CD40 on aortic (A-C), circulatory (D-F), lymphatic (G-I) and splenic (J-L) CD19⁺ B cells, CD11b⁺ myeloid cells and CD11b⁺, Ly6G⁺ neutrophils from Apoe$^{-/-}$ Cd40$^{fl/fl}$ Cd19 Cre^{wt} and their Cre-expressing littermates 28 days after AngII-induced AAA formation. Lack of CD40 on B cells was detected in all tested tissues (A, D, G, J). Mean ± SD. Apoe$^{-/-}$ Cd40$^{fl/fl}$ Cd19 Cre^{wt} n=3-6, Apoe$^{-/-}$ Cd40$^{fl/fl}$ Cd19 Cre^{tg} n=4-7. MFI = median fluorescence intensity. Unpaired Mann-Whitney test (two-tailed) (J) or unpaired Student's t test (two-tailed) (A-I,K,L) *p<0.05, **p<0.01, ****p<0.0001. Icons of tissues were used from BioRender.com.*

Myeloid cell-specific CD40 deficiency did not affect AAA formation and progression

AAA was induced in *Apoe*$^{-/-}$ *Cd40*$^{fl/fl}$ *Lyz2 Cre*^{wt} and their Cre^{tg} littermates via continuous infusion with AngII (1 µg/kg*min) for 28 days using subcutaneously implanted osmotic pumps. AngII treatment led to a similar survival rate in both genetic strains, specifically, 69.2% in Cre^{wt} mice and 66.67% in *Apoe*$^{-/-}$ *Cd40*$^{fl/fl}$ *Lyz2 Cre*^{tg} mice (Figure 37 A). Expansion of the abdominal aorta was assessed by non-invasive ultrasound imaging before and 28 days after the pump implantation. AAA diameter dilation was similar in myeloid-specific CD40-deficient mice compared to their Cre^{wt} littermates 28 days after AAA induction (Two-way ANOVA with Sidak's multiple comparisons post test; p=0.2000) (Figure 37 B). Furthermore, AAA incidences were comparable in both genetic strains. In detail, 12 out of 13 *Apoe*$^{-/-}$ *Cd40*$^{fl/fl}$ *Lyz2 Cre*^{wt} mice and 18 out of 21 *Apoe*$^{-/-}$ *Cd40*$^{fl/fl}$ *Lyz2 Cre*^{tg} mice developed an AAA after 28 days of AngII infusion, corresponding to AAA incidences of 92.3% and 85.7% (Figure 37 C).

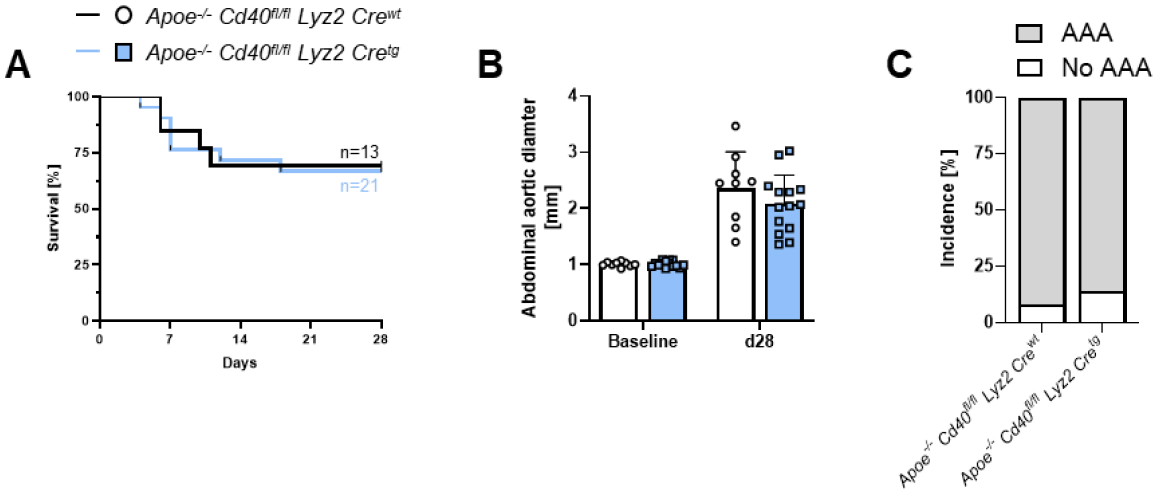

Figure 37: CD40 deficiency on myeloid cells did not affect rupture rate, AAA formation and development in an AngII model
AAAs were induced by continuous AngII infusion via implanted osmotic pumps into Apoe$^{-/-}$ *Cd40*$^{fl/fl}$ *Lyz2 Cre*^{wt} *mice and their Cre*^{tg} *littermates. (A) Kaplan-Meier curve shows the percentage survival of myeloid-specific CD40-deficient mice and their Cre*^{wt} *littermates. Apoe*$^{-/-}$ *Cd40*$^{fl/fl}$ *Lyz2 Cre*^{wt} *n=13, Apoe*$^{-/-}$ *Cd40*$^{fl/fl}$ *Lyz2 Cre*^{tg} *n=21 (B) Assessment of abdominal aortic diameter using ultrasound images before the pump implantation (baseline) and 28 days after AngII-induced AAA formation. Two-way ANOVA with Sidak's multiple comparisons post test; p=0.2000. Apoe*$^{-/-}$ *Cd40*$^{fl/fl}$ *Lyz2 Cre*^{wt} *n=9, Apoe*$^{-/-}$ *Cd40*$^{fl/fl}$ *Lyz2 Cre*^{tg} *n=14. (C) Incidence of AAA or no AAA in Apoe*$^{-/-}$ *Cd40*$^{fl/fl}$ *Lyz2 Cre*^{wt} *and their Cre-expressing littermates 28 days after AAA induction. Apoe*$^{-/-}$ *Cd40*$^{fl/fl}$ *Lyz2 Cre*^{wt} *n=13, Apoe*$^{-/-}$ *Cd40*$^{fl/fl}$ *Lyz2 Cre*^{tg} *n=21. Animals that died due to AAA rupture were Included. AAA formation was defined as an increase in aortic diameter of at least 1.5-fold.*

Numbers of circulatory immune cells was not changed in *Apoe*$^{-/-}$ *Cd40*$^{fl/fl}$ *Lyz2 Cre*^{tg} mice

Furthermore, the systemic effect of myeloid-specific CD40 deficiency compared to their Cre negative littermates on circulatory immune cells was investigated 28 days after AngII-induced AAA formation. Hematologic analysis revealed similar absolute numbers of blood leukocytes, lymphocytes, monocytes and neutrophils in both genetic strains (Figure 38).

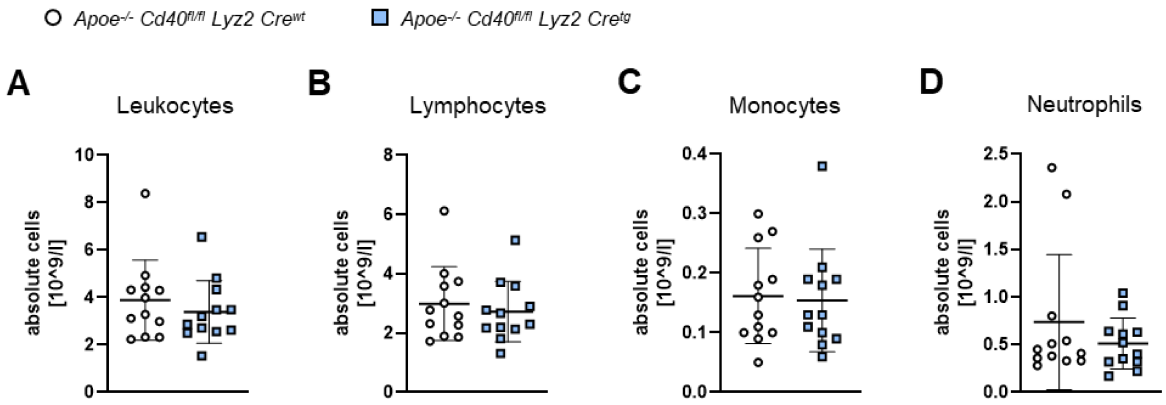

Figure 38: Lack of CD40 on myeloid cells did not affect the numbers of circulatory immune cells
Absolute cell numbers of leukocytes (A), lymphocytes (B), monocytes (C) and neutrophils (D) were measured in whole blood samples of Apoe$^{-/-}$ Cd40$^{fl/fl}$ Lyz2 Cre^{wt} and Apoe$^{-/-}$ Cd40$^{fl/fl}$ Lyz2 Cre^{tg} mice 28 days after AngII-induced AAA formation using an automated haematology analyser. Mean ± SD. Unpaired Mann-Whitney test (two-tailed) (A, C, D) or unpaired Student's t test (two-tailed) (B). Apoe$^{-/-}$ Cd40$^{fl/fl}$ Lyz2 Cre^{wt} n=12, Apoe$^{-/-}$ Cd40$^{fl/fl}$ Lyz2 Cre^{tg} n=12.

CD40 expression was not reduced on myeloid cells of *Apoe$^{-/-}$ Cd40$^{fl/fl}$ Lyz2 Cre^{tg}* mice

Cre recombinase expression in *Apoe$^{-/-}$ Cd40$^{fl/fl}$ Lyz2 Cre^{tg}* mice should result in reduced CD40 expression on myeloid cells, such as monocytes, macrophages and granulocytes. To validate CD40 deficiency on these cells, MFI of CD40 on CD11b^{+} myeloid cells, CD11b^{+}, Ly6G^{+} neutrophils and on CD19^{+} B cells was examined using flow cytometry. MFI of CD40 was determined on cells from aorta, blood, aortic lymph nodes and spleen. MFI of CD40 was similar on myeloid cells from blood, aortic lymph nodes and spleen in *Apoe$^{-/-}$ Cd40$^{fl/fl}$ Lyz2 Cre^{tg}* mice compared to their Cre^{wt} littermates (Figure 39 D, G, J). However, flow cytometric analysis revealed a 1.5-fold reduction of MFI of CD40 on myeloid cells from aorta between both genetic strains, but the change did not rise to the level of statistical significance (unpaired Student's t test (two-tailed) p=0.0628) (Figure 39 A). MFI of CD40 was significantly reduced on neutrophils from aortic lymph nodes from myeloid-specific CD40-deficient mice (Figure 39 H), whereas the expression of CD40 was changed on neutrophils from aorta, blood and spleen between both genetic strains (Figure 39 B, E, K). Moreover, MFI of CD40 of B cells from aorta, blood and spleen did not vary in *Apoe$^{-/-}$ Cd40$^{fl/fl}$ Lyz2 Cre^{tg}* mice compared to their Cre negative littermates (Figure 39 C, F, L). But MFI of CD40 on B cells from aortic lymph nodes was increased 1.2-fold, but the change did not rise to the level of statistical significance (unpaired Student's t test (two-tailed) p=0.0503) (Figure 39 I).

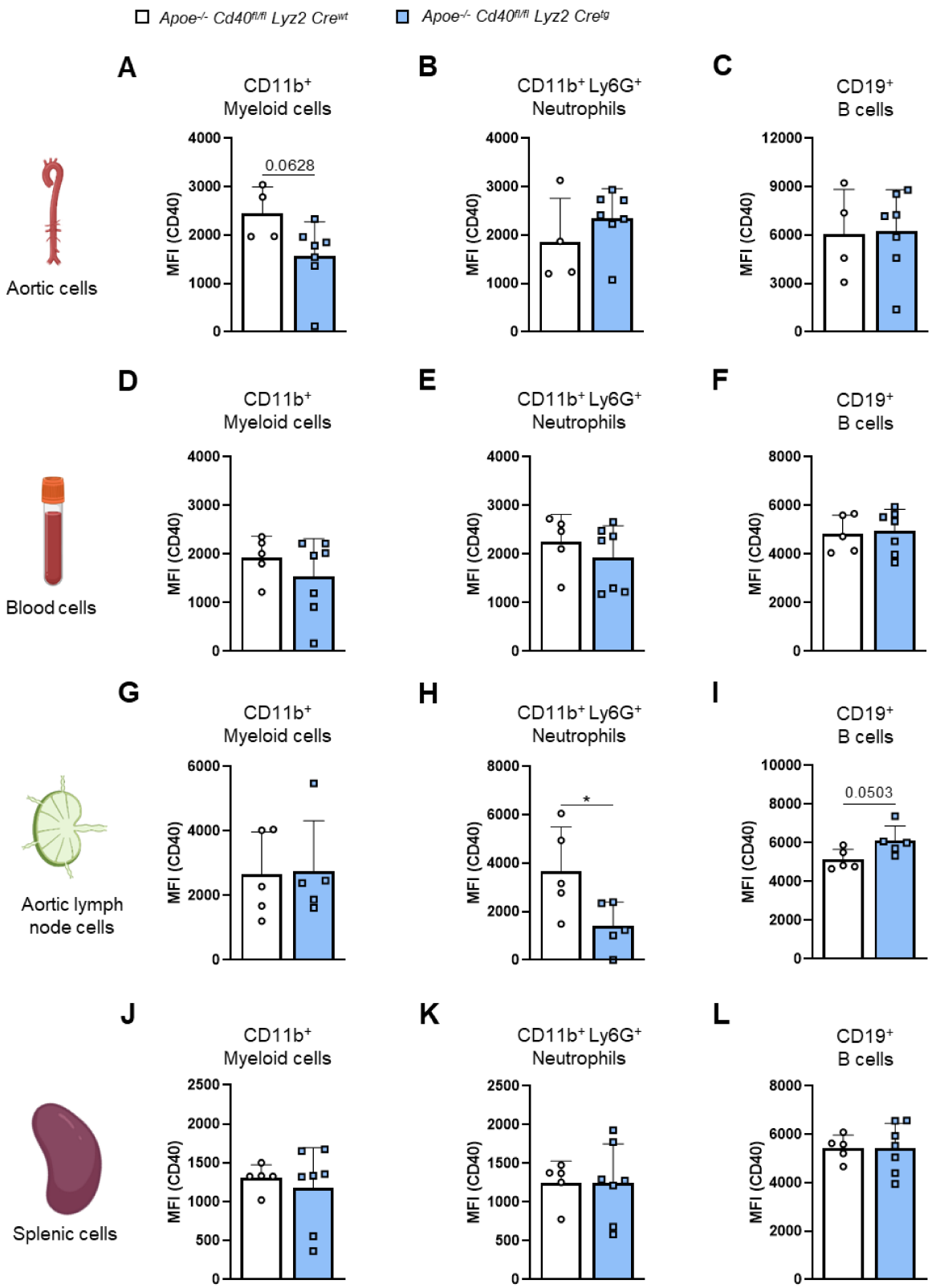

Figure 39: Flow cytometric analysis of CD40 expression on myeloid cells, neutrophils and B cells of *MFI of CD40 of aortic (A-C), circulatory (D-F), lymphatic (G-I) and splenic (J-L) CD11b+ myeloid cells, CD11b+, Ly6G+ neutrophils and CD19+ B cells were determined in Apoe-/- Cd40fl/fl Lyz2 Crewt and their Cre-expressing littermates 28 days after AngII-induced AAA formation. Trend of a reduction in CD40 expression on aortic myeloid cells (A) and significant decrease in CD40 expression on neutrophils from aortic lymph nodes (H). Unpaired Student's t test (two-tailed) *p<0.05. Mean ± SD. Apoe-/- Cd40fl/fl Lyz2 Crewt n=4-5, Apoe-/- Cd40fl/fl Lyz2 Cretg n=5-7. MFI = median fluorescence intensity. Icons of tissues were used from BioRender.com.*

Effects of T cell-specific CD40L deficiency on AAA formation and progression

The first part of this study showed that pharmacologic inhibition of CD40-TRAF6 signalling using TRAF-STOP could be a potential therapeutic target in the context of AAA pathology. However, TRAF-STOP treatment only blocks the signal transduction from CD40 to TRAF6 after CD40 activation and not the entire signalling pathway. Whether inhibiting the activation of CD40 by CD40L result in greater reduction in AAA progression as inhibiting only the signal transduction between CD40 and TRAF6, needs to be investigated. Therefore, this part further examined the effect of inhibiting CD40 activation by CD40L on AAA formation and progression using a genetic mouse strain. As CD40L is mainly expressed by T cells, a T cell-specific CD40L-deficient mouse strains was generated. *Apoe*$^{-/-}$ *Cd40lg*$^{fl/fl}$ *Cd4 Cre*^{tg} mice were used in the AngII model as well as *Cd40lg*$^{fl/fl}$ *Cd4 Cre*^{tg} mice in the PPE model.

T cell-specific CD40L deficiency did not affect AAA development and rupture after AngII-induced AAA formation

Continuous AngII infusion at a rate of 1 µg/kg*min for 28 days via subcutaneously implanted osmotic pumps was used to induce AAA formation in *Apoe*$^{-/-}$ *Cd40lg*$^{fl/fl}$ *Cd4 Cre*^{wt} mice and their Cre^{tg} littermates. It could be shown that the mortality rate was comparable in both genetic strains. Specifically, one out of seven *Apoe*$^{-/-}$ *Cd40lg*$^{fl/fl}$ *Cd4 Cre*^{wt} and three out of 13 *Apoe*$^{-/-}$ *Cd40lg*$^{fl/fl}$ *Cd4 Cre*^{tg} mice died in this experimental set up due to aortic rupture, corresponding to mortality rates of 14.3% and 23.1% respectively (Log-rank (Mantel-Cox) test p=0.6421) (Figure 40 A). Abdominal aortic dilation was assessed using non-invasive ultrasound imaging prior to and 28 days after pump implantation. Abdominal aortic diameter expanded similar in T cell-specific CD40L-deficient mice compared to their CD40L-expressing littermates 28 days after AAA induction (Figure 40 B). AAA incidence was comparable in both genetic strains. In detail, six out of seven *Apoe*$^{-/-}$ *Cd40lg*$^{fl/fl}$ *Cd4 Cre*^{wt} mice and nine out of 13 *Apoe*$^{-/-}$ *Cd40lg*$^{fl/fl}$ *Cd4 Cre*^{tg} mice developed an AAA 28 days after AngII pump implantation, corresponding to AAA incidences of 85.7% and 69.2% (Figure 40 C).

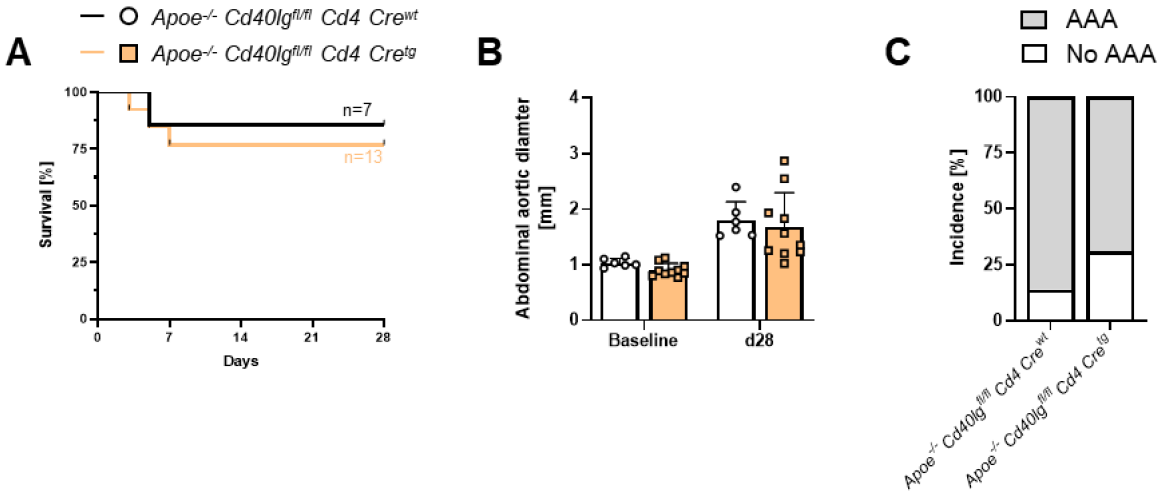

Figure 40: CD40L deficiency on T cells did not affect rupture rate, AAA formation and progression in the AngII model

Induction of AAAs was achieved by continuous AngII infusion into Apoe$^{-/-}$ *Cd40lg*$^{fl/fl}$ *Cd4 Cre*^{wt} *mice and their Cre-expressing littermates. (A) Kaplan-Meier curve shows the percentage survival of AngII-infused T cell-specific CD40L-deficient mice and their Cre negative littermates. Log-rank (Mantel-Cox) test p=0.6421. Apoe*$^{-/-}$ *Cd40lg*$^{fl/fl}$ *Cd4 Cre*^{wt} *n=7, Apoe*$^{-/-}$ *Cd40lg*$^{fl/fl}$ *Cd4 Cre*^{tg} *n=13. (B) Assessment of abdominal aortic diameter using*

non-invasive ultrasound imaging before the pump implantation (baseline) and 28 days after AngII-induced AAA formation. Mean ± SD. Apoe$^{-/-}$ Cd40lg$^{fl/fl}$ Cd4 Cre^{wt} n=6, Apoe$^{-/-}$ Cd40lg$^{fl/fl}$ Cd4 Cre^{tg} n=10. (C) Incidence of AAA or no AAA in Apoe$^{-/-}$ Cd40l$^{fl/fl}$ Cd4 Cre^{wt} and their Cre-expressing littermates 28 days post pump implantation. Two-sided Fisher's exact test; p=0.6126. Apoe$^{-/-}$ Cd40lg$^{fl/fl}$ Cd4 Cre^{wt} n=7, Apoe$^{-/-}$ Cd40lg$^{fl/fl}$ Cd4 Cre^{tg} n=13. Animals that died due to AAA rupture were included. Formation of AAA was defined as an increase in aortic diameter of at least 1.5-fold.

Lack of CD40L on T cells enhanced absolute numbers of circulatory leukocytes and lymphocytes 28 days after AngII-induced AAA formation

Systemic effects of T cell-specific CD40L deficiency on circulatory immune cells were investigated by measuring whole blood samples of *Apoe$^{-/-}$ Cd40lg$^{fl/fl}$ Cd4 Cre^{wt}* mice and their Cre-expressing littermates using an automated haematology analyser. Hematologic analysis resulted in a significant increase in absolute numbers of leukocytes as well as of lymphocytes in blood circulation of *Apoe$^{-/-}$ Cd40lg$^{fl/fl}$ Cd4 Cre^{tg}* mice compared to their Cre^{wt} littermates. Absolute cell numbers of circulatory monocytes and neutrophils were comparable in both genetic strains (Figure 41).

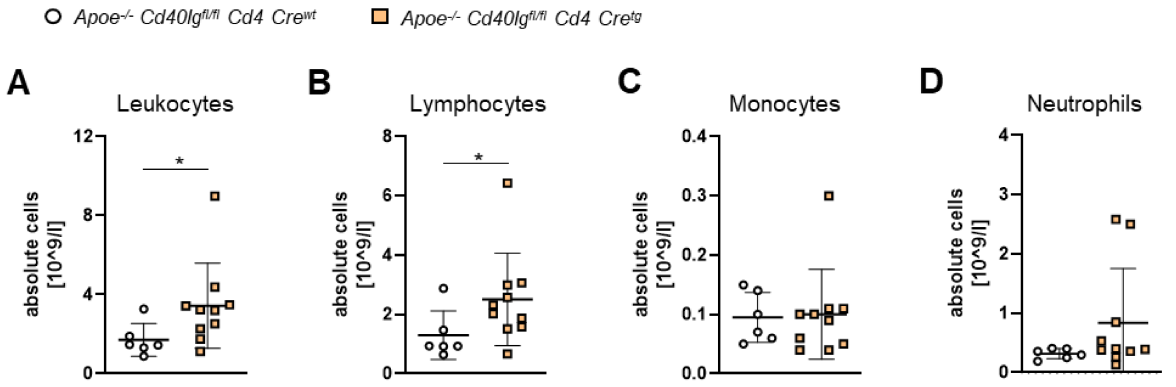

Figure 41: CD40L deficiency on T cells led to increased numbers of circulatory leukocytes and lymphocytes in the AngII model
*Absolute cell numbers of leukocytes (A), lymphocytes (B), monocytes (C) and neutrophils (D) was measured in whole blood samples from Apoe$^{-/-}$ Cd40lg$^{fl/fl}$ Cd4 Cre^{wt} mice and their Cre^{tg} littermates 28 days after AngII-induced AAA formation using an automated haematology analyser. Numbers of leukocytes as well as of lymphocytes were significantly increased in blood of Apoe$^{-/-}$ Cd40lg$^{fl/fl}$ Cd4 Cre^{tg} mice. Unpaired Mann-Whitney test (two-tailed); *p<0.05. Mean ± SD. Apoe$^{-/-}$ Cd40lg$^{fl/fl}$ Cd4 Cre^{wt} n=6, Apoe$^{-/-}$ Cd40lg$^{fl/fl}$ Cd4 Cre^{tg} n=10.*

Apoe$^{-/-}$ Cd40lg$^{fl/fl}$ Cd4 Cre^{tg} mice exhibited reduced CD40L expression on several T cell subsets

Evaluation of CD40L expression on overall CD3$^+$ T cells, CD8$^+$ cytotoxic T cells and CD4$^+$ Th cells from *Apoe$^{-/-}$ Cd40lg$^{fl/fl}$ Cd4 Cre^{wt}* mice and their Cre^{tg} littermates was performed using flow cytometric analysis. Single cell suspensions from blood, aortic lymph nodes and splenic tissue were stained and activated, followed by flow cytometric analysis. Flow cytometric measurements were analysed using a gating strategy that firstly excluded any cell debris and erythrocytes (SSC-A versus FSC-A), as well as cell doublets (FSC-H versus FSC-A). Thereafter, viable CD45$^+$ immune cells were identified. Further, CD3$^+$ T cells were identified and CD40L expression on T cells from *Apoe$^{-/-}$ Cd40lg$^{fl/fl}$ Cd4 Cre^{wt}* (Figure 42 A) and *Apoe$^{-/-}$ Cd40lg$^{fl/fl}$ Cd4 Cre^{tg}* (Figure 42 B) mice was determined. The exemplary dot plot showed a reduction in the number of CD40L-expressing overall CD3$^+$ T cells in *Apoe$^{-/-}$ Cd40lg$^{fl/fl}$ Cd4 Cre^{tg}* mice. Thereafter, the CD3$^+$ T cell population was used to identify CD8$^+$ cytotoxic T cells and CD4$^+$ Th cells. In addition, CD40L expression on these T cell subsets

was determined in single cell suspensions of *Apoe*$^{-/-}$ *Cd40lg*$^{fl/fl}$ *Cd4 Cre*^{wt} (Figure 42 C, E) and *Apoe*$^{-/-}$ *Cd40lg*$^{fl/fl}$ *Cd4 Cre*^{tg} mice (Figure 42 D, F). The exemplary dot plot shows a reduction in the amount of CD40L-expressing cytotoxic T cells and Th cells in *Apoe*$^{-/-}$ *Cd40lg*$^{fl/fl}$ *Cd4 Cre*^{tg} mice compared to Cre^{wt} mice (Figure 42 D, F).

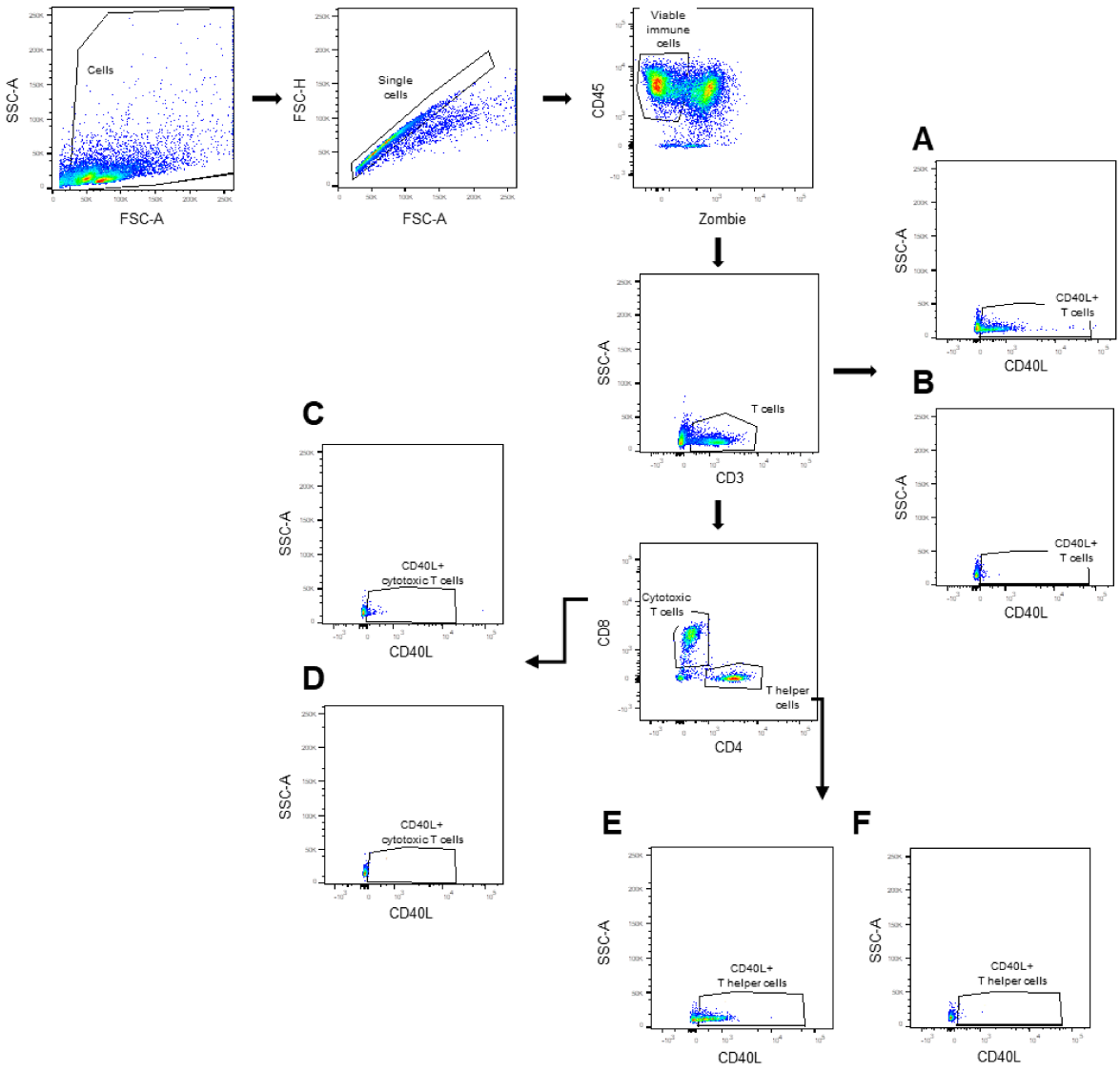

Figure 42: Flow cytometric gating strategy used to assess CD40L expression on T cell subsets
Representative gating strategy to determine CD40L expression on CD3$^+$ T cells, CD4$^+$ T helper cells and CD8$^+$ cytotoxic T cells in lymphatic and renal tissue as well as in blood circulation from Apoe$^{-/-}$ Cd40lg$^{fl/fl}$ Cd4 Cre^{wt} mice and their Cre-expressing littermates. Exemplary dot plots from flow cytometric analysis of CD40L-expressing cells from cell suspension from aortic lymph nodes of Apoe$^{-/-}$ Cd40l$^{fl/fl}$ Cd4 Cre^{wt} mice (A, C, E) and from Apoe$^{-/-}$ Cd40l$^{fl/fl}$ Cd4 Cre^{tg} mice (B, D, F).

To examine the CD40L expression on T cells, the MFI of CD40L on activated T cell subsets from *Apoe*$^{-/-}$ *Cd40lg*$^{fl/fl}$ *Cd4 Cre*^{wt} and *Apoe*$^{-/-}$ *Cd40lg*$^{fl/fl}$ *Cd4 Cre*^{tg} mice was quantified 28 days after AngII-induced AAA formation. Confirmation of CD40L deficiency was investigated on CD3$^+$ T cells, CD8$^+$ cytotoxic T cells and CD4$^+$ Th cells from blood, aortic lymph nodes and spleen. Cre recombinase activity led to a reduction in MFI of CD40L on T cells and Th cells from blood (Figure 43 A, B), aortic lymph nodes (Figure 43 D, E) and spleen (Figure 43 G, H) compared to *Apoe*$^{-/-}$ *Cd40lg*$^{fl/fl}$ *Cd4 Cre*^{wt} mice. MFI of CD40L on cytotoxic T cells was the lowest in all tested tissues compared to the other examined T cell subsets independent of

Cre recombinase expression. However, MFI of CD40L on cytotoxic T cells from blood, aortic lymph nodes and spleen from *Apoe*$^{-/-}$ *Cd40lg*$^{fl/fl}$ *Cd4 Cre*^{tg} mice was also slightly reduced compared to their Cre^{wt} littermates (Figure 43 C, F, I).

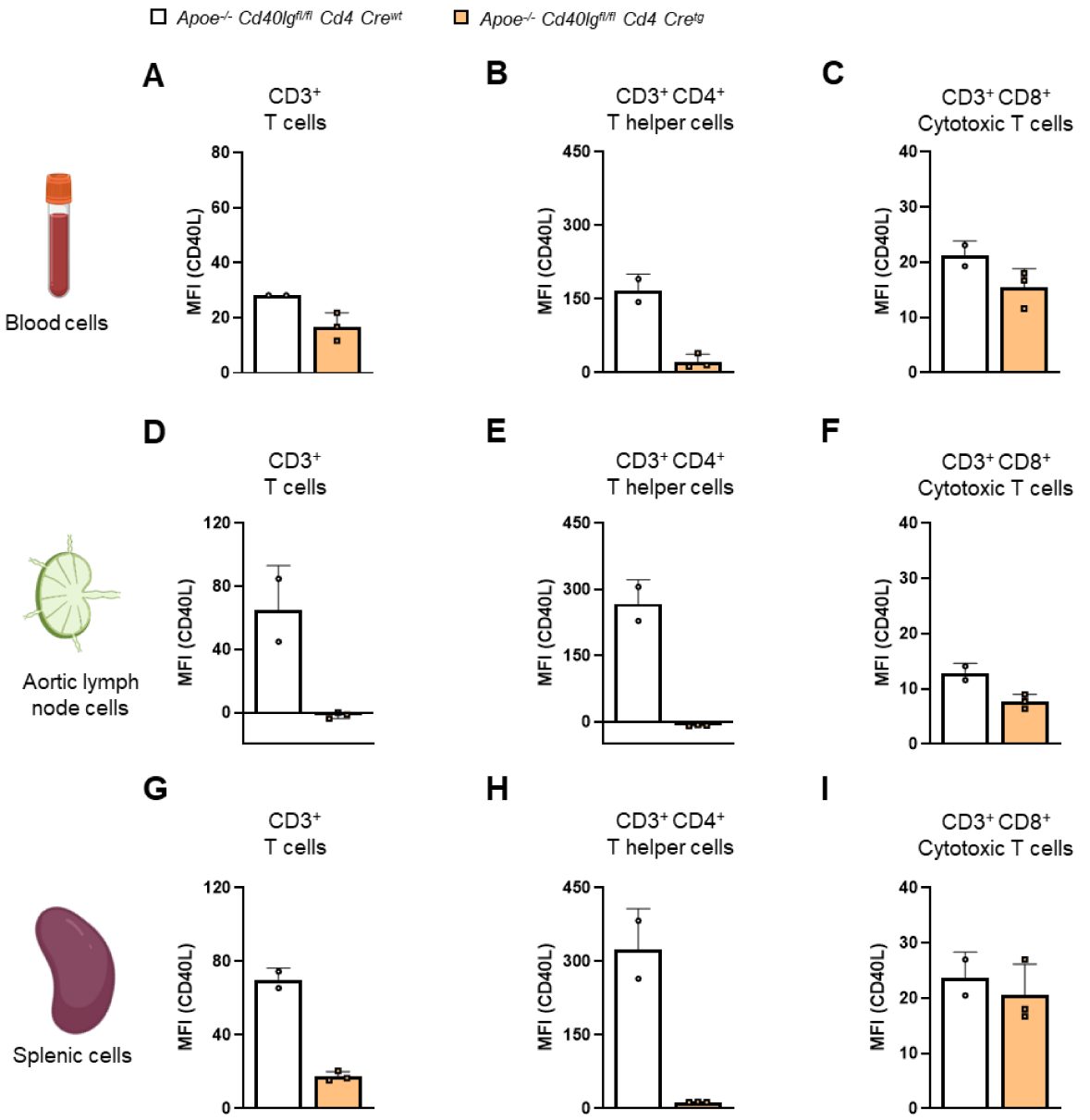

Figure 43: Reduced CD40L expression on T cell subsets from Apoe$^{-/-}$ Cd40lg$^{fl/fl}$ Cd4 Cre^{tg} mice
MFI of CD40L of circulatory (A-C), lymphatic (D-F) and splenic (G-I) activated overall CD3^{+} T cells, CD4^{+} T helper cells and CD8^{+} cytotoxic T cells from Apoe$^{-/-}$ Cd40lg$^{fl/fl}$ Cd4 Cre^{wt} and their Cre-expressing littermates 28 days after AngII-induced AAA formation. Evidence for reduced CD40L expression on all T cell subsets in all tested tissues. Mean ± SD. Apoe$^{-/-}$ Cd40lg$^{fl/fl}$ Cd4 Cre^{wt} n=2, Apoe$^{-/-}$ Cd40lg$^{fl/fl}$ Cd4 Cre^{tg} n=3. MFI = median fluorescence intensity. Tissue icons were used from BioRender.com.

CD40L deficiency on T cells did not affect aortic dilation and AAA incidence 28 days after PPE-induced AAA formation

In addition to the investigations in the AngII model, CD40L deficiency on T cells was examined in the PPE model in following part of this study. AAA was induced in *Cd40lg$^{fl/fl}$ Cd4 Cre^{wt}* mice and their Cre^{tg} littermates by temporarily, intraluminal perfusion of an isolated, infrarenal aortic segment with elastase solution. Dilation of the abdominal aorta was assessed via non-invasive ultrasound imaging before and 28 days after AAA induction. Analysis of aortic diameter revealed no differences in aortic expansion between the two genetic strains (Figure 44 A). Furthermore, AAA incidence was similar in *Cd40lg$^{fl/fl}$ Cd4 Cre^{wt}* compared to *Cd40lg$^{fl/fl}$ Cd4 Cre^{tg}* mice. In detail, twelve out of 18 *Cd40lg$^{fl/fl}$ Cd4 Cre^{wt}* mice and 18 out of 24 T cell-specific CD40L-deficient mice developed an AAA, corresponding to AAA incidences of 66.67% and 75% 28 days after PPE surgery (Figure 44 B).

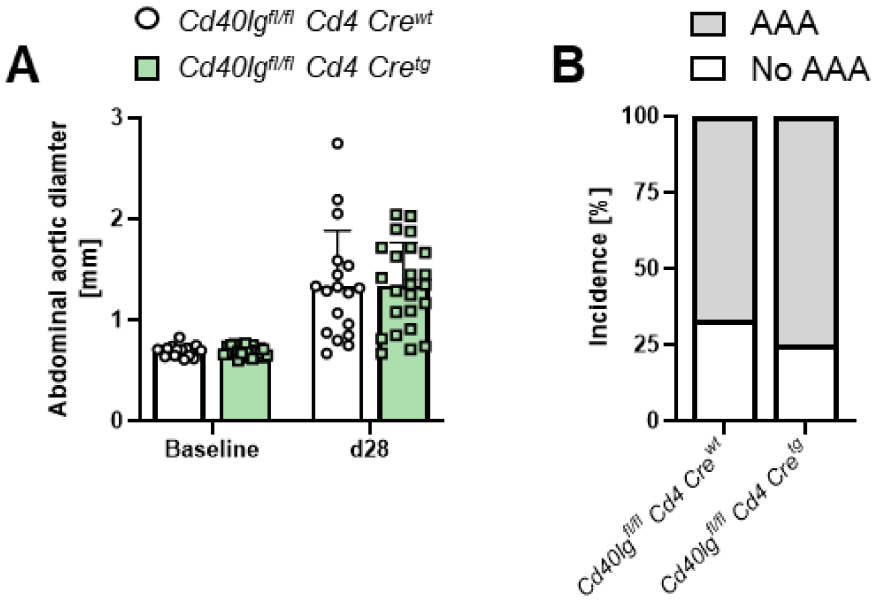

Figure 44: Lack of CD40L on T cells did not affect AAA formation and incidence in the PPE model
Induction of AAAs was achieved by PPE perfusion of an infrarenal aortic segment of Cd40lg$^{fl/fl}$ Cd4 Cre^{wt} mice and their Cre-expressing littermates. (A) Assessment of abdominal aortic diameter using ultrasound images before PPE surgery (baseline) and 28 days after AAA induction. Mean ± SD. (B) Incidence of AAA or no AAA in Cd40lg$^{fl/fl}$ Cd4 Cre^{wt} and Cd40lg$^{fl/fl}$ Cd4 Cre^{tg} mice 28 days after AAA induction. AAA was defined as an increase in aortic diameter of at least 1.5-fold. Cd40lg$^{fl/fl}$ Cd4 Cre^{wt} n=18, Cd40lg$^{fl/fl}$ Cd4 Cre^{tg} n=24.

Lack of CD40L on T cells led to no significant changes in circulatory immune cell numbers

The effect of CD40L deficiency on T cells on the accompanying systemic inflammation in whole blood samples of *Cd40lg$^{fl/fl}$ Cd4 Cre^{wt}* and *Cd40lg$^{fl/fl}$ Cd4 Cre^{tg}* mice was examined 28 days after PPE-induced AAA formation using an automated haematology analyser. Hematologic analysis revealed no changes in absolute numbers of circulating leukocytes, monocytes and neutrophils between the two genetic strains (Figure 45 A, C, D). However, the absolute number of circulating lymphocytes was increased 1.2-fold in mice deficient for CD40L on T cells compared to their Cre^{wt} littermates, but the change did not rise to the level of statistical significance (Unpaired Student's t test (two-tailed); p=0.0865) (Figure 45 B).

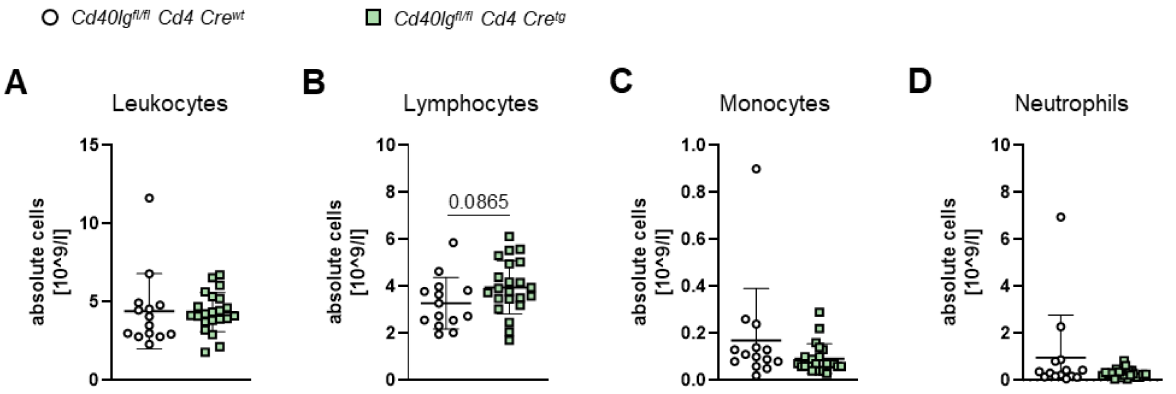

Figure 45: CD40L deficiency on T cells did not alter absolute numbers of circulatory immune cells in the PPE model

Absolute cell numbers of leukocytes (A), lymphocytes (B), monocytes (C) and neutrophils (D) were determined in whole blood samples from Cd40lg$^{fl/fl}$ Cd4 Cre^{wt} mice and their Cre-expressing Cd40lg$^{fl/fl}$ Cd4 Cre^{tg} littermates 28 days after PPE-induced AAA formation using an automated haematology analyser. Unpaired Student's t test (two-tailed) (B) or unpaired Mann-Whitney test (two-tailed) (A, C, D). Mean ± SD. Cd40lg$^{fl/fl}$ Cd4 Cre^{wt} n=14, Cd40lg$^{fl/fl}$ Cd4 Cre^{tg} n=22.

Discussion

Inflammatory processes play a key role in the pathology of AAA and these processes are among others regulated by the interaction of co-stimulatory molecules. The co-stimulatory dyad, CD40 and CD40L, is important in modulating cellular and humoral immune responses. Therefore, this study aimed to investigate the CD40/CD40L axis as potential therapeutic target in abdominal aortic aneurysm. A small molecule inhibitor, which blocks the interaction of TRAF6 to CD40, or lack of CD40 or CD40L on different cell types were used to interfere with CD40-CD40L signalling. AAA formation and the course of inflammatory and proteolytic processes were assessed after CD40-CD40L signalling inhibition post experimental aneurysm induction via PPE perfusion or continuous AngII infusion.

Inhibition of CD40-TRAF6 signalling as therapeutic target in AAA

The potential of modulating co-stimulatory molecules, such as CD40 and CD40L was already proven beneficial in models of chronic inflammatory diseases and other CVDs.[103, 105, 116] Specifically, genetic and pharmacologic inhibition of the binding of TRAF6 to CD40 abolished atherosclerotic plaque development in the thoracic aorta.[103, 106] To achieve pharmacologic inhibition, Zarzycka et al. developed small molecule inhibitors, named TRAF-STOPs, that specifically binds to the TRAF6 protein, thereby blocking the binding to CD40 and further signal transduction.[104] In addition, Kusters et al. already found that CD40L deficiency led to reduced aortic rupture and AAA incidence 28 days after AngII-induced AAA formation.[107] However, the present study was the first to investigate pharmacologic inhibition of CD40-TRAF6 signalling using TRAF-STOP 6860766 in AAA disease in two experimental models. We hypothesised that inhibiting the binding of TRAF6 to CD40 in the context of AAA using TRAF-STOP limits proteolytic and inflammatory processes resulting in decreased AAA pathology and thus reduced AAA formation and progression.

This study demonstrated that blocking the CD40-TRAF6 signalling pathway by TRAF-STOP was sufficient to limit AAA growth after PPE-induced AAA formation by reducing partially ECM degradation and inflammation. TRAF-STOP administration significantly reduced the abdominal aortic expansion quantified on day 14 and 28 after PPE surgery using the analysis of ultrasound and macroscopic images. In the AngII infusion model, TRAF-STOP treatment protected against AAA rupture in mice on chow diet as well as on WD. However, AAA dilation was only slightly decreased in the more severe model after CD40-TRAF6 inhibition, and aortic expansion was not altered in mice on chow diet 28 days after AngII-induced AAA formation. Our results after AngII-induced AAA formation in mice on chow diet are comparable to findings of Kusters et al. that showed already a protection against AAA rupture, whereas AAA expansion was not altered, in global CD40L-deficient *Apoe*$^{-/-}$ mice.[107] However, they also demonstrated a significantly reduced AAA incidence in *Apoe*$^{-/-}$ mice lacking CD40L 28 days after AAA induction, which could not be observed in our study. This may be due to the different methods used to interfere with the CD40/CD40L pathway after AAA induction. Kusters et al. used global CD40L gene-deficient mice, whereas this present study inhibited the CD40-TRAF6 signalling pathway pharmacologically using TRAF-STOP. Using global CD40L gene-deficient mice can not only interfere with the CD40/CD40L axis but also modulate other signalling pathways, as CD40L serves as ligand not only for CD40 but also for integrin receptors αMβ2, αIIbβ3, and α5β1.[117] The interaction of CD40L to αMβ2 on myeloid cells regulates cellular adhesion, binding to αIIbβ3 on platelets mediate thrombotic and haemostatic functions, whereas interaction with α5β1 activates ECs.[117] All these functions may also contribute to AAA pathology and thus enhance the effect of global

CD40L deficiency on AAA incidence. Moreover, these gene-deficient mice are devoid of CD40L from embryonic development on and could have developed compensatory mechanism to bypass potential detrimental effects caused by inhibited CD40-CD40L signalling. Lack of CD40L in these mice most likely also led to an altered immune system even if they developed compensatory mechanisms, as CD40/CD40L signalling is e.g. crucial for the formation of memory B cells and germinal centres.[87] In contrast, pharmacologic treatment using TRAF-STOP selectively inhibits the interaction of CD40 and TRAF6, while the signalling through other adaptor proteins is not affected.[104, 105] In the present study, TRAF-STOP administration was limited in time and started right after AAA induction, thus compensatory mechanisms could not arise. These differences could have led to lower effects on AAA incidence in TRAF-STOP-treated mice compared to global CD40L deficiency. On the other hand, the higher reduction in AAA incidence in CD40L gene-deficient mice may also be due to the different methods used to determine AAA incidence. Kusters et al. noted AAA incidence by macroscopic observations[107], whereas the present study used ultrasound technology and defined AAA formation as an increase in aortic diameter of at least 1.5-fold based on the baseline aortic diameter. The European Society for Vascular Surgery recommended this threshold for defining an AAA.[16] Therefore, it can be assumed that more AAAs were generally diagnosed in our study, as ultrasound measurements are more accurate compared to macroscopic determination. In addition, the accuracy of ultrasound technology may exclude some aortic dilations that do not exceed the AAA size threshold, although they might be counted in a macroscopic evaluation. In the present study, AAA expansion in five DMSO-treated mice and in two TRAF-STOP-treated mice were just below the threshold (Supplementary Figure 3). These mice might likely have been included if a macroscopic evaluation had been carried out as the primary read-out, which may have resulted in an enhanced difference in AAA incidence between the treatment groups. That would have resulted in a more beneficial effect of CD40-TRAF6 inhibition, which would have been more comparable to the results of Kusters et al.[107] Furthermore, in this study the maximum aortic diameter was assessed in ultrasound images using the LTL method of calliper placement (see Assessment of aortic diameter *in vivo*). This method was shown to have a high reproducibility such as the ITI method, whereas the OTO methods led to increased AAA size and thus higher number exceeding the size threshold[118], which makes the results of this study appear reliable.

CD40-TRAF6 inhibition resulted in significantly reduced AAA dilation 28 days after PPE-induced AAA formation, but not after continuous AngII infusion. One possible explanation is the different AAA pathomechanism underlying the individual experimental model. Mechanistically, the intraluminal perfusion of an isolated aortic segment results in the proteolytic degradation of medial elastic fibres accompanied by inflammatory processes, which then causes AAA formation.[8] In contrast, continuous AngII infusion using subcutaneously implanted osmotic pumps causes mostly medial dissection and subsequent haemorrhage followed by macrophage infiltration and ECM deposition. Thrombi and lumen dilation result in the formation of a pseudoaneurysm.[119] The effects of CD40-TRAF6 signalling in AAA pathology are poorly understood, but the results of this study led to the suggestion that TRAF-STOP treatment may modify proteolytic ECM turnover and thus impede AAA dilation following PPE-induced AAA formation. However, this treatment seem to be unable to inhibit medial dissection and thus aortic expansion following continuous AngII infusion. The possible alteration in proteolytic ECM degradation after CD40-TRAF6 signalling inhibition may also explain the reduced mortality rate following continuous AngII infusion. Here, extensive adventitial ECM degradation and subsequently weakening of the aortic wall lead to AAA rupture. Since aneurysm rupture commonly occurs in the AngII model but not in the PPE model,[109] this effect was only detected after AngII-induced AAA formation.

Using TAM-inducible, global CD40-deficient *Apoe*$^{-/-}$ *Cd40*$^{fl/fl}$ *CreER*^{tg} mice and their CreER^{wt} littermates in the AngII model supported these observations in our study. Results showed a reduction in mortality due to aortic rupture in *Apoe*$^{-/-}$ *Cd40*$^{fl/fl}$ *CreER*^{tg} mice 28 days after continuous AngII infusion, whereas AAA expansion was similar in both genetic strains. Together with findings of Kusters et al. in global CD40L-deficient *Apoe*$^{-/-}$ mice[107], this indicates a possible beneficial effect of interfering with the CD40-CD40L axis on AAA development, possibly by a reduction in ECM degradation. Therefore, the next step in the present study was therefore to investigate elastin degradation and collagen content in aneurysmal tissue after PPE-induced AAA formation.

Effects of CD40-TRAF6 signalling inhibition on ECM degradation

The amount and structure of ECM proteins within the aortic wall maintain elasticity as well as strength, and variations can influence these functions resulting in e.g. AAA formation.[10] In this study, pharmacological inhibition of CD40-TRAF6 signalling by TRAF-STOP limited collagen type IV but not elastin degradation 28 days after PPE-induced AAA formation. These findings probably resulted from reduced *Mmp2* mRNA expression in aneurysmal tissue in early disease stages. The PPE model utilizes the proteolytic degradation of medial elastic fibres to induce AAA formation.[8] In our experimental AAA model, the aorta was perfused with PPE at 120 mmHg pressure. Liu et al. had shown that the perfusion pressure has a major impact on elastin degradation.[120] A perfusion pressure of 100 mmHg halved the elastin content in aneurysmal tissue compared to a perfusion without pressure. A further increased perfusion pressure to 300 mmHg reduced the elastin content 4-fold. The perfusion pressure used to induce AAA formation in our study may have already caused an elastin degradation to such an extent that inhibition of CD40-TRAF6 signalling was not effective to reduce the degradation of elastic fibres. However, Kusters et al. also found no difference in elastin degradation in CD40L-deficient *Apoe*$^{-/-}$ mice 28 days after AngII-induced AAA formation.[107] This leads to the assumption that, contrary to our hypotheses, interfering with the CD40/CD40L axis may not be able to diminish elastic fibre degradation. Nevertheless, to verify this the effect of CD40-TRAF6 signalling inhibition on elastin degradation in aneurysmal tissue in different experimental models should be further investigated in the future.

Steffensen et al. demonstrated that collagen IV deficiency facilitates AAA development,[29] supporting our results and hypothesis that CD40-TRAF6 signalling inhibition may be beneficial in AAA pathology. Our study focussed on the determination of the collagen type IV amount in aneurysmal cross-sections using IF staining. Although, Urabe et al. showed that the orientation of adventitial collagen in the aortic wall is essential for tissue dynamics and strength and that disorganized collagen fibrils were increased in AAA tissue.[121] Therefore, future studies should investigate if inhibiting the CD40-TRAF6 signalling also affects other parameters such as the structure of adventitial collagen and thus the strength of the aortic wall.
Our findings provide no further information whether the inhibition of CD40-TRAF6 signalling reduced the degradation or increased the neo-synthesis of collagen. Previous studies have shown that both were present in aneurysmal tissue. Collagen type III degradation was shown to be increased in aneurysmal tissue of AAA patients. Enhanced turnover of collagen type III was also found to correlate with AAA diameter and positive symptomatology.[122] In contrast, Minion et al. investigated the content of collagen in the aneurysmal wall of AAA patients by amino acid analysis and found enhanced collagen amounts due to an increase in synthesis.[123] Bode et al. showed elevated levels of type III procollagen in the medial layer of aneurysmal cross-sections, whereas levels of type I procollagen were increased in the

intima, suggesting an enhanced metabolism of collagens in AAAs.[124] These differences may reflect different stages in ECM remodelling, and it seems to be important to maintain a balance in the amount of collagens in the aortic wall. Furthermore, these studies demonstrated that also collagen type III and I are of major interest in AAA pathology, and these collagens were additionally found to be the most abundant in the aorta.[25] Therefore, the amount of collagen types I and III, as well as further information about a possible neo-synthesis or degradation of each collage type should be collected in respect of a potential effect upon CD40-TRAF6 signalling inhibition in the future. Regarding the function and required integrity of collagens to prevent aortic rupture and the here shown protection against AAA rupture upon TRAF-STOP treatment in *Apoe*$^{-/-}$ mice after AngII-induced AAA formation, future studies should also investigate the effect of CD40-TRAF6 signalling inhibition on the collagen metabolism particularly after AngII-induced AAA formation.

Limiting ECM degradation by preventing MMP expression and activity in aneurysmal tissue is crucial to reduce AAA incidence and progression.[26] CD40 and CD40L interaction on various cell types plays an important role in inducing MMP production.[125] Gelatinases, MMP2 and MMP9, are known to degrade among others elastin and collagen type IV.[126] Accordingly, the effect of inhibiting CD40-TRAF6 signalling on gelatinase expression was investigated in this study. TRAF-STOP administration led to reduced *Mmp2* mRNA expression in AAA tissue 7 and 14 days after PPE-induced AAA formation revealed by gene expression profiling, whereas *Mmp9* mRNA expression was only decreased 14 days after AAA induction. However, the activity of MMP2 and MMP9 in aneurysmal tissue was not altered upon CD40-TRAF6 inhibition 14 days after AAA induction. Although this study is the first to investigate the effects of CD40-TRAF6 inhibition on MMP expression and activity after PPE-induced AAA formation, previous studies already investigated the CD40-CD40L axis in AAA pathology.[107, 127] In contrast to our findings, CD40L deficiency led to reduced MMP2 and MMP9 activity 28 days after AngII-induced AAA formation, whereas *Mmp2* and *Mmp9* mRNA expression was not significantly altered in AAA tissue 7 and 28 days after AAA induction.[107] Furthermore, Nagashima et al. demonstrated a decreased *MMP2* mRNA expression as well as MMP2 protein production in cultured aortic tissue from AAA patients after inhibition of the CD40-CD40L pathway by trapidil.[127] On the one hand, discrepancies in study results may derive from different experimental AAA models with distinct pathomechanisms.[8] On the other hand, three different methods were used to interfere with the CD40-CD40L pathway, genetic CD40L deficiency, treatment with trapidil or with TRAF-STOP. In assition, MMP activity was investigated at different time points after AAA induction. Combining the findings of Kusters et al and our data, provide evidence that proteolytic degradation of ECM proteins seems to be affected by the inhibition of CD40-CD40L signalling at later disease stages. However, MMP activity is regulated among others by the presence of TIMPs.[33] As our results did not provide information about mRNA expression and protein levels of TIMPs in aneurysmal tissue, these and the MMP2 and MMP9 activity in early and later disease stages (d7, d28) should be investigated in regard to a possible effect of CD40-TRAF6 inhibition in future studies.
The present study determined gene expression in two individual aneurysmal cross-sections from each treatment group 7 and 14 days after PPE-induced AAA formation by spatial transcriptomics as well as in isolated CD45^{+} cells from two pooled AAAs from DMSO- and TRAF-STOP-treated mice 7 days after AAA induction by CITE sequencing. To confirm our results on *Mmp2* and *Mmp9* expression, future studies needs to increase the amount of individual experiments. In addition, spatial transcriptomic technology was only performed on one cross-section from a whole AAA. In order to obtain an overview of the MMP expression in the entire aneurysmal tissue, several consecutive cross-sections should be used in further experiments.

Moreover, this study focussed on the expression and activity of gelatinases, even so collagen type IV as well as fibrillar collagen type I and III can be also degraded by collagenases (MMP1, 8, 13 and 18).[126] To validate whether the reduced collagen type IV amount in AAA tissue upon TRAF-STOP treatment is due to the decreased *Mmp2* mRNA expression shown in this study or whether this is also a result of reduced collagenases, should be further examined. Specifically, additional investigations of the presence and activity of collagenases in aneurysmal tissue after CD40-TRAF6 signalling inhibition in different experimental AAA models would be of interest.
MMP2 is predominantly synthesised by SMCs and fibroblast, as well as partially macrophages, whereas MMP9 is mainly derived from macrophages and partially neutrophils.[36] To provide insights, whether reduced MMP expression in aneurysmal tissue of TRAF-STOP-treated mice emerged from actual decreased cellular expression or from reduced numbers of MMP-expressing cells in AAA tissue upon CD40-TRAF6 inhibition, this study further investigated the distribution of several immune cell types in AAA tissue.

Effects of CD40-TRAF6 signalling inhibition on the immune response

Development and progression of AAA is driven by chronic inflammation caused by the infiltration and activation of various immune cells into the aneurysmal tissue.[40] Among others macrophages, neutrophils, NK cells, B cells and T cells were shown to play a crucial role in AAA formation.[40] The co-stimulatory dyad CD40-CD40L regulates various immune and inflammatory processes.[87] Accordingly, we hypothesised that inhibition of CD40-TRAF6 signalling may contribute to reduced immune cell infiltration into the aneurysmal tissue, and thus, led to a reduced inflammatory response resulting in attenuated AAA progression.

In general, various immune cells were found in aneurysmal tissue and their contribution to AAA formation and progression was demonstrated in plenty studies.[40] However, this contribution was mostly investigated in one experimental AAA model, e.g. effects on macrophages in AAA tissue were examined after AngII-induced AAA formation in 16 studies, whereas only in 2 studies after PPE-induced AAA formation.[40] Therefore, the results obtained in one experimental model need to be interpreted with caution and not related to the AAA pathology in general, especially as all experimental models has limitations and only mimic parts of the human disease. One single immune cell type can function differently or have another activation status resulting in a different immune response in the aortic wall and thus may contribute differently to AAA pathology based on the AAA induction method used. To overcome this restriction, this study investigated the immune cell proportions in AAA tissue after PPE and AngII-induced AAA formation and demonstrated that CD40-TRAF6 signalling inhibition seem to have different effects on the immune cell content depending on the AAA induction method.
This study demonstrated a significantly reduced proportion of myeloid cells, whereas the proportions of B cells and Th cells were remarkably enhanced, upon TRAF-STOP treatment 28 days post PPE-induced AAA formation. In aneurysmal tissue of *Apoe*$^{-/-}$ mice on chow diet CD40-TRAF6 inhibition led to a minor reduction in the T cell proportion. Using the severe AngII model, inhibition of CD40-TRAF6 signalling resulted in a significantly increased proportion of T cells 28 days after AAA induction, whereas the proportion of neutrophils was significantly reduced in AAA tissue of *Apoe*$^{-/-}$ mice. These results show that treatment with TRAF-STOP led to different results in the distribution of immune cells in aneurysmal tissue in the different experimental models. Highlighting the importance of investigate AAA pathology in several experimental models.

Our findings are partially in line with the previous study from Kusters et al. that showed a significantly reduced amount of macrophages and a decrease in the T cell content in aneurysmal tissue of CD40L-deficient *Apoe*$^{-/-}$ mice 28 days after AngII-induced AAA formation.[107] However, with regard to the used AAA induction methods, their results would be most comparable to ours obtained with the AngII model in *Apoe*$^{-/-}$ mice on chow diet, but our results in this model did not demonstrate a reduction in macrophages. This discrepancy may be due to the different methods used to inhibit the CD40/CD40L axis after AAA induction. As mentioned above, Kusters et al. used global CD40L gene-deficient mice, thereby also inhibiting other signalling pathways involving CD40L and the integrin receptors αMβ2, αIIbβ3, and α5β1. This could also affect the presence of various immune cells in aneurysmal tissue, e.g. the reduced macrophage content demonstrated by Kusters et al.[107] It seems that blocking only parts of the CD40/CD40L axis by TRAF-STOP administration, is not sufficient to reduce the macrophage population in AAA tissue in the AngII model using *Apoe*$^{-/-}$ mice on chow diet. Besides, this difference may also be due to the different methods used to determine the immune cell content in aneurysmal tissue. Kusters et al. used immunohistochemistry staining of individual AAA cross-sections, which only provides a brief insight of the presence of immune cells in the aneurysm, whereas in the present study the whole AAA tissue was digested and used for flow cytometric examination. On the other hand, we focused on the determination of immune cell proportions in aneurysmal tissue. Additional investigations that concentrate on the absolute numbers of immune cells in AAA tissue would be of interest, as proportions of immune cell population may vary compared to the determination of absolute cell numbers in aneurysmal tissue. If the proportion of one immune cell population shifts, this has an impact on the proportion of other populations. To avoid this limitation one could determine absolute cell numbers and future studies should then investigate the effect of CD40-TRAF6 inhibition on immune cell infiltration into the aneurysmal tissue.

In contrast to our hypothesis, CD40-TRAF6 inhibition slightly enhanced B and T cell proportions after PPE-induced AAA formation and led to a significant increase in the T cell proportion after AngII-induced AAA formation in *Apoe*$^{-/-}$ mice on WD. However, previous studies showed that in the context of AAA, the role of B cells is controversial and depending on the T cell subset, they can promote or attenuate AAA progression.[65, 67, 70, 72] The present study focussed on general immune cell types and not on specific immune cell subsets, thus, future studies should investigate this to obtain more precise information about the underlying mechanism of CD40-TRAF6 inhibition on immune cell content in AAA tissue.

This study found no alterations in the macrophage proportion in AAA tissue of *Apoe*$^{-/-}$ mice upon CD40-TRAF6 inhibition 28 days after AngII-induced AAA formation. Although it has been shown that treatment with TRAF-STOP was particularly effective in macrophages to reduce experimental atherosclerosis.[106] However, interfering with the CD40-TRAF6 signalling pathway was also found to polarize macrophages toward a more anti-inflammatory phenotype.[103] Since this study determined the proportion of macrophages in AAA tissue and did not investigate the activation status and polarization of them, this should be further examined to clarify the inflammatory response of immune cells in AAA tissue upon CD40-TRAF6 inhibition.

Moreover, our results further support a coherence between altered immune cell presence in AAA tissue and reduced AAA expansion upon CD40-TRAF6 signalling inhibition. TRAF-STOP treatment led to reduced AAA expansion after PPE surgery in C57BL/6J mice and after continuous AngII infusion in *Apoe*$^{-/-}$ mice on WD. In both models, administration of TRAF-STOP also led to differences in the immune cell content in the aneurysm, whereas no changes in AAA dilation as well as in immune cell proportions were detected in *Apoe*$^{-/-}$ mice on chow diet upon CD40-TRAF6 inhibition after AngII-induced AAA formation.

With regard to the number of MMP-expressing cells in AAA tissue upon CD40-TRAF6 signalling inhibition, this study only demonstrated a reduced proportion of myeloid cells

28 days after aneurysm induction, although the expression of *Mmp2* and *Mmp9* was reduced partially in early disease stages. Accordingly, this study did not reveal whether the demonstrated reduction in MMP expression upon TRAF-STOP treatment emerged from an actual decrease in cellular expression or from a reduction in the numbers of MMP-expressing cells. Thus, additional studies could investigate the amount of MMP-expressing cells such as myeloid cells and neutrophils upon CD40-TRAF6 inhibition at later disease stages. Of interest could also be the potential effect of TRAF-STOP treatment on the amount of non-hematopoietic cells like ECs, SMCs and fibroblasts in AAA tissue, which are known to express CD40 as well as collagenases.[20, 85]

Furthermore, cytokines and chemokines are important regulators of inflammatory processes and thus play a key role in AAA pathology.[74] Interaction of CD40 and CD40L on various cell types is crucial to induce the production of chemokines and cytokines.[125] Therefore, we hypothesized that inhibition of CD40-TRAF6 binding and further inhibition of downstream inflammatory signalling pathways may result in reduced expression and release of inflammatory mediators such as cytokines and chemokines. Accordingly, this study demonstrated that TRAF-STOP administration led to a reduction in *Tnfa* mRNA expression in aneurysmal tissue 7 and 14 days after PPE-induced AAA formation using spatial transcriptomics technology. This is in line with findings of Kusters et al. that showed a significant reduction in *Tnfa* mRNA expression in AAA tissue of CD40L-deficient *Apoe*$^{-/-}$ mice 7 days after AngII-induced AAA formation.[107] Our results indicate that the reduction in *Tnfa* mRNA expression is due to an absolute decrease in cellular expression. Since the present study did not found a reduction in the proportions of the major TNFα-expressing cells, macrophages and neutrophils, in AAA tissue upon CD40-TRAF6 signalling inhibition 7 days after AAA induction. However, the results of reduced *Tnfa* mRNA expression must be interpreted with caution, as the limitations of spatial transcriptomics and CITE sequencing experiments performed in this study as described above also apply here. Additional studies should confirm the potential beneficial reduction of TNFα upon TRAF-STOP treatment by increasing the amount of individual experiments.

Pro-inflammatory cytokines such as TNFα, IL-12, and IL-17 are considered to exacerbate AAA disease.[74] Xiong et al. showed that inhibition of TNFα led to reduced $CaCl_2$-induced AAA formation and IL-12 blockage was found to alleviate AAA disease in the PPE model.[78, 128] In addition, genetic IL-17 deficiency as well as inhibiting Th17 cell differentiation by digoxin resulted in reduced AAA development in different experimental murine models.[69, 70] Yet, in mice treated with TRAF-STOP, we observed a decrease in plasma levels of IL-12 and IL-17 28 days after PPE-induced AAA formation, as well as slightly reduced TNFα levels in plasma of *Apoe*$^{-/-}$ mice on chow diet 28 days after AngII pump implantation. These findings support our hypothesis that CD40-TRAF6 signalling inhibition results in reduced inflammatory responses and thus reduced AAA formation.

Furthermore, in the severe AngII model TRAF-STOP treatment led to increased plasma levels of IL-10 in *Apoe*$^{-/-}$ mice on WD 28 days after AngII-induced AAA formation. This is consistent with previous studies, which have demonstrated that IL-10 plays a protective role in AAA pathology and its presence is required for the maintenance of a healthy vessel wall.[83, 129] This result support the evidence that inhibition of CD40-TRAF6 signalling shifts the pro-inflammatory phenotype towards an anti-inflammatory profile.[103] In contrast, the concentration of the pro-inflammatory cytokines, IL-1β and GM-CSF were also increased in plasma of *Apoe*$^{-/-}$ mice on WD after CD40-TRAF6 blockage 28 days after AngII-induced AAA formation. Although some studies demonstrated a detrimental role for these cytokines in AAA disease,[79, 130] there are some contradictory studies reporting conflicting outcomes.[131] This discrepancy seems to be due to the experimental AAA-induction method used. Pharmacological inhibition of IL-1β prevented AAA formation in the AngII model and GM-

CSF was shown to be important in patients with aortic dissection but not in AAA patients.[132, 133] These results indicate that TRAF-STOP treatment is not able to limit the secretion of all AAA-promoting cytokines, but is still sufficient to reduce AAA formation and rupture in the severe AngII model.

Zarzycka et al. showed an inhibition of NF-κB signalling with IC_{50} values in the low µM range using TRAF-STOP 6860766 via a luciferase NF-κB assay.[104] Furthermore, TRAF-STOP limited IL-1β and IL-6 expression induced by CD40 in bone marrow-derived macrophages and increased survival rates of mice in an experimental model of polymicrobial sepsis. The compound did not show toxicity in an *in vitro* viability assay and did not cause abnormalities in 13 organs analysed.[104] In addition, Lameijer et al. has proven that an HDL-based nano-immunotherapy using the analogue, TRAF-STOP 6877002, was beneficial to treat inflammation in atherosclerosis in mice and they strengthened the potential of CD40-TRAF6 inhibition for clinical translation, as the treatment was proven to be safe in non-human primates.[134] These findings together with the limitations of a general blockage of CD40 or CD40L, as this caused severe side effects,[95] and our study results support the use of small molecule inhibitors for the treatment of CVDs such as AAA and the clinical translational potential of this therapy.
The present study is the first that demonstrated the beneficial effects of CD40-TRAF6 inhibition on AAA pathology after PPE-induced aneurysm formation. Furthermore, different cytokines, chemokines and proteases and therefore ECM degradation seem to be affected by the blockage of CD40-TRAF6 interaction at different disease stages. The altered proportions of immune cells as well as pro-inflammatory cytokines in AAA tissue upon TRAF-STOP treatment points toward a generalized decrease in the inflammatory status of these mice, which emphasises the strong pro-inflammatory functions of the CD40-CD40L axis.[125]
However, only minor effects of CD40-TRAF6 signalling inhibition on AAA expansion and rupture in the AngII model were found, indicating an experimental model-dependent effect. The meta-analysis of Trachet et al. revealed that treatment studies using the AngII model should be interpreted with caution as it features some limitations when reporting only the aortic expansion as outcome.[135] Instead, these studies should focus among others on structural changes in the aortic wall, thus, future studies need to investigate the effects of CD40-TRAF6 inhibition on ECM proteins, proteases as well as on the inflammatory response in the AngII model.

Cell type-specific CD40 and CD40L signalling in AAA

In the context of AAA, many immune cells were shown to contribute to AAA formation and progression.[40] This study indicated a possible coherence between significant changes in immune cell distribution in aneurysmal tissue 28 days after AAA induction and aortic expansion upon CD40-TRAF6 inhibition. CD40 as well as TRAF6 are widely expressed in a variety of immune cells, including monocytes, macrophages, B cells, DCs and T cells.[85, 136] Corresponding B cell- or myeloid cell-specific CD40-deficient mice as well as T cell-specific CD40L-deficient mice were generated using the Cre/lox P system[137], to allow a direct and indirect inhibition of CD40 signalling in experimental AAA models. We hypothesized that depleting CD40 on B cells or myeloid cells as well as depleting CD40L on T cells could reduce the activation of CD40 signalling and thereby limit proteolytic and inflammatory processes, thus, reduce AAA formation. This approach is also able to reveal, which CD40- or CD40L-expressing cell type is mainly involved in CD40 signalling during AAA pathology.

Effects of cell type-specific CD40 deficiency in AAA

Our generated *Apoe*$^{-/-}$ *Cd40*$^{fl/fl}$ *Cd19 Cre*^{tg} mice contain B cells with significantly reduced CD40 expression in all tested organs, specifically in blood, aortic lymph nodes, spleen, and aorta. However, on myeloid cells the CD40 expression was also affected in aorta and in aortic lymph nodes. Nevertheless, this study demonstrated no effect on systemic inflammation shown by similar numbers of immune cells in the blood circulation 28 days after AngII-induced AAA formation. Lacking CD40 on B cells did not influence AAA rupture, size and incidence compared to their CD40-expressing littermates after AngII-induced AAA formation. These findings are in contrast to our hypothesis, particularly as CD40 signalling in B cells plays a crucial role in maintaining B cell functions including T cell-dependent immunoglobulin class switching and germinal centre formation.[90] It has been shown that B cells and Igs are abundantly present in the adventitial layer of the aneurysmal wall and have been activated there.[138, 139] In addition, it has already been demonstrated that B cell activation is contributing to AAA development in experimental AAA models. B cell-deficient mice and the usage of B cell neutralizing antibodies prevented $CaCl_2$- and elastase-induced AAA formation.[65, 66] However, these beneficial effects were observed in experimental AAA induction models other than the model used in the present study. Since all three experimental mouse model exhibit other pathomechanisms,[8] this leads to the assumption that the detrimental role of B cells in AAA pathology is more crucial after $CaCl_2$- and elastase-induced aneurysm formation compared to continuous AngII infusion. It is important to emphasise, that these previous studies showed beneficial effects after complete B cell depletion, whereas in the present study we specifically inhibit CD40 signalling in B cells. Nevertheless, Tay et al. could previously demonstrate the importance of CD40 signalling in B cells in atherosclerosis. They found that CD40 on B cells was important for their atherogenic effects and that genetic deletion of CD40 on B cells led to decreased atherosclerosis and IgG plasma levels.[140] A study by Meher et al. highlighted that the role of B cells in AAA pathology is not fully understood yet, as B cell deficiency did not affect AAA growth in the PPE model.[67]
Taken together, these studies show a controversial role of B cells in AAA but the overall process seem to include B cell activation and Ig class switching in the adventitial AAA wall, which is dependent on CD40. Therefore, our results tend to suggest that the overall effect of CD40-dependent Ig class switching is at best small and that this plays a minor role in the AngII model. This may be due to the minor contribution of CD40 signalling in B cells on proteolytic processes, one of the main hallmarks of AAA disease, since e.g. gelatinases are mostly expressed by SMCs and fibroblast, macrophages and neutrophils.[36] However, future studies should also investigate the contribution of B cell-specific CD40 signalling in other experimental models to verify this suggestion.

Macrophages are important cells of the innate immune system, contributing to the formation and progression of AAA by, among others, releasing pro-inflammatory mediators and proteases.[47, 56] Therefore, the next step in this study was to investigate the effect of inhibiting CD40 signalling in myeloid cells on AAA development using *Apoe*$^{-/-}$ *Cd40*$^{fl/fl}$*Lyz2 Cre*^{tg} mice and their Cre^{wt} littermates. This study did not reveal a beneficial impact on AAA rupture rate, expansion and incidence in mice deficient for CD40 on myeloid cells 28 days after AngII-induced aneurysm formation. Systemic inflammation was also not affected in *Apoe*$^{-/-}$ *Cd40*$^{fl/fl}$*Lyz2 Cre*^{tg} mice demonstrated by similar numbers of blood leukocytes, lymphocytes, monocytes and neutrophils. These results tend to suggest that CD40-mediated pro-inflammatory signalling in myeloid cells is not as important in AAA pathology as assumed. This could be due to the various mediators that can activate pro-inflammatory signalling pathways, e.g. NFκB signalling in macrophages, and thus contribute to the development of AAA. Receptors that facilitate the activation of NFκB in myeloid cells include, beside CD40,

TNFR1/2, IL-1 receptor type 1 (IL1R1) as well as TLRs.[141] It has already been shown that the TLR4 receptor as well as TNFα and IL-1β, which interact with TNFR1/2 and IL1R1 respectively, play a crucial role in AAA pathology.[78, 79, 142] This indicates that the inhibition of the CD40 signalling pathway in myeloid cells and the potential resulting reduction in pro-inflammatory mediators may have been compensated by the stimulation of other receptors that facilitate inflammatory responses.
These claims can only be considered if the efficiency of CD40 deficiency on myeloid cells has been verified in the genetically-modified mouse strain used. In this study, flow cytometric analysis revealed no significant reduction in CD40 expression on $CD11b^+$ myeloid cells from aorta, blood, aortic lymph nodes and spleen. Notably, only the CD40 expression on neutrophils from aortic lymph nodes was significantly decreased. Based on these findings, myeloid cell-specific Cre recombinase expression seem to be not efficient to reduce CD40 expression on these cells in *Apoe*$^{-/-}$ *Cd40*$^{fl/fl}$ *Lyz2 Cre*^{tg} mice. The *Lyz2* gene encodes for the lysozyme M protein, which is expressed in myelomonocytic cells including monocytes, macrophages and granulocytes in mice.[143] In 1999, Clausen et al. developed the Lyz2-Cre mouse to permanently inactivate target genes in myeloid cells using the Cre/lox P recombination system.[144] Since then, these animals have been used in many studies to inactivate myeloid-specific genes and investigate the effects on various diseases. It has been demonstrated that myeloid-specific netrin-1-deficient and JMJD3-deficient mice were protected from AAA formation.[145, 146] In atherosclerosis, Bosmans et al. could already show that myeloid-specific CD40 deficiency led to reduced lesion size and necrotic core size.[147] All these studies used the *Lyz2*-Cre strain, and successfully verified the genetic deletion by immunofluorescence staining,[145] by quantitative polymerase chain reaction (qPCR) or western blotting.[147] Flow cytometric analysis failed to show a reduction in myeloid cell-specific CD40 expression in blood and spleen from the *Lyz2*-Cre mouse in the context of atherosclerosis.[147] These findings are consistent with our results from the flow cytometric analysis. Macrophages have been shown to exhibit high autofluorescence and are notorious for unspecific binding of antibodies due to their extent expression of Fc receptors.[148, 149] This may cause difficulties when analysing macrophages using flow cytometry and could explain the lack of reduction of myeloid cell-specific CD40 expression. Thus, additional methods, such as those used in the other studies, are required to verify the decrease in CD40 expression on myeloid cells.
The *Lyz2*-Cre strain can result in deletion of the target gene not only in monocytes and macrophages but also in granulocytes as neutrophils as well as in DCs due to their close linage relationship.[146] Based on their great heterogeneity under physiological and pathological conditions, Shi et al. emphasized that a transgenic Cre strain, which is completely specific for macrophages would be impossible.[143] Nevertheless, macrophages play a crucial role in AAA pathology. Our study demonstrated great beneficial effects of CD40-TRAF6 inhibition using TRAF-STOP on AAA development, which may be partly due to a reduced proportion of macrophages in the aneurysmal wall in the PPE model. These TRAF-STOP-mediated effects could not be replicated in the AngII model. Therefore, future studies need to examine the macrophage-derived CD40 signalling in the context of AAA pathology in more detail in respect of the experimental AAA-induction model used and the method of CD40 signalling inhibition using genetic ablation.

Effects of T cell-specific CD40L deficiency in AAA

Cell type-specific depletion of CD40L on T cells was investigated with respect on AAA formation and development in the AngII and PPE model using *Apoe*$^{-/-}$ *Cd40lg*$^{fl/fl}$ *Cd4 Cre*^{tg} and *Cd40lg*$^{fl/fl}$ *Cd4 Cre*^{tg} mice. Our study demonstrated that our generated *Apoe*$^{-/-}$ *Cd40lg*$^{fl/fl}$ *Cd4 Cre*^{tg} mice contain reduced CD40L expression on $CD3^+$ T cells and $CD4^+$ Th cells from blood, aortic lymph nodes and spleen. This is in line with the study of Lacy et al. verifying

CD40L deficiency in these mice using immunofluorescence staining and flow cytometric analysis.[150] Consistent with our work, they found that T cell-specific CD40L-deficient mice exhibit a slightly increased number of leukocytes and lymphocytes in peripheral blood compared to their CD40L-expressing littermates. Using the AngII model, we detected an even higher and significant increase in the numbers of circulatory leukocytes and lymphocytes in *Apoe*$^{-/-}$*Cd40lg*$^{fl/fl}$ *Cd4 Cre*^{tg} mice. Therefore, the basally change in the leukocyte and lymphocyte content in peripheral blood due to the CD40L deficiency must be taken into account when examining AAA pathology using the experimental AngII model.
In atherosclerosis, T cell-specific CD40L deficiency was sufficient to protect mice from developing advanced atherosclerotic plaques.[150] With respect of this and the previous study of Kusters et al. showing a reduction in AAA rupture and formation in overall CD40L-deficient mice,[107] this study hypothesized that lack of CD40L on T cells would interfere with CD40 signalling and resulted in reduced AAA development. However, CD40L deficiency on T cells did not affect aortic dilation and rupture after AngII- and PPE-induced AAA formation. These results tend to suggest that CD40L expression on T cells is not a main driver in AAA pathology. However, it was found that platelets are the main source of sCD40L. After platelet stimulation, CD40L is rapidly expressed on their surface, from which it can subsequently cleaved.[151, 152] Previous studies have demonstrated that platelet manipulation positively influence AAA formation in animals.[153, 154] Therefore platelet-derived sCD40L may interact with CD40 on several other cell types triggering enhanced inflammatory and proteolytic processes that promote AAA pathology, thus compensating the potential beneficial effect of CD40L deficiency on T cells. Considering that a global CD40L deficiency protected mice from AngII-induced AAA rupture,[107] but in our study T cell-specific lack of CD40L was not sufficient to reduce AAA formation, future studies should investigate the effect of platelet-derived CD40L in AAA pathology.

Conclusion and outlook

The major impact of CVDs worldwide, and in particular the asymptomatic progressing of AAA disease with often fatal outcome, highlights the urgent need to understand the underlying mechanism of AAA pathology in order to develop non-surgical treatment for patients. For this purpose, the primary aim of this study was to examine the CD40/CD40L axis as potential therapeutic target in abdominal aortic aneurysm. Our data revealed that pharmacological inhibition of CD40-TRAF6 signalling using TRAF-STOP decelerate AAA growth by partially reducing ECM degradation and inflammatory processes in the PPE model. In addition, CD40-TRAF6 signalling inhibition remarkably decreases mortality rate due to AAA rupture of *Apoe*$^{-/-}$ on standard chow and WD in the AngII model. Although, this study demonstrated that TAM-inducible global CD40 deficiency protects *Apoe*$^{-/-}$ mice from aortic rupture after AngII-induced AAA formation, lack of CD40 on B cells or on myeloid cells did not affect AAA development and rupture after AAA induction. Furthermore, T cell-specific CD40L deficiency did not alter AAA formation and rupture after AngII- and PPE-induced aneurysm formation. Taken together, these findings highlight the potential beneficial effect of inhibiting the CD40/CD40L signalling in AAA pathology. In addition, this study emphasises the importance of using several experimental models to investigate AAA pathology. The wide expression of CD40 and CD40L on various immune cells and the results obtained with our generated cell type-specific CD40- or CD40L-deficient mice stresses the complexity of the numerous CD40/CD40L mediated inflammatory processes and lead to the suggestion that not only one cell type expressing CD40/CD40L is a main driver in AAA pathology.

Further research on the inhibition of the CD40/CD40L signalling by TRAF-STOP is needed to obtain further information on the underlying mechanisms that limit AAA pathology. Thereby, future studies should focus on the influence of CD40-TRAF6 signalling inhibition on proteolytic and inflammatory processes in experimental AAA models that best mimic human AAA disease such as the PPE model. Since the CD40/CD40L dyad is expressed on many cell types and involved in various inflammatory processes, and as the present study could not identify the main cell type responsible for observed beneficial effects in AAA, further investigations need to examine the cell-type specific effects of CD40/CD40L inhibition. In this context, the contribution to AAA pathology of other cell types such as platelets, fibroblasts and SMCs, which also express CD40 and CD40L and which play a crucial role in ECM metabolism, needs to attract more attention in future studies. Together with the findings of the present study, this may promote the development of targeted therapeutic strategies directed against a specific cell type to treat AAA disease. These examinations are necessary to determine the frequency and duration of potential treatment and to anticipate and limit undesired side effects.

References

1. Puertas-Umbert L, Almendra-Pegueros R, Jiménez-Altayó F, Sirvent M, Galán M, Martínez-González J, Rodríguez C. *Novel pharmacological approaches in abdominal aortic aneurysm*. Clin Sci (Lond). 2023;137(15):1167-94.http://dx.doi.org/10.1042/cs20220795
2. Wei L, Bu X, Wang X, Liu J, Ma A, Wang T. *Global Burden of Aortic Aneurysm and Attributable Risk Factors from 1990 to 2017*. Glob Heart. 2021;16(1):35.http://dx.doi.org/10.5334/gh.920
3. Song P, He Y, Adeloye D, Zhu Y, Ye X, Yi Q, Rahimi K, Rudan I. *The Global and Regional Prevalence of Abdominal Aortic Aneurysms: A Systematic Review and Modelling Analysis*. Ann Surg. 2022;277(6):912-9.http://dx.doi.org/10.1097/sla.0000000000005716
4. Cornuz J, Sidoti Pinto C, Tevaearai H, Egger M. *Risk factors for asymptomatic abdominal aortic aneurysm: systematic review and meta-analysis of population-based screening studies*. Eur J Public Health. 2004;14(4):343-9.http://dx.doi.org/10.1093/eurpub/14.4.343
5. Keisler B, Carter C. *Abdominal aortic aneurysm*. Am Fam Physician. 2015;91(8):538-43
6. Kent KC. *Clinical practice. Abdominal aortic aneurysms*. N Engl J Med. 2014;371(22):2101-8.http://dx.doi.org/10.1056/NEJMcp1401430
7. Sakalihasan N, Michel JB, Katsargyris A, Kuivaniemi H, Defraigne JO, Nchimi A, Powell JT, Yoshimura K, Hultgren R. *Abdominal aortic aneurysms*. Nat Rev Dis Primers. 2018;4(1):34.http://dx.doi.org/10.1038/s41572-018-0030-7
8. Busch A, Bleichert S, Ibrahim N, Wortmann M, Eckstein H-H, Brostjan C, Wagenhäuser MU, Goergen CJ, Maegdefessel L. *Translating mouse models of abdominal aortic aneurysm to the translational needs of vascular surgery*. JVS: Vascular Science. 2021.http://dx.doi.org/10.1016/j.jvssci.2021.01.002
9. Gasser TC, Ogden RW, Holzapfel GA. *Hyperelastic modelling of arterial layers with distributed collagen fibre orientations*. J R Soc Interface. 2006;3(6):15-35.http://dx.doi.org/10.1098/rsif.2005.0073
10. Tsamis A, Krawiec JT, Vorp DA. *Elastin and collagen fibre microstructure of the human aorta in ageing and disease: a review*. J R Soc Interface. 2013;10(83):20121004.http://dx.doi.org/10.1098/rsif.2012.1004
11. Powell JT, Greenhalgh RM. *Clinical practice. Small abdominal aortic aneurysms*. N Engl J Med. 2003;348(19):1895-901.http://dx.doi.org/10.1056/NEJMcp012641
12. Secretariat MA. *Ultrasound screening for abdominal aortic aneurysm: an evidence-based analysis*. Ont Health Technol Assess Ser. 2006;6(2):1-67
13. Kapila V, Jetty P, Wooster D, Vucemilo V, Dubois L. *Screening for abdominal aortic aneurysms in Canada: 2020 review and position statement of the Canadian Society for Vascular Surgery*. Can J Surg. 2021;64(5):E461-e6.http://dx.doi.org/10.1503/cjs.009120
14. Aune D, Schlesinger S, Norat T, Riboli E. *Tobacco smoking and the risk of abdominal aortic aneurysm: a systematic review and meta-analysis of prospective studies*. Sci Rep. 2018;8(1):14786.http://dx.doi.org/10.1038/s41598-018-32100-2
15. Bahia SS, Vidal-Diez A, Seshasai SR, Shpitser I, Brownrigg JR, Patterson BO, Ray KK, Holt PJ, Thompson MM, Karthikesalingam A. *Cardiovascular risk prevention and all-cause mortality in primary care patients with an abdominal aortic aneurysm*. Br J Surg. 2016;103(12):1626-33.http://dx.doi.org/10.1002/bjs.10269
16. Wanhainen A, Verzini F, Van Herzeele I, et al. *Editor's Choice - European Society for Vascular Surgery (ESVS) 2019 Clinical Practice Guidelines on the Management of Abdominal Aorto-iliac Artery Aneurysms*. Eur J Vasc Endovasc Surg. 2019;57(1):8-93.http://dx.doi.org/10.1016/j.ejvs.2018.09.020
17. Golledge J, Moxon JV, Singh TP, Bown MJ, Mani K, Wanhainen A. *Lack of an effective drug therapy for abdominal aortic aneurysm*. J Intern Med. 2020;288(1):6-22.http://dx.doi.org/10.1111/joim.12958
18. Hungerford JE, Little CD. *Developmental biology of the vascular smooth muscle cell: building a multilayered vessel wall*. J Vasc Res. 1999;36(1):2-27.http://dx.doi.org/10.1159/000025622
19. Wagenseil JE, Mecham RP. *Vascular extracellular matrix and arterial mechanics*. Physiol Rev. 2009;89(3):957-89.http://dx.doi.org/10.1152/physrev.00041.2008
20. Stepien KL, Bajdak-Rusinek K, Fus-Kujawa A, Kuczmik W, Gawron K. *Role of Extracellular Matrix and Inflammation in Abdominal Aortic Aneurysm*. Int J Mol Sci. 2022;23(19).http://dx.doi.org/10.3390/ijms231911078
21. Campa JS, Greenhalgh RM, Powell JT. *Elastin degradation in abdominal aortic aneurysms*. Atherosclerosis. 1987;65(1-2):13-21.http://dx.doi.org/10.1016/0021-9150(87)90003-7
22. Anidjar S, Salzmann JL, Gentric D, Lagneau P, Camilleri JP, Michel JB. *Elastase-induced experimental aneurysms in rats*. Circulation. 1990;82(3):973-81.http://dx.doi.org/10.1161/01.cir.82.3.973
23. Pyo R, Lee JK, Shipley JM, Curci JA, Mao D, Ziporin SJ, Ennis TL, Shapiro SD, Senior RM, Thompson RW. *Targeted gene disruption of matrix metalloproteinase-9 (gelatinase B) suppresses development of experimental abdominal aortic aneurysms*. The Journal of clinical investigation. 2000;105(11):1641-9.http://dx.doi.org/10.1172/jci8931
24. McLean SE, Mecham BH, Kelleher CM, Mariani TJ, Mecham RP. Extracellular matrix gene expression in the developing mouse aorta. Advances in Developmental Biology. 15: Elsevier; 2005. p. 81-128.
25. Kelleher CM, McLean SE, Mecham RP. Vascular Extracellular Matrix and Aortic Development. Current Topics in Developmental Biology. 62: Academic Press; 2004. p. 153-88.
26. Abdul-Hussien H, Soekhoe RG, Weber E, von der Thüsen JH, Kleemann R, Mulder A, van Bockel JH, Hanemaaijer R, Lindeman JH. *Collagen degradation in the abdominal aneurysm: a conspiracy of matrix*

metalloproteinase and cysteine collagenases. Am J Pathol. 2007;170(3):809-17.http://dx.doi.org/10.2353/ajpath.2007.060522
27. Powell JT, Adamson J, Macsweeney STR, Greenhalgh RM, Humphries SE, Henney AM. *Influence of type III collagen genotype on aortic diameter and disease*. British Journal of Surgery. 2005;80(10):1246-8.http://dx.doi.org/10.1002/bjs.1800801008
28. Steffensen LB, Rasmussen LM. *A role for collagen type IV in cardiovascular disease?* Am J Physiol Heart Circ Physiol. 2018;315(3):H610-h25.http://dx.doi.org/10.1152/ajpheart.00070.2018
29. Steffensen LB, Stubbe J, Lindholt JS, et al. *Basement membrane collagen IV deficiency promotes abdominal aortic aneurysm formation*. Sci Rep. 2021;11(1):12903.http://dx.doi.org/10.1038/s41598-021-92303-y
30. Nagase H, Woessner JF, Jr. *Matrix metalloproteinases*. J Biol Chem. 1999;274(31):21491-4.http://dx.doi.org/10.1074/jbc.274.31.21491
31. Visse R, Nagase H. *Matrix metalloproteinases and tissue inhibitors of metalloproteinases: structure, function, and biochemistry*. Circ Res. 2003;92(8):827-39.http://dx.doi.org/10.1161/01.Res.0000070112.80711.3d
32. Verma RP, Hansch C. *Matrix metalloproteinases (MMPs): Chemical–biological functions and (Q)SARs*. Bioorganic & Medicinal Chemistry. 2007;15(6):2223-68.http://dx.doi.org/https://doi.org/10.1016/j.bmc.2007.01.011
33. Löffek S, Schilling O, Franzke C-W. *Biological role of matrix metalloproteinases: a critical balance*. European Respiratory Journal. 2011;38(1):191-208.http://dx.doi.org/10.1183/09031936.00146510
34. Quintana RA, Taylor WR. *Cellular Mechanisms of Aortic Aneurysm Formation*. Circ Res. 2019;124(4):607-18.http://dx.doi.org/10.1161/circresaha.118.313187
35. Longo GM, Xiong W, Greiner TC, Zhao Y, Fiotti N, Baxter BT. *Matrix metalloproteinases 2 and 9 work in concert to produce aortic aneurysms*. The Journal of clinical investigation. 2002;110(5):625-32.http://dx.doi.org/10.1172/jci15334
36. Maguire EM, Pearce SWA, Xiao R, Oo AY, Xiao Q. *Matrix Metalloproteinase in Abdominal Aortic Aneurysm and Aortic Dissection*. Pharmaceuticals. 2019;12(3):118
37. Lindholt JS, Vammen S, Fasting H, Henneberg EW, Heickendorff L. *The plasma level of matrix metalloproteinase 9 may predict the natural history of small abdominal aortic aneurysms. A preliminary study*. Eur J Vasc Endovasc Surg. 2000;20(3):281-5.http://dx.doi.org/10.1053/ejvs.2000.1151
38. Wilson WRW, Anderton M, Choke EC, Dawson J, Loftus IM, Thompson MM. *Elevated Plasma MMP1 and MMP9 are Associated with Abdominal Aortic Aneurysm Rupture*. European Journal of Vascular and Endovascular Surgery. 2008;35(5):580-4.http://dx.doi.org/https://doi.org/10.1016/j.ejvs.2007.12.004
39. Zhang X, Shen YH, LeMaire SA. *Thoracic aortic dissection: are matrix metalloproteinases involved?* Vascular. 2009;17(3):147-57.http://dx.doi.org/10.2310/6670.2008.00087
40. Marquez-Sanchez AC, Koltsova EK. *Immune and inflammatory mechanisms of abdominal aortic aneurysm*. Front Immunol. 2022;13:989933.http://dx.doi.org/10.3389/fimmu.2022.989933
41. Rosales C. *Neutrophil: A Cell with Many Roles in Inflammation or Several Cell Types?* Frontiers in Physiology. 2018;9.http://dx.doi.org/10.3389/fphys.2018.00113
42. Fontaine V, Jacob MP, Houard X, Rossignol P, Plissonnier D, Angles-Cano E, Michel JB. *Involvement of the mural thrombus as a site of protease release and activation in human aortic aneurysms*. Am J Pathol. 2002;161(5):1701-10.http://dx.doi.org/10.1016/s0002-9440(10)64447-1
43. Klopf J, Brostjan C, Neumayer C, Eilenberg W. *Neutrophils as Regulators and Biomarkers of Cardiovascular Inflammation in the Context of Abdominal Aortic Aneurysms*. Biomedicines. 2021;9(9).http://dx.doi.org/10.3390/biomedicines9091236
44. Eliason JL, Hannawa KK, Ailawadi G, et al. *Neutrophil Depletion Inhibits Experimental Abdominal Aortic Aneurysm Formation*. Circulation. 2005;112(2):232-40.http://dx.doi.org/doi:10.1161/CIRCULATIONAHA.104.517391
45. van Furth R, Cohn ZA. *The origin and kinetics of mononuclear phagocytes*. J Exp Med. 1968;128(3):415-35.http://dx.doi.org/10.1084/jem.128.3.415
46. Ziegler-Heitbrock L, Ancuta P, Crowe S, et al. *Nomenclature of monocytes and dendritic cells in blood*. Blood. 2010;116(16):e74-e80.http://dx.doi.org/10.1182/blood-2010-02-258558
47. Raffort J, Lareyre F, Clement M, Hassen-Khodja R, Chinetti G, Mallat Z. *Monocytes and macrophages in abdominal aortic aneurysm*. Nat Rev Cardiol. 2017;14(8):457-71.http://dx.doi.org/10.1038/nrcardio.2017.52
48. Ghigliotti G, Barisione C, Garibaldi S, et al. *CD16(+) monocyte subsets are increased in large abdominal aortic aneurysms and are differentially related with circulating and cell-associated biochemical and inflammatory biomarkers*. Dis Markers. 2013;34(2):131-42.http://dx.doi.org/10.1155/2013/836849
49. Mellak S, Ait-Oufella H, Esposito B, Loyer X, Poirier M, Tedder TF, Tedgui A, Mallat Z, Potteaux S. *Angiotensin II Mobilizes Spleen Monocytes to Promote the Development of Abdominal Aortic Aneurysm in Apoe^{−/−} Mice*. Arteriosclerosis, thrombosis, and vascular biology. 2015;35(2):378-88.http://dx.doi.org/doi:10.1161/ATVBAHA.114.304389
50. Moran CS, Jose RJ, Moxon JV, Roomberg A, Norman PE, Rush C, Körner H, Golledge J. *Everolimus limits aortic aneurysm in the apolipoprotein E-deficient mouse by downregulating C-C chemokine receptor 2 positive monocytes*. Arteriosclerosis, thrombosis, and vascular biology. 2013;33(4):814-21.http://dx.doi.org/10.1161/atvbaha.112.301006
51. Wynn TA, Chawla A, Pollard JW. *Macrophage biology in development, homeostasis and disease*. Nature. 2013;496(7446):445-55.http://dx.doi.org/10.1038/nature12034

52. Sreejit G, Fleetwood AJ, Murphy AJ, Nagareddy PR. *Origins and diversity of macrophages in health and disease*. Clinical & Translational Immunology. 2020;9(12):e1222.http://dx.doi.org/https://doi.org/10.1002/cti2.1222
53. Park MD, Silvin A, Ginhoux F, Merad M. *Macrophages in health and disease*. Cell. 2022;185(23):4259-79.http://dx.doi.org/10.1016/j.cell.2022.10.007
54. Rateri DL, Howatt DA, Moorleghen JJ, Charnigo R, Cassis LA, Daugherty A. *Prolonged infusion of angiotensin II in apoE(-/-) mice promotes macrophage recruitment with continued expansion of abdominal aortic aneurysm*. Am J Pathol. 2011;179(3):1542-8.http://dx.doi.org/10.1016/j.ajpath.2011.05.049
55. Davis FM, Rateri DL, Daugherty A. *Abdominal aortic aneurysm: novel mechanisms and therapies*. Curr Opin Cardiol. 2015;30(6):566-73.http://dx.doi.org/10.1097/hco.0000000000000216
56. Rizas KD, Ippagunta N, Tilson MDI. *Immune Cells and Molecular Mediators in the Pathogenesis of the Abdominal Aortic Aneurysm*. Cardiology in Review. 2009;17(5):201-10.http://dx.doi.org/10.1097/CRD.0b013e3181b04698
57. Okuno K, Cicalese S, Eguchi S. *Depletion of CD11c+ cell attenuates progression of abdominal aortic aneurysm*. Clinical Science. 2020;134(1):33-7.http://dx.doi.org/10.1042/cs20191083
58. Krishna SM, Moran CS, Jose RJ, Lazzaroni S, Huynh P, Golledge J. *Depletion of CD11c+ dendritic cells in apolipoprotein E-deficient mice limits angiotensin II-induced abdominal aortic aneurysm formation and growth*. Clin Sci (Lond). 2019;133(21):2203-15.http://dx.doi.org/10.1042/CS20190924
59. Yan H, Zhou H-F, Akk A, Hu Y, Springer LE, Ennis TL, Pham CTN. *Neutrophil Proteases Promote Experimental Abdominal Aortic Aneurysm via Extracellular Trap Release and Plasmacytoid Dendritic Cell Activation*. Arteriosclerosis, thrombosis, and vascular biology. 2016;36(8):1660-9.http://dx.doi.org/doi:10.1161/ATVBAHA.116.307786
60. Perera Molligoda Arachchige AS. *Human NK cells: From development to effector functions*. Innate Immunity. 2021;27(3):212-29.http://dx.doi.org/10.1177/17534259211001512
61. Fu B, Tian Z, Wei H. *Subsets of human natural killer cells and their regulatory effects*. Immunology. 2014;141(4):483-9.http://dx.doi.org/10.1111/imm.12224
62. Hinterseher I, Schworer CM, Lillvis JH, Stahl E, Erdman R, Gatalica Z, Tromp G, Kuivaniemi H. *Immunohistochemical analysis of the natural killer cell cytotoxicity pathway in human abdominal aortic aneurysms*. Int J Mol Sci. 2015;16(5):11196-212.http://dx.doi.org/10.3390/ijms160511196
63. Koch AE, Haines GK, Rizzo RJ, Radosevich JA, Pope RM, Robinson PG, Pearce WH. *Human abdominal aortic aneurysms. Immunophenotypic analysis suggesting an immune-mediated response*. Am J Pathol. 1990;137(5):1199-213
64. Sage AP, Tsiantoulas D, Binder CJ, Mallat Z. *The role of B cells in atherosclerosis*. Nature Reviews Cardiology. 2019;16(3):180-96.http://dx.doi.org/10.1038/s41569-018-0106-9
65. Schaheen B, Downs EA, Serbulea V, et al. *B-Cell Depletion Promotes Aortic Infiltration of Immunosuppressive Cells and Is Protective of Experimental Aortic Aneurysm*. Arteriosclerosis, thrombosis, and vascular biology. 2016;36(11):2191-202.http://dx.doi.org/10.1161/atvbaha.116.307559
66. Furusho A, Aoki H, Ohno-Urabe S, et al. *Involvement of B Cells, Immunoglobulins, and Syk in the Pathogenesis of Abdominal Aortic Aneurysm*. J Am Heart Assoc. 2018;7(6).http://dx.doi.org/10.1161/jaha.117.007750
67. Meher AK, Johnston WF, Lu G, et al. *B2 cells suppress experimental abdominal aortic aneurysms*. Am J Pathol. 2014;184(11):3130-41.http://dx.doi.org/10.1016/j.ajpath.2014.07.006
68. Dale MA, Ruhlman MK, Baxter BT. *Inflammatory cell phenotypes in AAAs: their role and potential as targets for therapy*. Arteriosclerosis, thrombosis, and vascular biology. 2015;35(8):1746-55.http://dx.doi.org/10.1161/atvbaha.115.305269
69. Sharma AK, Lu G, Jester A, et al. *Experimental Abdominal Aortic Aneurysm Formation Is Mediated by IL-17 and Attenuated by Mesenchymal Stem Cell Treatment*. Circulation. 2012;126(11_suppl_1):S38-S45.http://dx.doi.org/doi:10.1161/CIRCULATIONAHA.111.083451
70. Wei Z, Wang Y, Zhang K, et al. *Inhibiting the Th17/IL-17A–Related Inflammatory Responses With Digoxin Confers Protection Against Experimental Abdominal Aortic Aneurysm*. Arteriosclerosis, thrombosis, and vascular biology. 2014;34(11):2429-38.http://dx.doi.org/doi:10.1161/ATVBAHA.114.304435
71. Sakaguchi S, Yamaguchi T, Nomura T, Ono M. *Regulatory T Cells and Immune Tolerance*. Cell. 2008;133(5):775-87.http://dx.doi.org/10.1016/j.cell.2008.05.009
72. Yodoi K, Yamashita T, Sasaki N, et al. *Foxp3⁺ Regulatory T Cells Play a Protective Role in Angiotensin II–Induced Aortic Aneurysm Formation in Mice*. Hypertension. 2015;65(4):889-95.http://dx.doi.org/doi:10.1161/HYPERTENSIONAHA.114.04934
73. Zhou HF, Yan H, Cannon JL, Springer LE, Green JM, Pham CT. *CD43-mediated IFN-γ production by CD8+ T cells promotes abdominal aortic aneurysm in mice*. J Immunol. 2013;190(10):5078-85.http://dx.doi.org/10.4049/jimmunol.1203228
74. Puchenkova OA, Soldatov VO, Belykh AE, Bushueva O, Piavchenko GA, Venediktov AA, Shakhpazyan NK, Deykin AV, Korokin MV, Pokrovskiy MV. *Cytokines in Abdominal Aortic Aneurysm: Master Regulators With Clinical Application*. Biomark Insights. 2022;17:11772719221095676.http://dx.doi.org/10.1177/11772719221095676
75. Middleton RK, Lloyd GM, Bown MJ, Cooper NJ, London NJ, Sayers RD. *The pro-inflammatory and chemotactic cytokine microenvironment of the abdominal aortic aneurysm wall: a protein array study*. J Vasc Surg. 2007;45(3):574-80.http://dx.doi.org/10.1016/j.jvs.2006.11.020
76. Golledge AL, Walker P, Norman PE, Golledge J. *A systematic review of studies examining inflammation associated cytokines in human abdominal aortic aneurysm samples*. Dis Markers. 2009;26(4):181-8.http://dx.doi.org/10.3233/DMA-2009-0629

77. Třeška V, Topolčan O, Pecen L. *Cytokines as Plasma Markers of Abdominal Aortic Aneurysm*. 2000;38(11):1161-4.http://dx.doi.org/doi:10.1515/CCLM.2000.178
78. Xiong W, MacTaggart J, Knispel R, Worth J, Persidsky Y, Baxter BT. *Blocking TNF-alpha attenuates aneurysm formation in a murine model*. J Immunol. 2009;183(4):2741-6.http://dx.doi.org/10.4049/jimmunol.0803164
79. Johnston WF, Salmon M, Su G, Lu G, Stone ML, Zhao Y, Owens GK, Upchurch GR, Jr., Ailawadi G. *Genetic and pharmacologic disruption of interleukin-1β signaling inhibits experimental aortic aneurysm formation*. Arteriosclerosis, thrombosis, and vascular biology. 2013;33(2):294-304.http://dx.doi.org/10.1161/atvbaha.112.300432
80. Nishihara M, Aoki H, Ohno S, Furusho A, Hirakata S, Nishida N, Ito S, Hayashi M, Imaizumi T, Fukumoto Y. *The role of IL-6 in pathogenesis of abdominal aortic aneurysm in mice*. PLoS One. 2017;12(10):e0185923.http://dx.doi.org/10.1371/journal.pone.0185923
81. Gschwandtner M, Derler R, Midwood KS. *More Than Just Attractive: How CCL2 Influences Myeloid Cell Behavior Beyond Chemotaxis*. Frontiers in Immunology. 2019;10.http://dx.doi.org/10.3389/fimmu.2019.02759
82. Moehle CW, Bhamidipati CM, Alexander MR, Mehta GS, Irvine JN, Salmon M, Upchurch GR, Jr., Kron IL, Owens GK, Ailawadi G. *Bone marrow-derived MCP1 required for experimental aortic aneurysm formation and smooth muscle phenotypic modulation*. J Thorac Cardiovasc Surg. 2011;142(6):1567-74.http://dx.doi.org/10.1016/j.jtcvs.2011.07.053
83. Adam M, Kooreman NG, Jagger A, et al. *Systemic Upregulation of IL-10 (Interleukin-10) Using a Nonimmunogenic Vector Reduces Growth and Rate of Dissecting Abdominal Aortic Aneurysm*. Arteriosclerosis, thrombosis, and vascular biology. 2018;38(8):1796-805.http://dx.doi.org/10.1161/atvbaha.117.310672
84. Chen L, Flies DB. *Molecular mechanisms of T cell co-stimulation and co-inhibition*. Nature Reviews Immunology. 2013;13(4):227-42.http://dx.doi.org/10.1038/nri3405
85. Elgueta R, Benson MJ, de Vries VC, Wasiuk A, Guo Y, Noelle RJ. *Molecular mechanism and function of CD40/CD40L engagement in the immune system*. Immunol Rev. 2009;229(1):152-72.http://dx.doi.org/10.1111/j.1600-065X.2009.00782.x
86. Quezada SA, Jarvinen LZ, Lind EF, Noelle RJ. *CD40/CD154 interactions at the interface of tolerance and immunity*. Annu Rev Immunol. 2004;22:307-28.http://dx.doi.org/10.1146/annurev.immunol.22.012703.104533
87. Schönbeck U, Libby P. *The CD40/CD154 receptor/ligand dyad*. Cell Mol Life Sci. 2001;58(1):4-43.http://dx.doi.org/10.1007/pl00000776
88. Mazzei GJ, Edgerton MD, Losberger C, Lecoanet-Henchoz S, Graber P, Durandy A, Gauchat JF, Bernard A, Allet B, Bonnefoy JY. *Recombinant soluble trimeric CD40 ligand is biologically active*. J Biol Chem. 1995;270(13):7025-8.http://dx.doi.org/10.1074/jbc.270.13.7025
89. Kambayashi T, Laufer TM. *Atypical MHC class II-expressing antigen-presenting cells: can anything replace a dendritic cell?* Nature Reviews Immunology. 2014;14(11):719-30.http://dx.doi.org/10.1038/nri3754
90. Lai J-H, Luo S-F, Ho L-J. *Targeting the CD40-CD154 Signaling Pathway for Treatment of Autoimmune Arthritis*. Cells. 2019;8(8):927
91. Pullen SS, Miller HG, Everdeen DS, Dang TT, Crute JJ, Kehry MR. *CD40-tumor necrosis factor receptor-associated factor (TRAF) interactions: regulation of CD40 signaling through multiple TRAF binding sites and TRAF hetero-oligomerization*. Biochemistry. 1998;37(34):11836-45.http://dx.doi.org/10.1021/bi981067q
92. Bishop GA, Moore CR, Xie P, Stunz LL, Kraus ZJ. *TRAF proteins in CD40 signaling*. Adv Exp Med Biol. 2007;597:131-51.http://dx.doi.org/10.1007/978-0-387-70630-6_11
93. Goronzy JJ, Weyand CM. *T-cell co-stimulatory pathways in autoimmunity*. Arthritis Research & Therapy. 2008;10(1):S3.http://dx.doi.org/10.1186/ar2414
94. Callard RE, Armitage RJ, Fanslow WC, Spriggs MK. *CD40 ligand and its role in X-linked hyper-IgM syndrome*. Immunol Today. 1993;14(11):559-64.http://dx.doi.org/10.1016/0167-5699(93)90188-q
95. Daub S, Lutgens E, Münzel T, Daiber A. *CD40/CD40L and Related Signaling Pathways in Cardiovascular Health and Disease-The Pros and Cons for Cardioprotection*. Int J Mol Sci. 2020;21(22).http://dx.doi.org/10.3390/ijms21228533
96. Wagner AH, Güldenzoph B, Lienenlüke B, Hecker M. *CD154/CD40-Mediated Expression of CD154 in Endothelial Cells: Consequences for Endothelial Cell–Monocyte Interaction*. Arteriosclerosis, thrombosis, and vascular biology. 2004;24(4):715-20.http://dx.doi.org/doi:10.1161/01.ATV.0000122853.99978.b1
97. Mach F, Schönbeck U, Bonnefoy J-Y, Pober JS, Libby P. *Activation of Monocyte/Macrophage Functions Related to Acute Atheroma Complication by Ligation of CD40*. Circulation. 1997;96(2):396-9.http://dx.doi.org/doi:10.1161/01.CIR.96.2.396
98. Hausding M, Jurk K, Daub S, et al. *CD40L contributes to angiotensin II-induced pro-thrombotic state, vascular inflammation, oxidative stress and endothelial dysfunction*. Basic Research in Cardiology. 2013;108(6):386.http://dx.doi.org/10.1007/s00395-013-0386-5
99. Mach F, Schönbeck U, Sukhova GK, Atkinson E, Libby P. *Reduction of atherosclerosis in mice by inhibition of CD40 signalling*. Nature. 1998;394(6689):200-3.http://dx.doi.org/10.1038/28204
100. Schönbeck U, Sukhova GK, Shimizu K, Mach F, Libby P. *Inhibition of CD40 signaling limits evolution of established atherosclerosis in mice*. Proceedings of the National Academy of Sciences of the United States of America. 2000;97(13):7458-63.http://dx.doi.org/10.1073/pnas.97.13.7458
101. Yazdany J, Davis J. *The role of CD40 ligand in systemic lupus erythematosus*. Lupus. 2004;13(5):377-80.http://dx.doi.org/10.1191/0961203304lu1030oa

102. Donners MMPC, Beckers L, Lievens D, et al. *The CD40-TRAF6 axis is the key regulator of the CD40/CD40L system in neointima formation and arterial remodeling*. Blood. 2008;111(9):4596-604.http://dx.doi.org/10.1182/blood-2007-05-088906
103. Lutgens E, Lievens D, Beckers L, et al. *Deficient CD40-TRAF6 signaling in leukocytes prevents atherosclerosis by skewing the immune response toward an antiinflammatory profile*. J Exp Med. 2010;207(2):391-404.http://dx.doi.org/10.1084/jem.20091293
104. Zarzycka B, Seijkens T, Nabuurs SB, et al. *Discovery of small molecule CD40-TRAF6 inhibitors*. J Chem Inf Model. 2015;55(2):294-307.http://dx.doi.org/10.1021/ci500631e
105. Chatzigeorgiou A, Seijkens T, Zarzycka B, et al. *Blocking CD40-TRAF6 signaling is a therapeutic target in obesity-associated insulin resistance*. Proceedings of the National Academy of Sciences of the United States of America. 2014;111(7):2686-91.http://dx.doi.org/10.1073/pnas.1400419111
106. Seijkens TTP, van Tiel CM, Kusters PJH, et al. *Targeting CD40-Induced TRAF6 Signaling in Macrophages Reduces Atherosclerosis*. J Am Coll Cardiol. 2018;71(5):527-42.http://dx.doi.org/10.1016/j.jacc.2017.11.055
107. Kusters PJH, Seijkens TTP, Beckers L, et al. *CD40L Deficiency Protects Against Aneurysm Formation*. Arteriosclerosis, thrombosis, and vascular biology. 2018;38(5):1076-85.http://dx.doi.org/10.1161/ATVBAHA.117.310640
108. Daugherty A, Manning MW, Cassis LA. *Angiotensin II promotes atherosclerotic lesions and aneurysms in apolipoprotein E-deficient mice*. The Journal of clinical investigation. 2000;105(11):1605-12.http://dx.doi.org/10.1172/jci7818
109. Golledge J, Krishna SM, Wang Y. *Mouse models for abdominal aortic aneurysm*. British journal of pharmacology. 2022;179(5):792-810.http://dx.doi.org/10.1111/bph.15260
110. Bhamidipati CM, Mehta GS, Lu G, Moehle CW, Barbery C, DiMusto PD, Laser A, Kron IL, Upchurch GR, Ailawadi G. *Development of a novel murine model of aortic aneurysms using peri-adventitial elastase*. Surgery. 2012;152(2):238-46.http://dx.doi.org/https://doi.org/10.1016/j.surg.2012.02.010
111. Chiou AC, Chiu B, Pearce WH. *Murine Aortic Aneurysm Produced by Periarterial Application of Calcium Chloride*. Journal of Surgical Research. 2001;99(2):371-6.http://dx.doi.org/https://doi.org/10.1006/jsre.2001.6207
112. Trachet B, Aslanidou L, Piersigilli A, Fraga-Silva RA, Sordet-Dessimoz J, Villanueva-Perez P, Stampanoni MFM, Stergiopulos N, Segers P. *Angiotensin II infusion into ApoE-/- mice: a model for aortic dissection rather than abdominal aortic aneurysm?* Cardiovasc Res. 2017;113(10):1230-42.http://dx.doi.org/10.1093/cvr/cvx128
113. Hu D, Yin C, Mohanta SK, Weber C, Habenicht AJ. *Preparation of Single Cell Suspensions from Mouse Aorta*. Bio-protocol. 2016;6(11).http://dx.doi.org/10.21769/bioprotoc.1832
114. Hao Y, Hao S, Andersen-Nissen E, et al. *Integrated analysis of multimodal single-cell data*. Cell. 2021;184(13):3573-87.e29.http://dx.doi.org/10.1016/j.cell.2021.04.048
115. Kobeissi E, Hibino M, Pan H, Aune D. *Blood pressure, hypertension and the risk of abdominal aortic aneurysms: a systematic review and meta-analysis of cohort studies*. Eur J Epidemiol. 2019;34(6):547-55.http://dx.doi.org/10.1007/s10654-019-00510-9
116. Bosch L, de Haan J, Seijkens T, van Tiel C, Brans M, Pasterkamp G, Lutgens E, de Jager S. *Small molecule-mediated inhibition of CD40-TRAF6 reduces adverse cardiac remodelling in pressure overload induced heart failure*. International Journal of Cardiology. 2019;279:141-4.http://dx.doi.org/10.1016/j.ijcard.2018.12.076
117. Michel NA, Zirlik A, Wolf D. *CD40L and Its Receptors in Atherothrombosis—An Update*. Frontiers in Cardiovascular Medicine. 2017;4.http://dx.doi.org/10.3389/fcvm.2017.00040
118. Borgbjerg J, Bøgsted M, Lindholt JS, Behr-Rasmussen C, Hørlyck A, Frøkjær JB. *Superior Reproducibility of the Leading to Leading Edge and Inner to Inner Edge Methods in the Ultrasound Assessment of Maximum Abdominal Aortic Diameter*. European Journal of Vascular and Endovascular Surgery. 2018;55(2):206-13.http://dx.doi.org/10.1016/j.ejvs.2017.11.019
119. Daugherty A, Cassis LA, Lu H. *Complex pathologies of angiotensin II-induced abdominal aortic aneurysms*. J Zhejiang Univ Sci B. 2011;12(8):624-8.http://dx.doi.org/10.1631/jzus.B1101002
120. Liu X, Qu C, Zhang Y, Fang J, Teng L, Shen C. *Perfusion pressure of elastase impacts the formation ratio and diameters of abdominal aortic aneurysms in rats*. Exp Ther Med. 2023;25(5):190.http://dx.doi.org/10.3892/etm.2023.11889
121. Urabe G, Hoshina K, Shimanuki T, Nishimori Y, Miyata T, Deguchi J. *Structural analysis of adventitial collagen to feature aging and aneurysm formation in human aorta*. Journal of Vascular Surgery. 2016;63(5):1341-50.http://dx.doi.org/10.1016/j.jvs.2014.12.057
122. Treska V, Topolcan O. *Plasma and tissue levels of collagen types I and III markers in patients with abdominal aortic aneurysms*. Int Angiol. 2000;19(1):64-8
123. Minion DJ, Davis VA, Nejezchleb PA, Wang Y, McManus BM, Baxter BT. *Elastin is increased in abdominal aortic aneurysms*. J Surg Res. 1994;57(4):443-6.http://dx.doi.org/10.1006/jsre.1994.1168
124. Bode MK, Soini Y, Melkko J, Satta J, Risteli L, Risteli J. *Increased amount of type III pN-collagen in human abdominal aortic aneurysms: evidence for impaired type III collagen fibrillogenesis*. J Vasc Surg. 2000;32(6):1201-7.http://dx.doi.org/10.1067/mva.2000.109743
125. Lievens D, Eijgelaar WJ, Biessen EA, Daemen MJ, Lutgens E. *The multi-functionality of CD40L and its receptor CD40 in atherosclerosis*. Thromb Haemost. 2009;102(2):206-14.http://dx.doi.org/10.1160/th09-01-0029
126. Overall CM. *Molecular determinants of metalloproteinase substrate specificity*. Molecular Biotechnology. 2002;22(1):51-86.http://dx.doi.org/10.1385/MB:22:1:051

127. Nagashima H, Aoka Y, Sakomura Y, Uto K, Sakuta A, Aomi S, Kurosawa H, Hagiwara N, Kawana M, Kasanuki H. *Matrix metalloproteinase 2 is suppressed by trapidil, a CD40-CD40 ligand pathway inhibitor, in human abdominal aortic aneurysm wall*. J Vasc Surg. 2004;39(2):447-53.http://dx.doi.org/10.1016/j.jvs.2003.07.005
128. Yan H, Hu Y, Akk A, Ye K, Bacon J, Pham CTN. *Interleukin-12 and -23 blockade mitigates elastase-induced abdominal aortic aneurysm*. Sci Rep. 2019;9(1):10447.http://dx.doi.org/10.1038/s41598-019-46909-y
129. Ait-Oufella H, Wang Y, Herbin O, et al. *Natural Regulatory T Cells Limit Angiotensin II–Induced Aneurysm Formation and Rupture in Mice*. Arteriosclerosis, thrombosis, and vascular biology. 2013;33(10):2374-9.http://dx.doi.org/doi:10.1161/ATVBAHA.113.301280
130. Ye P, Chen W, Wu J, et al. *GM-CSF contributes to aortic aneurysms resulting from SMAD3 deficiency*. The Journal of clinical investigation. 2013;123(5):2317-31.http://dx.doi.org/10.1172/jci67356
131. Batra R, Suh MK, Carson JS, et al. *IL-1β (Interleukin-1β) and TNF-α (Tumor Necrosis Factor-α) Impact Abdominal Aortic Aneurysm Formation by Differential Effects on Macrophage Polarization*. Arteriosclerosis, thrombosis, and vascular biology. 2018;38(2):457-63.http://dx.doi.org/10.1161/atvbaha.117.310333
132. Brangsch J, Reimann C, Kaufmann JO, et al. *Molecular MR-Imaging for Noninvasive Quantification of the Anti-Inflammatory Effect of Targeting Interleukin-1β in a Mouse Model of Aortic Aneurysm*. Mol Imaging. 2020;19:1536012120961875.http://dx.doi.org/10.1177/1536012120961875
133. Son B-K, Sawaki D, Tomida S, et al. *Granulocyte macrophage colony-stimulating factor is required for aortic dissection/intramural haematoma*. Nature Communications. 2015;6(1):6994.http://dx.doi.org/10.1038/ncomms7994
134. Lameijer M, Binderup T, van Leent MMT, et al. *Efficacy and safety assessment of a TRAF6-targeted nanoimmunotherapy in atherosclerotic mice and non-human primates*. Nat Biomed Eng. 2018;2(5):279-92.http://dx.doi.org/10.1038/s41551-018-0221-2
135. Trachet B, Fraga-Silva RA, Jacquet PA, Stergiopulos N, Segers P. *Incidence, severity, mortality, and confounding factors for dissecting AAA detection in angiotensin II-infused mice: a meta-analysis*. Cardiovasc Res. 2015;108(1):159-70.http://dx.doi.org/10.1093/cvr/cvv215
136. Wang J, Wu X, Jiang M, Tai G. *Mechanism by which TRAF6 Participates in the Immune Regulation of Autoimmune Diseases and Cancer*. BioMed Research International. 2020;2020:4607197.http://dx.doi.org/10.1155/2020/4607197
137. Kim H, Kim M, Im S-K, Fang S. *Mouse Cre-LoxP system: general principles to determine tissue-specific roles of target genes*. lar. 2018;34(4):147-59.http://dx.doi.org/10.5625/lar.2018.34.4.147
138. Walton LJ, Powell JT, Parums DV. *Unrestricted usage of immunoglobulin heavy chain genes in B cells infiltrating the wall of atherosclerotic abdominal aortic aneurysms*. Atherosclerosis. 1997;135(1):65-71.http://dx.doi.org/https://doi.org/10.1016/S0021-9150(97)00152-4
139. Cerro-Pardo I, Lindholt JS, Núñez E, et al. *Combined Immunoglobulin Free Light Chains Are Novel Predictors of Cardiovascular Events in Patients With Abdominal Aortic Aneurysm*. European Journal of Vascular and Endovascular Surgery. 2022;63(5):751-8.http://dx.doi.org/https://doi.org/10.1016/j.ejvs.2021.11.025
140. Tay C, Liu Y-H, Kanellakis P, et al. *Follicular B Cells Promote Atherosclerosis via T Cell–Mediated Differentiation Into Plasma Cells and Secreting Pathogenic Immunoglobulin G*. Arteriosclerosis, thrombosis, and vascular biology. 2018;38(5):e71-e84.http://dx.doi.org/doi:10.1161/ATVBAHA.117.310678
141. Mussbacher M, Derler M, Basílio J, Schmid JA. *NF-κB in monocytes and macrophages - an inflammatory master regulator in multitalented immune cells*. Front Immunol. 2023;14:1134661.http://dx.doi.org/10.3389/fimmu.2023.1134661
142. Qin Z, Bagley J, Sukhova G, Baur WE, Park H-J, Beasley D, Libby P, Zhang Y, Galper JB. *Angiotensin II-induced TLR4 mediated abdominal aortic aneurysm in apolipoprotein E knockout mice is dependent on STAT3*. Journal of Molecular and Cellular Cardiology. 2015;87:160-70.http://dx.doi.org/https://doi.org/10.1016/j.yjmcc.2015.08.014
143. Shi J, Hua L, Harmer D, Li P, Ren G. *Cre Driver Mice Targeting Macrophages*. Methods Mol Biol. 2018;1784:263-75.http://dx.doi.org/10.1007/978-1-4939-7837-3_24
144. Clausen BE, Burkhardt C, Reith W, Renkawitz R, Förster I. *Conditional gene targeting in macrophages and granulocytes using LysMcre mice*. Transgenic Res. 1999;8(4):265-77.http://dx.doi.org/10.1023/a:1008942828960
145. Hadi T, Boytard L, Silvestro M, et al. *Macrophage-derived netrin-1 promotes abdominal aortic aneurysm formation by activating MMP3 in vascular smooth muscle cells*. Nat Commun. 2018;9(1):5022.http://dx.doi.org/10.1038/s41467-018-07495-1
146. Davis FM, Tsoi LC, Melvin WJ, et al. *Inhibition of macrophage histone demethylase JMJD3 protects against abdominal aortic aneurysms*. J Exp Med. 2021;218(6).http://dx.doi.org/10.1084/jem.20201839
147. Bosmans LA, van Tiel CM, Aarts S, et al. *Myeloid CD40 deficiency reduces atherosclerosis by impairing macrophages' transition into a pro-inflammatory state*. Cardiovasc Res. 2023;119(5):1146-60.http://dx.doi.org/10.1093/cvr/cvac084
148. Viksman MY, Liu MC, Schleimer RP, Bochner BS. *Application of a flow cytometric method using autofluorescence and a tandem fluorescent dye to analyze human alveolar macrophage surface markers*. Journal of Immunological Methods. 1994;172(1):17-24.http://dx.doi.org/https://doi.org/10.1016/0022-1759(94)90374-3
149. Andersen MN, Al-Karradi SNH, Kragstrup TW, Hokland M. *Elimination of erroneous results in flow cytometry caused by antibody binding to Fc receptors on human monocytes and macrophages*. Cytometry Part A. 2016;89(11):1001-9.http://dx.doi.org/https://doi.org/10.1002/cyto.a.22995

150. Lacy M, Bürger C, Shami A, et al. *Cell-specific and divergent roles of the CD40L-CD40 axis in atherosclerotic vascular disease*. Nature Communications. 2021;12(1):3754.http://dx.doi.org/10.1038/s41467-021-23909-z
151. Henn V, Slupsky JR, Gräfe M, Anagnostopoulos I, Förster R, Müller-Berghaus G, Kroczek RA. *CD40 ligand on activated platelets triggers an inflammatory reaction of endothelial cells*. Nature. 1998;391(6667):591-4.http://dx.doi.org/10.1038/35393
152. André P, Nannizzi-Alaimo L, Prasad SK, Phillips DR. *Platelet-Derived CD40L*. Circulation. 2002;106(8):896-9.http://dx.doi.org/doi:10.1161/01.CIR.0000028962.04520.01
153. Liu O, Jia L, Liu X, Wang Y, Wang X, Qin Y, Du J, Zhang H. *Clopidogrel, a platelet P2Y12 receptor inhibitor, reduces vascular inflammation and angiotensin II induced-abdominal aortic aneurysm progression*. PLoS One. 2012;7(12):e51707.http://dx.doi.org/10.1371/journal.pone.0051707
154. Wagenhäuser MU, Mulorz J, Krott KJ, et al. *Crosstalk of platelets with macrophages and fibroblasts aggravates inflammation, aortic wall stiffening and osteopontin release in abdominal aortic aneurysm*. Cardiovasc Res. 2023.http://dx.doi.org/10.1093/cvr/cvad168

Supplement

```
1  run("Duplicate...", "title=title");
2  run("Duplicate...", "title=title2");
3  run("Gaussian Blur...", "sigma=15");
4  setOption("BlackBackground", true);
5  run("Convert to Mask");
6  run("Dilate");
7  run("Dilate");
8  setAutoThreshold("Default dark");
9  run("Threshold...");
10 setThreshold(129, 255);
11 run("Convert to Mask");
12 run("Close");
13 run("Measure");
14 selectWindow("title");
15 run("Split Channels");
16 selectWindow("title (blue)");
17 close();
18 close();
19 setAutoThreshold("Default dark");
20 run("Threshold...");
21 setThreshold(70, 255);
22 run("Convert to Mask");
23 run("Close");
24 run("Measure");
```

Supplementary Figure 1: Semi-automated macro for analysing collagen type IV amount in ImageJ software
This macro was created to semi-automatically analyse the amount of collagen type IV in aneurysmal cross-sections after IF staining. The first series of commands (1-13) allowed the determination of the whole AAA area using the WGA staining. The second series of commands (13-24) allowed the calculation of the area that was covered with collagen type IV positive signal.

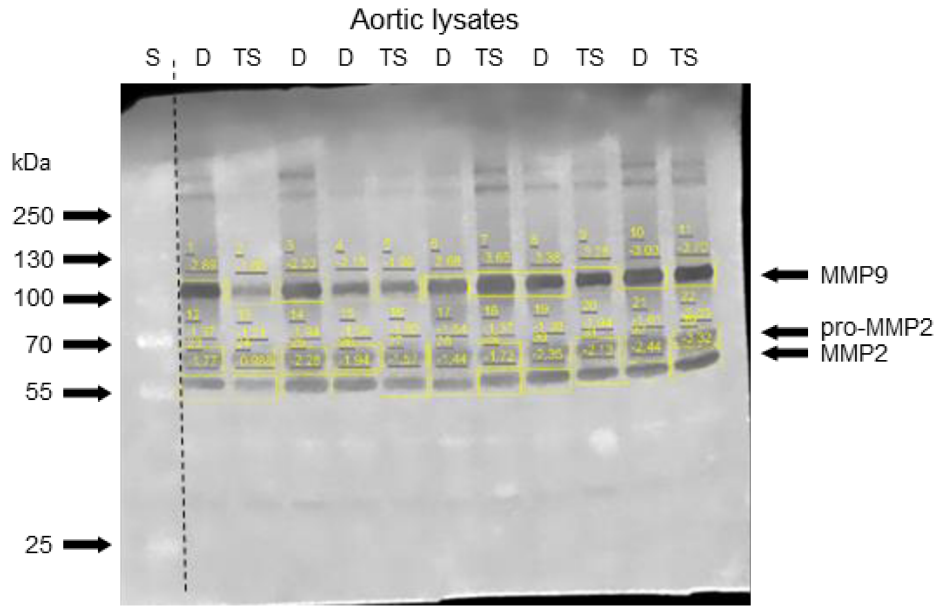

Supplementary Figure 2: Analysis of MMP9, pro-MMP2 and MMP2 activity in aortic lysates
Gelatin gel zymography of aortic lysates from DMSO- and TRAF-STOP-treated mice 14 days after PPE-induced AAA formation. Black bands indicate proteolytic activity. Protein size standard was loaded into the first lane. In every other lane 20 µg of total aortic protein lysate was loaded. Yellow boxes represent the area in which signal intensity of bands was measured. Results of signal intensity are displayed above boxes.
S = Size standard, D = DMSO, TS = TRAF-STOP; DMSO n=6, TRAF-STOP n=5.

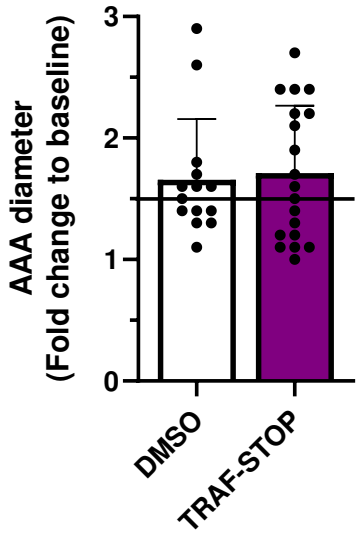

Supplementary Figure 3: TRAF-STOP treatment did not alter AAA diameter changes in the AngII model
Changes in the abdominal aortic diameter in DMSO- and TRAF-STOP-treated mice 28 days after AngII-induced AAA formation. AAA diameter was assessed using non-invasive ultrasound imaging, and changes after 28 days were calculated compared to baseline measurements. Expansion of aneurysm was similar in both treatment groups. An increase of ≥ 1.5-fold in aortic diameter was defined as AAA. Mean ± SD. DMSO n=14, TRAF-STOP n=19.

Danksagung

Alle Gedanken sind niedergeschrieben, der letzte Punkt ist gesetzt, alle Korrekturen sind eingearbeitet, das heißt: meine Dissertation ist fertig… nun bleibt es an mir auf eine Zeit zurückzublicken, in der ich tief in die Wissenschaft und Forschung eingetaucht bin. Es war eine Zeit in der ich viele Erfahrungen sammeln konnte, meinen Horizont erweitert habe, viele Lösungen für Probleme gesucht und glücklicherweise auch oftmals gefunden habe, die ich vorher nicht gehabt habe. Eine Zeit in der es auch manches Mal Frustration und Kummer gab, jedoch auch geprägt war von Glücksmomenten, Freude und Freundschaften.

Für diese Zeit möchte ich mich hiermit bei einigen Personen gesondert bedanken, denn ohne sie wäre diese Arbeit und der Weg zum Ziel nicht möglich gewesen. Mein Dank geht an Prof. Dr. Malte Kelm, dem Direktor der Klinik für Kardiologie, Pneumologie und Angiologie, dass ich meine Forschung im kardiovaskulären Forschungslabor Labor durchführen konnte. Außerdem danke ich dem TRR259 für die Finanzierung meines Projekts und der dazugehörigen Graduiertenschule, die mir geholfen hat meine Kenntnisse und Fähigkeiten zu verbessern. Natürlich geht auch ein Dank raus an alle Kooperationspartner, die mit ihrer Hilfe zu dieser Dissertation beigetragen haben. Ein besonderes Dankeschön geht an Prof. Dr. Norbert Gerdes, meinen Doktorvater und Leiter der Arbeitsgruppe, in der ich über vier Jahre ein Teil sein konnte. Deine Begeisterung für die Wissenschaft und dieses - mein - Projekt war ansteckend. Danke für deine Betreuung und Förderung in dieser Zeit. Natürlich möchte ich mich auch bei der Arbeitsgruppe selbst bedanken. Ihr standet mir mit Rat und Tat zur Seite und habt mit mir Tag ein, Tag aus die Forschung der Arbeitsgruppe gewuppt. Danke „Zirkus Halligerdes“ und einen besonderen Dank an Tanja, Susi, Chrissi, Sven, Ashley, Alex. Ich möchte hiermit auch allen anderen Arbeitsgruppen im CVRL danken. Das Arbeiten im Labor war mit euch geprägt von einem freundschaftlichen Miteinander, von helfenden Händen und konstruktiven Vorschlägen. Wir sind zusammengewachsen und haben die Aufs und Abs im stetigen Laboralltag zusammen gemeistert - Isabella, Vithya, Marcel und Maike. Natürlich möchte ich hier auch den zwei guten Seelen im Labor, Steffi und Julia, danken, ohne euch wäre alles nicht so reibungslos gelaufen.

Ich habe viel (Frei-) Zeit im CVRL verbracht um an meinem Projekt zu forschen, aber ohne die Hilfe von „außerhalb“ wäre das alles nicht möglich gewesen. Denn ohne die Unterstützung meiner Freunde und Familie hätte ich es nicht geschafft. Meine Freunde begleiten mich schon seit den Kindertagen und obwohl der räumliche Abstand größer geworden ist, bin ich sehr dankbar für euren emotionalen Beistand, für euer hartnäckiges Nachfragen und dass ich jederzeit auf euch zählen kann. Mein größter Dank gehört jedoch meiner Familie. Mein ganzes Leben begleitet ihr mich schon, haltet meinen Rücken frei und unterstützt mich in all meinen Entscheidungen. Ihr helft wo ihr nur könnt und eure grenzenlose Liebe hat mich zu dem gemacht, was ich heute bin. In dieser für mich sehr aufregenden und abenteuerlichen Zeit habt ihr an mich geglaubt und nun ist es vollbracht. Danke Mama, Papa, Caro mit Benny und Josie und Pascal!